Cytochromes *c*′: Biological Models for the $S = {}^3/_2,{}^5/_2$ Spin-State Admixture?

Raymond Weiss,† Avram Gold,*,‡ and James Terner§

Laboratoire de Chimie Supramoléculaires, Institut de Science et d'Ingénierie Supramoléculaires, Université Louis Pasteur de Strasbourg, 8 Allée Gaspard Monge, B.P.70028, F-67083 Strasbourg Cedex, France, Department of Environmental Sciences and Engineering, The University of North Carolina at Chapel Hill, Chapel Hill, North Carolina 27599-7431, and Department of Chemistry, Virginia Commonwealth University, Richmond, Virginia 23284-2006

Received June 24, 2005

Contents

* To whom correspondence should be addressed: e-mail, golda@email.unc.edu; phone, 919 966 7304; fax, 919 966 4711.
† Université Louis Pasteur de Strasbourg 8.
‡ The University of North Carolina at Chapel Hill.
§ Virginia Commonwealth University.

1. Introduction

The electronic ground state of most known ferric heme proteins is either low-spin ($S = {}^1/_2$) or high-spin ($S = {}^5/_2$). However, a small number of these proteins do not conform to this regime. This group includes the bacterial ferricytochromes *c*′ (earlier known as RHP, cytochromoids *c*, cytochromes *cc*′),[1−4] whose magnetic properties have been the subject of debate. In the earliest investigations, magnetic moments of 5.1 and 4.9 μ_B were deduced from solution magnetic susceptibility measurements made at physiological pH and room temperature for the ferricytochromes *c*′ isolated from the *Rhodospirillum rubrum* (*Rs. rubrum*), *Chromatium vinosum* (*Ch. vinosum*), and *Rhodopseudomonas palustris* (*Rp. palustris*) bacteria.[5] Between 1.4 and 4.2 K, the magnetic moment of the ferricytochrome *c*′ from *Ch. vinosum* was determined to be 3.4 μ_B by magnetic susceptibility measurements.[6] The unusual magnetic properties led Ehrenberg and Kamen[5] to propose that the electronic structure could be described by a low-spin ($S = {}^1/_2$)/high-spin ($S = {}^5/_2$) thermal equilibrium. Maltempo *et al.*[6−8] subsequently proposed a ground state in which the unperturbed mid-spin ($S = {}^3/_2$) and high-spin ($S = {}^5/_2$) states are quantum mechanically admixed. Further studies have indicated that magnetic properties vary among the ferricytochromes *c*′ isolated from different bacteria. Based largely on EPR spectroscopy, these proteins appear to be comprised of two groups. The first group, isolated from *Rp. palustris*, *Rhodobacter capsulatus* (*Rb. capsulatus*), and *Ch. vinosum*, displays a large mid-spin ($S = {}^3/_2$) contribution to an admixed ground state ranging from 40 to 57%.[7,9,10]

The second group, isolated from *Rs. rubrum*, *Rhodospirillum molischianum* (*Rs. molischianum*), *Achromobacter xylosoxidans* NCIMB 11015 (*Ach. xylosoxidans* NCIMB 11015; formerly *Alcaligenes sp* NCIMB 11015), GIFU 543, GIFU 1048, GIFU 1051, and GIFU 1764, has a much smaller mid-spin contribution of around 10−15%.[10,11] Continuing efforts to characterize the ferricytochromes *c*′ have led to

10.1021/cr040416l CCC: $59.00
Published on Web 06/01/2006

Raymond Weiss was born and raised in Alsace, France, and educated at the University of Strasbourg and the University of Nancy (Ph.D.). His research interests are centered around the structure and properties of synthetic metalloporphyrins and the nature and structure of reaction intermediates in heme protein catalysis. He is currently Professor Emeritus at Université Louis Pasteur, Strasbourg, France.

Avram Gold is a native of New York City. He received both his B.A. and Ph.D. degrees in Chemistry from Harvard University. Following postdoctoral fellowships with Weston Borden and Richard Holm, he was appointed Research Associate at the Harvard School of Public Health, where work in cytochrome P450-mediated activation of xenobiotic toxics led to an interest in porphyrins. Dr. Gold joined the faculty of the Department of Environmental Sciences and Engineering at the University of North Carolina at Chapel Hill, where he is currently Professor.

inconsistent conclusions on the relative importance of the $S = {}^3/_2,{}^5/_2$ spin admixture in these proteins. Resonance Raman studies are in accord with the conclusion that the spin state of the *Rp. palustris* ferricytochrome c' may be $S = {}^3/_2$,[12] while EXAFS studies were compatible with a significant mid-spin contribution to admixed ground states of the ferricytochromes c' from *Rs. molischianum* and *Rs. rubrum*.[13] In contrast, EPR and Mössbauer studies of the ferricytochrome c' from the latter bacterium,[14] resonance Raman studies of the ferricytochrome c' from *Methylococcus capsulatus* Bath (*M. capsulatus* Bath),[15] and ^{1}H NMR studies of the ferricytochromes c' conclude that, with the possible exception of *Ch. vinosum*, the ground state of these proteins is essentially high-spin.[16−20]

James Terner is Professor of Chemistry at Virginia Commonwealth University. He was born in Reading, England, but grew up in the Boston, Massachusetts, area and did undergraduate studies at Brandeis University. He received his Ph.D. in Chemistry in 1979, working with Prof. M. A. El-Sayed at UCLA, after which he was an NIH postdoctoral fellow with Professor T. G. Spiro at Princeton University. He joined the faculty of Virginia Commonwealth University in 1981 as Assistant Professor of Chemistry, and was an Alfred P. Sloan Fellow from 1985 to 1987. Current research interests are in the area of resonance Raman spectroscopy of unstable heme protein intermediates. His outside interests include mountain climbing and long distance bicycling.

In summary, the electronic ground state of the ferricytochromes c' has been and continues to be the subject of debate, and evidence for a quantum mechanically admixed $S = {}^3/_2,{}^5/_2$ ground state in these molecules has often been challenged.[21] As a result of the ongoing discussions, a large number of spectroscopic studies and several X-ray structures have been undertaken. Based on mechanisms postulated by Maltempo *et al.*[6−8] to account for the ground state of the heme iron of the ferricytochrome c' from *Ch. vinosum*, a number of model complexes have now been investigated and characterized as quantum mechanical $S = {}^3/_2,{}^5/_2$ spin-state admixtures.[22−24] This work reviews, first, work on model heme complexes in which the properties of the $S = {}^3/_2,{}^5/_2$ spin-state admixture have been established, and then, the studies related to the ground-state properties of the heme iron centers in the ferricytochromes c'. The results of studies on the proteins will be described and discussed in light of the knowledge accumulated on five- and six-coordinate ferric porphyrin model complexes, in which the iron centers display well characterized quantum mechanical $S = {}^3/_2,{}^5/_2$ spin admixed ground states with varying degrees of mid-spin contribution. From the outset, it is important to emphasize that the physicochemical data available on the cytochromes c' are fragmented, and to date, a comprehensive set of data cannot be assembled for any single protein to enable a definitive assessment of spin state.

1.1. Characterization and Function of Cytochromes c'

The cytochromes c' are usually isolated as soluble homodimers, composed of two identical subunits of approximately 130 residues (molecular mass of ≈14 kDa) containing a *c*-type heme. However, the proteins derived from the three photosynthetic bacteria, *Rp. palustris*, *Rb. capsulatus*, and *Rhodobacter sphaeroides* (*Rb. sphaeroides*), are exceptions to this generality.[25] The *Rp. palustris* protein is entirely monomeric, while the proteins from *Rb. capsulatus* and *Rb. sphaeroides* are a mixture of monomers and dimers.[26] Although the cytochrome c' derived from the purple pho-

Table 1. Mössbauer Parameters of $S = {}^3/_2,{}^5/_2$ Spin Admixed and Pure Mid-spin Iron(III) Porphyrin Complexes

compound	T (K)	δ[a] (mm s^{-1})	ΔE_Q (mm s^{-1})	%($S = {}^3/_2$)[b]
$Fe^{III}(tpp)SbF_6 \cdot C_6H_5F$[c]	4.2	0.39	4.29	~98
$Fe^{III}(tpp)B_{11}CH_{12} \cdot C_7H_8$[c]	RT		3.77	
	4.2	0.33	4.12	~92
$Fe^{III}(tpp)Co(B_9C_2H_{11})_2$[d]	295		3.69	
$Fe^{III}(tpp)ClO_4$[e,f]	RT	0.30	2.79	
(0.5 *m*-xylene)	195	0.34	3.17	
	77	0.38	3.48	
	4.2	0.38	3.50	~65
$Fe^{III}(tpp)AsF_6$[d]	4.2		3.25	
$Fe^{III}(tpp)SO_3CF_3$[d]	RT		2.39	~30
$Fe^{III}(tpp)BF_4$[c]	RT		1.60	
$[Fe^{III}(oep)(2\text{-}MeImH)]^+$[g]	4.2	0.40	1.39	~0
$Fe^{III}(tpp)ReO_4$[d]	78		1.32	
$Fe^{III}(oep)ClO_4$[f,h]	RT	0.37	3.16	
	115	0.37	3.52	
	4.2	0.37	3.57	~80
$Fe^{III}(oep)ClO_4$[i]	RT	0.31	3.14	
	77	0.39	3.57	
	4.2	0.40	3.54	~100
$[Fe^{III}(oep)(EtOH)_2]ClO_4$[f,g]	RT	0.29	2.97	
	115	0.36	3.32	
	4.2	0.38	3.47	
$[Fe^{III}(oep)(THF)_2]ClO_4$[j]	RT	0.31	3.03	
	77	0.42	3.34	
$[Fe^{III}(oep)(3\text{-}Clpy)]ClO_4$[k]	4.2	0.36	3.23	~81
$Fe^{III}(oetpp)Cl$[l]	280	0.35	0.92	4−10
$Fe^{III}(dpp)Cl$[m]	280	0.35	0.95	~7
$[Fe^{III}(t^i prp)(THF)_2]ClO_4$[n]	76	0.34	3.71	~100
$[Fe^{III}(oetpp)(THF)_2]ClO_4$[n]	290	0.50	3.50	~100

[a] /αFe. [b] Based on $g^{eff}_{\perp}$ values. [c] Reference 93. [d] Reference 24. [e] Reference 22. [f] Reference 134. [g] Reference 94. [h] Reference 87. [i] Reference 119. [j] Reference 63. [k] Reference 219. [l] Reference 108. [m] Reference 110. [n] Reference 95.

tosynthetic bacterium *Ch. vinosum* is dimeric, it is unique in that ligand binding to the heme iron causes dimer dissociation.[27,28]

The cytochromes *c*′ form a unique group of heme proteins belonging to class II of the cytochromes *c*, characterized by (i) a heme attachment near the C-terminal region of the polypeptide chain; (ii) axial ligation to an imidazole ring of a His residue; (iii) absence of a second axial ligand; and (iv) wide-ranging, relatively low redox potentials ranging from −205 to +202 mV (Table 2).[29,30] As evident from the bacterial sources in Table 2, members of this group are found in a wide variety of bacteria with different metabolic pathways including photosynthetic, denitrifying, and nitrogen-fixing as well as methanotrophic and sulfur oxidizing activity.[15,29,31] The cytochromes *c*′ isolated from the denitrifying bacteria clearly have the highest redox potentials ($E_{m,7} \geq 110$ mV). The redox potentials of the sulfur and nonsulfur phototrophs span an intermediate range, while the redox potential of the methanotroph *M. capsulatus* Bath is significantly below those of the other proteins. As yet, no functional significance can be attributed to the differences in redox potentials, and with the exception of the protein from *M. capsulatus* Bath, the physiological role of the cytochromes *c*′ is not well understood. The cytochrome *c*′ from *M. capsulatus* Bath is proposed to serve as electron shuttle between cytochrome P460 ($-380 < E_{m,7} < 300$ mV), which catalyzes

Table 2. Redox Potential ($E_{m,7}$) of Cytochromes *c*′

$E_{m,7}$ (mV)	bacterial source of cytochromes *c*′
+202	*Paracoccus denitrificans*[a]
+132 to +90	*Achromobacter xylosoxidans* NCIMB 11015[b−d]
+110	*Achromobacter xylosoxidans* GIFU 543[e]
+105 to +94	*Rhodopseudomonas palustris*[c]
+95	*Rhodospirillum salexigens*[c,f,g]
+60	*Rhodocyclus gelatinosus*[c]
+51	*Rhodobacter capsulatus*[c,d]
+45	*Rhodospirillum tenuis 3761*[c]
+30	*Rhodobacter sphaeroides*[c,h]
+30	*Ectothorhodospira halophila*[c]
+18	*Chromatium vinosum*[c,d]
+14	*Rhodospirillum molischianum*[c]
+14	*Rhodospirillum photometricum*[c]
+3	*Rhodospirillum rubrum*[c,i]
+3	*Rhodospeudomonas purpureus*[c]
−205	*Methylococcus capsulatus* Bath[j]

[a] Gilmour, R.; Goodhew, C. F.; Pettigrew, G. W. *Biochim. Biophys. Acta* **1991**, *1059*, 233. [b] Cusanovich, M. A.; Tedro, S. M.; Kamen, M. D. *Arch. Biochem. Biophys.* **1970**, *141*, 557. [c] Reference 147. [d] Meyer, T. E.; Cusanovich, M. A. *Biochim. Biophys. Acta* **1989**, *975*, 1. [e] Shidara, S.; Iwasaki, H.; Yoshimura, T.; Suzuki, S.; Nakahara, A. *J. Biochem.* **1986**, *99*, 1749. [f] De Klerk, H.; Bartsch, R. G.; Kamen, M. D. *Biochim. Biophys. Acta* **1965**, *97*, 275. [g] Dus, K.; De Klerk, H.; Bartsch, R. G.; Horio, T.; Kamen, M. D. *Proc. Natl. Acad. Sci. U.S.A.* **1967**, *57*, 367. [h] Meyer, T. E.; Cusanovich, M. A. *Biochim. Biophys. Acta* **1985**, *807*, 308. [i] Kakuno, T.; Hosoi, K.; Higuti, T.; Horio, T. *J. Biochem.* **1973**, *74*, 1193. [j] Reference 15.

a four-electron oxidation of hydroxylamine to nitrite, and cytochrome c_{555} ($+175$ mV $< E_{m,7} < +195$ mV).[15,32] In general, it has long been assumed that the cytochromes *c*′ are involved in electron transfer.[33] They are able to bind neutral ligands such as CO, NO, and alkylisocyanides,[34−41] as well as anionic ligands such as cyanide.[42,43] In addition to binding NO in vitro, it has been shown that NO binds to whole cells of the denitrifying bacterium *Ach. xylosoxidans* NCIMB 11015 under denitrifying conditions,[44] and it has been suggested that the cytochromes *c*′ present in the denitrifying bacteria may bind nitric oxide, which is a freely diffusible intermediate during denitrification.[41,45] It has also been proposed that some cytochromes *c*′ may function as NO carriers[46] and help to alleviate nitrosative stress in bacteria.[47,48] In a physiological environment, the cytochromes *c*′ seem to function in the reduced oxidation state, as the characteristic EPR spectrum of ferricytochromes *c*′ has not been detected in vivo.[49,50]

2. $S = {}^3/_2,{}^5/_2$ Spin-State Admixture in Model Heme Complexes

2.1. Spin States of Ferric Porphyrin Complexes

Based on crystal-field and quantum-mechanical calculations[51−56] and EPR and NMR spectroscopic data,[57,58] it is now well accepted that, in a field of tetragonal (or nearly tetragonal) symmetry, the d^5 orbital population of iron(III) can be formally classified into three spin states:

(i) A high-spin state ($S = {}^5/_2$) with the d-electron configuration $d(xy)^1d(xz,yz)^2d(z^2)^1d(x^2-y^2)^1$. In C_{4v} symmetry, the ground term of this configuration is $^6A_1$. The orbital occupancy pattern arises because the energy gaps between the 3d-orbitals are smaller than the spin pairing energies. A large number of five-coordinate, purely high-spin ferric porphyrin complexes having one moderately strong anionic ligand are known. A small number of six-coordinate complexes having two neutral, weakly basic axial ligands are

also known. Many high-spin ferric heme proteins in which the heme iron is five-coordinate are known.

(ii) A low-spin state ($S = {}^1/_2$) with the d-electron configuration $d(xy)^2d(xz,yz)^3d(z^2)^0d(x^2-y^2)^0$. In D_{4h} symmetry, the ground term is ^2E. The low-spin configuration is the result of an energy gap between the $d(xz,yz)$ and $d(z^2)$ orbitals which is larger than the spin pairing energy. It has recently been shown that, with ligands which are σ-donors and strong π-acceptors, the relative energies of the $d(xy)$ and $d(xz,yz)$ orbitals can be reversed, leading to the electronic configuration $d(xz,yz)^4d(xy)^1d(z^2)^0d(x^2-y^2)^0$ having the ground term $^2B_1$.[58] A large number of six-coordinate, low-spin iron(III) porphyrin model heme complexes have been synthesized, and many six-coordinate, low-spin ferric heme proteins have been isolated and characterized. A few five-coordinate, low-spin iron(III) model complexes have been reported, confined predominantly to compounds with iron−carbon σ-bonds, and no low-spin, five-coordinate ferric heme protein has been characterized.

(iii) A mid-spin state ($S = {}^3/_2$) with the electron configuration $d(xy)^2d(xz,yz)^2d(z^2)^1d(x^2-y^2)^0$. The ground term in the C_{4v} point group is $^4A_2$. This spin state arises when the energy gap between the $d(z^2)$ and $d(x^2-y^2)$ orbitals is larger than the spin pairing energy.

Coordination of one weak-field anionic axial ligand,[59,60] one neutral basic ligand,[61,62] two neutral weakly basic ligands,[63−67] or a combination of a weakly coordinating anionic ligand and a weakly basic neutral ligand[68,69] can induce the mid-spin configuration. Several examples of almost pure mid-spin iron(III) porphyrin model complexes have been reported.[59,60] The less common mid-spin configuration $d(xz,yz)^3d(xy)^1d(z^2)^1(dx^2-y^2)^0$ with the ground state ^4E has been described for severely ruffled and saddled *meso* tetraalkyl model hemes.[70−72] There are currently no examples of heme proteins in a pure, or "nearly pure", mid-spin state.

When the energy separation of the mid-spin and high-spin states approaches the magnitude of the spin−orbit coupling parameter, the electronic ground state of the heme is best described as a quantum mechanical admixture of the two spin states. Many model heme complexes displaying the quantum mechanically admixed $S = {}^3/_2,{}^5/_2$ ground state are known.[58] Based on resonance Raman, EPR, NMR, and electronic spectra, several class III peroxidases have been characterized as $S = {}^3/_2,{}^5/_2$ spin state admixtures,[73,74] Although assignment of the $S = {}^3/_2,{}^5/_2$ spin-state admixture to these proteins has not, to date, provoked a debate similar to that surrounding the cytochromes c', rigorous physicochemical characterization has not been performed on all the class III peroxidases.

2.1.1. Theoretical Basis for the $S = {}^3/_2,{}^5/_2$ Quantum Mechanical Spin-State Admixture

In studies based on model complexes, the quantum mechanical $S = {}^3/_2,{}^5/_2$ spin admixed ground state was initially proposed to explain the magnetic properties of the moderately acidic or neutral pH form of the ferricytochrome c' from the photosynthetic bacteria *Ch. vinosum*.[6−8] In a model proposed by Maltempo, the mid- and high-spin states interact when their energy separation is of the same order of magnitude as, or smaller than, the spin−orbit coupling parameter λ. In C_{4v} symmetry, the ground state may be described by a linear combination of the sextet $^6A_1$ and quartet $^4A_2$ states, resulting in a $d(x^2-y^2)$ orbital occupancy <1 and a $d(xy)$ orbital occupancy >1. According to Mitra *et al.*,[75] the Maltempo model explains only the gross magnetic behavior of the complexes and mixing with low-lying excited spin states (^4E, ^2E, $^2B_2$) should also be considered. As shown diagrammatically by Figure 1,[76] the relative contributions of $S = {}^3/_2$ and $S = {}^5/_2$ states to the ground state of spin-admixed systems varies depending upon the energy of the $d(x^2-y^2)$ orbital. As the energy of this orbital increases, the ground state will change from predominantly $S = {}^5/_2$ to predominantly $S = {}^3/_2$.[68]

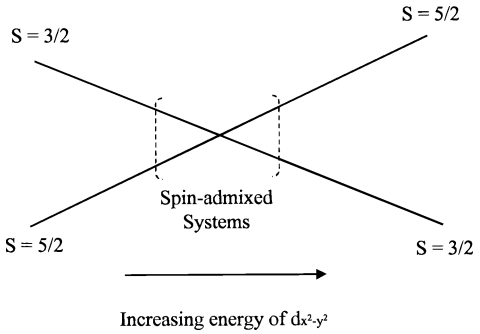

Figure 1. Possible relative energies of the $S = {}^3/_2$ and $S = {}^5/_2$ states in spin-admixed systems and their variation in energy as a function of increasing energy of the $d(x^2-y^2)$ orbital. Reprinted with permission from ref 76. Copyright 2000 American Chemical Society.

2.1.2. Magnetic Properties of Spin-Admixed Ferric Porphyrin Complexes: Effects of Porphyrin Structure and Ligation State.

2.1.2.1. General Features. Effective $g_\perp$ values of EPR transitions reported for $S = {}^3/_2,{}^5/_2$ spin-admixed complexes vary between 4, the theoretical value for pure mid-spin complexes, and 6, the value for pure high-spin complexes.[77] Because of the approximate axial symmetry of the ligand field of iron in mid-spin, spin-admixed, and high-spin electronic configurations, $g_\perp$ lines in EPR spectra of randomly oriented samples appear as broad, derivative-shaped curves.

The distribution of unpaired electron spin, as reflected in NMR hyperfine shifts of ^1H and ^{13}C NMR signals, serves as an extremely sensitive probe of spin admixture. For pure high-spin iron(III) porphyrins without significant core distortion, the predominating mechanism of spin delocalization is via a σ pathway from $d(x^2-y^2)$ to the porphyrin framework. Thus, the signals of the pyrrole β-H of iron(III) tetraarylporphyrins (Fe^{III}(tap)) experience large shifts downfield to $\sim +80$ ppm. The α-CH proton signals of high-spin octaethyl- (oep) and etio-type (etio) porphyrins are similarly shifted downfield to $\sim +60$ ppm. As the $d(x^2-y^2)$ orbital becomes depopulated with the increasing $S = {}^3/_2$ admixture, the pyrrole proton signals of the tetraarylporphyrin shift upfield to a limiting postion of ~ -60 ppm in mid-spin complexes. The situation for signals of protons on pyrrole β alkyl substituents is less straightforward. The α-CH_2 proton signals of the severely saddle-distorted pentacoordinate complex iodo 2,3,7,8,12,13,17,18-octaethyl-5,10,15,20-tetraphenylporphinatoiron(III) (Fe^{III}(oetpp)I), which has been characterized by EPR and magnetic susceptibility measurements as a nearly pure mid-spin complex, range from 47.3 to 11.9 ppm,[78] with an average shift of 30.2 ppm, only slightly upfield from the average shifts of the α-CH_2 signals of high-spin Fe^{III}(oetpp)F (35.7 ppm) and Fe^{III}(oetpp)Cl (34.0 ppm) complexes. The average of the α-CH_2 proton signals of the mid-spin hexacoordinate complexes $[Fe^{III}(oetpp)(thf)_2]^+$ and [Fe^{III}-

$(oetpp)(MeOH)_2]^+$ is shifted to a slightly higher field at ~20 ppm. However, the difference between α-CH_2 shifts in high-spin and mid-spin complexes is still much less pronounced than that for the pyrrole protons of the Fe^{III}(tap). The relative insensitivity of α-CH proton shifts to the proportion of $S = {}^3/_2$ admixture is ascribed to a combination of rapid attenuation of spin transfer through σ bonds and conformational effects relating to the orientation of the β alkyl groups.[72] The *meso* carbons lie in a nodal plane of the σ system, and spin transfer occurs via a π-mechanism through a $d(z^2)-a_{2u}$ interaction.[79] Thus, in high-spin complexes, *meso* protons are shifted far upfield of the diamagnetic region (−54 ppm in Fe^{III}(oep)-Cl). As iron moves toward the porphyrin mean plane in spin-admixed complexes, the $d(z^2)-a_{2u}$ interaction becomes less favorable, and *meso* proton signals move downfield toward the diamagnetic region while protons at *meso* α-CH postions move *up*field toward the diamagnetic region.[72]

The isotropic shifts of proton signals of $S = {}^3/_2,{}^5/_2$ spin-admixed complexes show an anti-Curie temperature dependence,[24,62,80−83] as a result of the dependence of spin-state admixture on temperature. The non-Curie behavior of proton resonances has been studied in the chloro, perchlorato, bis-[4-(dimethylamino)pyridine], bis(1-methylimidazolate), and bis(cyanide) iron(III) complexes of the sterically crowded β-pyrrole-substituted octamethyltetraphenylporphyrin (omtpp), octaethyltetraphenylporphyrin (oetpp), octaethyltetrapentafluorophenylporphyrin (oepfpp), and tetra-β,β′-tetramethylenetetraphenylporphyrin (tc_6tpp).[84] An expanded form of the Curie law that includes a contribution from the Boltzmann population of a thermally accessible excited state has been developed to allow the spin multiplicities and energy separation of ground and excited states to be determined by fitting the temperature dependence of proton resonances. The ground-state assignments based on fitting the expanded Curie-law equation were in agreement with assignments based on EPR, with the exception of the case of $Fe^{III}(tc_6tpp)Cl$. While the EPR spectrum of this complex indicated a high-spin ground state, the best fit for the temperature dependence of the phenyl and methylene protons was obtained based on the assumption of a mid-spin ground state. The authors have proposed a thermal equilibrium between the two spin states that makes the $S = {}^3/_2$ state lowest in energy over the temperature range of the NMR experiments.

^{13}C NMR signals of pyrrole α- and β-carbons in planar hexacoordinate high-spin complexes of the type $[Fe^{III}(tap)]^+$ are shifted strongly downfield, to ~1600 and 1250 ppm, respectively, by σ-donation of unpaired spin from the half-filled $d(x^2-y^2)$ orbital to the porphyrin framework. Decreasing $d(z^2)-a_{2u}$ interaction with movement of the iron toward the porphyrin mean plane leads to a shift of *meso* carbon signals close to the diamagnetic region at ~20 ppm. On strong ruffling of the porphyrin core in the hexacoordinate high-spin complex iron(III) *meso*-tetra(isopropylporphyrin) ($[Fe^{III}(t^iPrp)]^+$), a small upfield shift of the pyrrole α-carbon signal by 15 ppm and small downshifts of the *meso* carbon by 60 ppm and the pyrrole β-carbon by 40 ppm are ascribed to contraction of the $Fe-N_p$ bonds and interaction between the $d(xy)$ and a_{2u} orbitals. Saddle distortion in hexacoordinate high-spin $[Fe^{III}(oetpp)]^+$ results in pronounced upfield shifts of both α- and β-pyrrole carbon signals to ~700 and 900 ppm, respectively, through decreased σ-donation from Fe $d(x^2-y^2)$ and a slight downfield shift of the *meso* carbon to ~40 ppm through $d(x^2-y^2)-a_{2u}$ interaction. In hexacoordinate planar $[Fe^{III}(tap)]^+$ complexes characterized as predominantly mid-spin, $d(xz,yz)-3e_g$ interaction is proposed to lead to a large upfield pyrrole α-carbon shift to ~ −200 ppm and a smaller *meso* carbon downfield shift to ~80 ppm. In hexacoordinate spin-admixed complexes where strong ruffling of the porphyrin core causes inversion of the $d(xy)$ and $d(xz,yz)$ orbital energies to give the electronic configuration $d(xz,yz)^3d(xy)^1d(z^2)^1d(x^2-y^2)^0$, as in the case of $[Fe^{III}(t^iPrp)]^+$, a decrease in $d(xz,yz)-3e_g$ interaction accompanied by development of a $d(xy)-a_{2u}$ interaction is proposed to lead to large downfield shifts of both the pyrrole α-carbon signal (to 24 ppm) and the *meso* carbon signal (to 145 ppm). Saddling in $[Fe^{III}(oetpp)]^+$ allows $d(x^2-y^2)-a_{2u}$ interaction in addition to $3e_g-d(xz,yz)$ interaction, causing a strong downfield shift of the α-carbon signal to ~400 ppm and a large *meso* carbon shift upfield to −270 ppm.

^{13}C NMR shifts of porphyrin ring carbons have recently been investigated as a probe for spin state.[72] For spin-admixed planar complexes $[Fe^{III}(tpp)L_2]^+$ and strongly ruffled complexes $[Fe^{III}(t^iPr)L_2]^+$, shifts of the pyrrole H were correlated with shifts of pyrrole α, β, and *meso* carbon signals. The correlations were proposed as a basis for estimating mid-spin content from ^{13}C NMR spectra. Deviation of ^{13}C shifts of $[Fe^{III}(t^iPr)L_2]^+$ from the correlation curves for L = MeOH, thf, 2-Me-thf, and dioxane were attributed to the unusual mid-spin configuration $d(xz,yz)^3d(xy)^1d(z^2)^1d(x^2-y^2)^0$, and a separate correlation curve was constructed for this configuration. In the case of the strongly saddle-distorted $[Fe^{III}(oetpp)L_2]^+$, a good correlation was established between the ^{13}C NMR shift of the Py-C_α attached to the pyrrole and the shifts of the α, β, and *meso* carbons.

These studies have shown that ^1H and ^{13}C NMR are useful tools for defining the spin states of complexes at ambient conditions and for determining whether the spin state is due to a thermally accessible state or a thermodynamic equilibrium between spin states or both.[85]

The structural, spectroscopic, and magnetic properties of quantum mechanically spin-admixed iron(III) porphyrin complexes, particularly iron(III) tetraphenylporphyrin complexes, have been used as the basis of a "magnetochemical" series to rank ligand field strength,[24,60] analogous to the spectrochemical series. In line with expectations, the metrics of the spin-admixed complexes lie between the limits of pure high-spin and pure mid-spin complexes according to the relative proportions of the spin states in the admixture.

2.1.2.2. Specific Studies on Mid-Spin and Spin-Admixed Model Complexes. A large body of work has appeared characterizing spin-admixed model compounds. The $S = {}^3/_2,{}^5/_2$ quantum mechanically admixed ground state has been reported for five- and six-coordinate ferric tetraaryl- and octaalkylporphyrin complexes ligated to (i) one weak-field or weakly basic anionic ligand such as $B_{11}CH_{12}^-$,[59] SbF_6^-,[59] AsF_6^-,[24] ClO_4^-,[22,86,87] $C(CN)_3^-$,[81,88] $CF_3SO_3^-$,[81,89] or BF_4^-,[24] (ii) one neutral ligand such as imidazole, alkyl-substituted imidazoles, or benz- or halogenated imidazoles,[61,62] (iii) two neutral, weakly basic ligands such as THF,[63] 3-chloropyridine,[64,65] or 3,5-dichloropyridine,[66,67] or (iv) one weakly coordinating anionic ligand and one neutral weakly basic ligand such as N_3^- + DMF[69] or $CF_3SO_3^-$ + H_2O.[68] It has also been shown that the relative proportion of the mid-spin contribution ($S = {}^3/_2$) to the $S = {}^3/_2,{}^5/_2$ spin-admixed state can be varied by unfavorable steric interactions between axial ligands and *ortho* substituents of ferric 2,6- and 2,4,6-substituted tetraarylporphyrin complexes that result in weak-

ened axial coordination.[76,90,91] Magnetic susceptibility measurements have established magnetic moments ranging from 3.9 to 5.9 μ_B. The temperature-dependent magnetic susceptibility has been described over the range 6−300 K for Fe^{III}(oep)(3-Clpy),[92] Fe^{III}(tpp)($B_{11}CH_{12}$)·C_7H_8,[59] Fe^{III}(tpp)($FSbF_5$)·C_6H_5F,[93] and Fe^{III}(oep)(2-MeImH)$^+$,[94] and over the range 1.9−300 K for Fe^{III}(oep)(3,5-Cl_2py)$_2ClO_4$.[66] With the exception of the mono(2-MeImH) complex, these complexes were identified as spin-admixed, and the temperature-dependent curves were characterized by a clear inflection at ∼130 K. A good fit to the experimental data was obtained by the Maltempo model when weak antiferromagnetic coupling was included in the calculated susceptibility values of the 5-coordinate complexes. The mono(2-MeImH) complex showed no spin transition and was best treated as high-spin (see section 2.2).

The five-coordinate iron(III) porphyrin complexes of weakly coordinating anionic ligands, such as the mono(imidazole) complexes [Fe(tmp)L]ClO_4 (L = imidazole, alkyl-substituted imidazoles, or benz- or halogenated imidazoles), have been studied by a variety of spectroscopic techniques.[62,70,85,95−99] As discussed in section 2.2, the degree of spin-state admixture could generally be rationalized by the relative ligand field strength estimated as a function of steric bulk and electronic effects. Exceptions (also discussed in section 2.2) were complexes of the sterically bulky ligands 2-^{t}BuImH and 2-(1-(EtPr))ImH, which were essentially high-spin.

In addition to stabilization of d(z^2) by coordination of a weak-field axial ligand, the mid-spin state may be stabilized through raising the energy of d(x^2-y^2) by increasing the field strength of the porphyrin ligand. The nearly pure mid-spin states of the chloroiron(III) complexes of phthalocyanine[100,101] and octamethyltetraazaporphyrin,[102,103] are attributed to the smaller cavities of these ligands relative to those of the tetraaryl- and octaalkylporphyrins. The result is a substantially higher energy d(x^2-y^2) orbital through the increased field strength of these tetrapyrrolic ligands.[104] It has also been shown that the relative proportion of the mid-spin state in the $S = {}^3/_2,{}^5/_2$ admixture can be varied by electron-releasing or -withdrawing *para*-phenyl substituents of iron(III) *meso*-tetraarylporphyrin complexes that modulate the field strength of the porphyrin ligand.[76,90,91]

As discussed above, nonplanar distortions of the porphyrin ligand have recently been proposed to increase equatorial field strength. Based on this observation, a saddle deformation of the heme has been suggested to mediate the electronic structure of the bacterial ferricytochromes c'.[105] EHT and INDO calculations of Cheng and Chen[106] predict that saddle deformations decrease the symmetry of the porphyrin coordination sphere and can cause stronger interaction between the macrocycle and the coordinated metal with a net effect of elevating the energy of d(x^2-y^2) relative to d(z^2). The $S = {}^3/_2,{}^5/_2$ spin-admixed chloroiron(III) complexes of the sterically crowded porphyrin dianions omtpp and oetpp contain porphyrins that are severely saddle shaped. A quantum mechanical $S = {}^3/_2,{}^5/_2$ spin admixture with a mid-spin contribution of about 40% was determined by EPR spectroscopy for the complex Fe^{III}(oetpp)Cl.[105]

The temperature dependence of the magnetic behavior of six-coordinate saddle-distorted complexes [Fe^{III}(oetpp)(L)$_2$]$^+$ with weakly coordinating axial ligands L = tetrahydrofuran (thf), 4-cyanopyridine (4-CNpy), pyridine (py), or 4-dimethylaminopyridine (4-dma-py) has been investigated.[95,96,107] The bis(4-dma-py) complex, [Fe(oetpp)(4-dma-py)$_2$]ClO_4, maintained a low-spin state over the temperature range 2−300 K. The bis(py) complex was in the $S = {}^3/_2$ spin state at room temperature and underwent a novel spin transition from mid-spin to low-spin ($S = {}^1/_2$) at about 150 K. The bis(4-CNpy) complex showed similar behavior in the solid state, but in solution it remained in the mid-spin state. The bis(thf) complex [Fe^{III}(oetpp)]$^+$ maintained a pure mid-spin state over the temperature range 5−300 K.[96] The bis(thf) complex of strongly ruffled [Fe^{III}(t^iPrp)(thf)$_2$]$^+$ was characterized as being in an essentially pure $S = {}^3/_2$ spin state between 50 and 300 K. The major considerations put forward for the increasing stabilization of the mid-spin state in the [Fe^{III}(oetpp)(L)$_2$]$^+$ complexes (L = thf, 4-CNpy, py) were short Fe−N_p bond distances occurring in highly nonplanar distorted porphyrins and weak coordination of the axial ligands. These results indicate that both the nonplanar distortions of the porphyrin core and the coordination strength of the axial ligand play an important role in tuning the spin states of iron(III).

The electronic states of the pyrrole β-substituted complexes [Fe^{III}(omtpp)(L)$_2$]$^+$ and iron(III) tetra-β,β'-tetramethylenetetra(3,5-dimethylphenyl)porphyrin (tbtxp), [Fe^{III}(tbtxp)(L$_2$)]$^+$ (L = thf, 4-CNpy, py, 4-dma-py), have also been studied in liquid and frozen solution. While the bis(4-dma-py) complexes maintain the low-spin state, the bis(thf) derivatives exhibit an essentially pure mid-spin state over a wide range of temperature. The bis(py) and bis(4-CNpy) complexes exhibit an $S = {}^3/_2 \rightarrow {}^1/_2$ spin transition as the temperature is decreased from 300 to 200 K. [97] Close examination of the NMR and EPR data revealed that at low temperature these complexes adopt the less common d(xz,yz)^{4}d(xy)^1 low-spin state electronic configuration in contrast to the case of [Fe^{III}(oetpp)(py)$_2$]$^+$, which shows the more common d(xy)^{2}d(xz,yz)^3 configuration.[97] [Fe^{III}(omtpp)(py)$_2$]$^+$ has been found to behave quite differently from [Fe^{III}(oetpp)(py)$_2$]$^+$ in the microcrystalline state. While the oetpp derivative was found to exhibit the $S = {}^3/_2 \rightarrow {}^1/_2$ spin transition, the omtpp derivative maintained a low-spin state. The difference in magnetic behavior between [Fe^{III}(omtpp)(py)$_2$]$^+$ and [Fe^{III}(oetpp)(py)$_2$]$^+$ has been ascribed to the difference in the molecular packing of the crystals, with the former complex adopting a densely packed cubic crystal system while the latter crystallizes in a less condensed monoclinic system.[99] The results indicate that loosely packed crystal systems and wide cavities around the axial ligands are important requirements for the occurrence of the spin crossover in the solid state.[99]

More recently, magnetic properties of bis(4-CNpy) complexes of iron(III) octamethyl-, octaphenyl-, and tetra-β,β'-tetramethylenetetraphenylporphyrin were analyzed by NMR and EPR spectroscopy and the crystal structures of two different forms of [Fe^{III}(oetpp)(4-CNpy)$_2$]ClO_4 and one form of [Fe^{III}(omtpp)(4-CNpy)$_2$]ClO_4 were determined.[85] This study shows the coordination strength of the axial ligand as well as short Fe−N_p bond distances to be an important factor in tuning the ground state of the iron(III) porphyrins. While most of the conclusions of this study are in agreement with the studies of Nakamura *et al.*[95,96,107] discussed above, large negative phenyl H chemical shift differences $\delta_m - \delta_o$ and $\delta_m - \delta_p$ in the ^{1}H NMR spectra indicate that the actual electronic state of [Fe^{III}(oetpp)(4-CNpy)$_2$]ClO_4 involves a significant, but as yet not quantified, contribution from a high-spin ($S = 2$) iron(II) center antiferromagnetically coupled to an $S = {}^1/_2$ porphyrin π-cation radical.[85]

However, the importance of saddle distortion, per se, has been questioned in studies of fluoro- and chloroiron(III) (oetpp) complexes,[78,108] as well as the chloroiron(III) complexes of other pyrrole β-ethyl and phenyl *meso*-tetraphenylporphyrins.[109,110] These complexes show only a weakly spin-admixed ground state, although the porphyrin ligands display very large saddle distortions and are often also slightly ruffled. In contrast, the mid-spin contributions to the ground electronic state of the bromo and iodo complexes of Fe^{III}(oetpp), in which the field strength of the axial ligands is weaker, have been found to be ~89 and 98%, respectively.[78] The ground state of the perchlorato iron(III) complex Fe^{III}(oetpp)ClO_4, with both a weak-field ligand and severe saddle distortion, is almost pure $S = {}^3/_2$.[111] Taken as a whole, these reports suggest that a weak-field ligand and saddle distortion may act in combination to cause a significant mid-spin component in an $S = {}^3/_2,{}^5/_2$ admixture.

Hoard[112] has shown that D_{2d} ruffling of the porphyrin core allows the relief of strain in metalloporphyrins which require core contraction to accommodate short $M-N_p$ bond distances.[113] Since core contraction increases the field strength, a ruffled core should elevate the energy of the $d(x^2-y^2)$ orbital and therefore stabilize the mid-spin state. Nevertheless, despite a short $Fe-N_p$ average distance of 2.034(9) Å, the ruffled chiroporphyrin complex Fe(tmcp)Cl (tmcp = tetramethylchiroporphyrin)[114] is high-spin.[115] However, the combination of ruffling and axial coordination by a weak-field alcohol ligand in the six-coordinate bis(ethanol) complex $[Fe^{III}(tmcp)(EtOH)_2]^+$ and in three variants of the mixed ethanol−water complex $[Fe^{III}(tmcp)(EtOH)(H_2O)]^+$ leads to strong tetragonal distortions with a ground state that is either pure mid-spin or very close to pure mid-spin. While the spin states of the five-coordinate halide-ligated iron(III) complexes of the highly ruffled *meso*-tetraalkylporphyrins, Fe^{III}(trp)X (*r* = 1-ethylpropyl (1-EtPr) or isopropyl (^{i}Pr); X = F, Cl, Br,) are demonstrated to be high-spin in CD_2Cl_2 solution, the iodo and perchlorato complexes of these porphyrins exhibit strongly $S = {}^3/_2,{}^5/_2$ spin-admixed states, with mid-spin contributions of 87−96%.[98] On the basis of ^{13}C NMR hyperfine shifts, which are downfield for the *meso* carbons and upfield for pyrrole α-carbons, the unusual electronic configuration $d(xz,yz)^3d(xy)^1d(z^2)^1$ $\{S = {}^3/_2\ (d(xy))\}$ has been proposed for the $S = {}^3/_2,{}^5/_2$ admixture.[98] The six-coordinate complexes of these porphyrins, such as $[Fe^{III}(trp)(thf)_2]^+$, have virtually pure mid-spin ground states.[95,98] ^{13}C NMR shifts of the *meso* and pyrrole α-carbons of the six-coordinate complexes are also consistent with the $d(xz,yz)^3d(xy)^1d(z^2)^1$ electronic configuration.[70,98] The occurrence of short $Fe-N_p$ bond lengths in highly ruffled porphyrin derivatives was confirmed by the structure of $[Fe^{III}(t^iPrp)(thf)_2]ClO_4$.[95] The average $Fe-N_p$ bond distance of 1.967(12) Å observed in this compound is clearly smaller than that observed in the quantum mechanically $S = {}^3/_2,{}^5/_2$ spin-admixed bis(thf) derivatives $[Fe^{III}(oep)(thf)_2]ClO_4$ and $[Fe^{III}(tpp)(thf)_2]ClO_4$.[116,117] The *meso* carbons of $[Fe^{III}(t^iPrp)(thf)_2]ClO_4$ deviate by ca. 0.68 Å above and below the porphyrin core mean plane.[118]

2.1.3. X-ray Structural Studies on Spin-Admixed Ferric Porphyrin Complexes: Bond Distances, Out-of-Plane Displacements, and Porphyrin Conformation

As observed above, the d-electron distribution in the iron(III) porphyrin complexes having weak-field axial ligands and displaying a significant $S = {}^3/_2$ contribution to the $S = {}^3/_2,{}^5/_2$ admixed ground state differs from those in a pure high-spin state by increased occupation of the d(*xy*) orbital and a corresponding decrease in the $d(x^2-y^2)$ orbital in the direction of the equatorial pyrrole nitrogens. For both 5- and 6-coordinate complexes, the changes in the d-electron distribution are reflected in significantly smaller average $Fe-N_p$ bond lengths and, in 5-coordinate complexes, in smaller out-of-plane displacements Δ(core). In the strongly spin-admixed complexes, $Fe-N_p$ bond lengths are generally ≤2.00 Å, compared to >2.00 Å in pure high-spin complexes. In the 5-coordinate spin-admixed complexes, Δ(core) is generally <0.3 Å compared to >0.45 Å in high-spin complexes.[22,89,113,116,117,119−121] Similar observations have been reported for the six-coordinate iron(III) octaalkyl- and tetraarylporphyrins and weakly basic axial ligands.[63,65,66,68,88,113,122] In several pyridine-ligated six-coordinate iron(III) porphyrin $S = {}^3/_2,{}^5/_2$ spin-admixed compounds, the dihedral angle ϕ formed by the plane containing two opposite pyrrole nitrogens and the axial ligand mean plane is close to 0°.[66]

Similar properties were observed in complexes in which the porphyrin ligands are saddle shaped or ruffled. In the saddle-distorted five-coordinate $S = {}^3/_2,{}^5/_2$ spin-admixed complexes Fe^{III}(omtpp)Cl, Fe^{III}(oetpp)Cl (two crystalline forms), and Fe^{III}(dodecaphenylporphyrin)Cl (Fe^{III}(dpp)Cl), in which the mid-spin contributions are probably small, average $Fe-N_p$ bond distances are 2.034(9), 2.040(6), and 2.056 Å, respectively.[105,108,110] The average $Fe-N_p$ bond distance observed in the high-spin five-coordinate chloroiron(III) chiroporphyrin complex, Fe^{III}(tmcp)Cl, in which the porphyrin dianion (tmcp) is highly ruffled, is very similar to the values observed in Fe^{III}(oetpp)Cl and Fe^{III}(dpp)Cl.[115] However, as discussed above, five- and six-coordinate iron(III) complexes displaying an almost pure mid-spin state have been obtained by a combination of weak-field axial ligation and severe porphyrin saddling or ruffling. Considerable radial contraction takes place in such complexes. In the five-coordinate complex $Fe^{III}(oetpp)ClO_4$ the average $Fe-N_p$ bond distance is 1.963(7) Å.[111] In the six-coordinate species, $[Fe^{III}(tmcp)(EtOH)_2]^+$, $[Fe^{III}(tmcp)(EtOH)(H_2O)]^+$, $[Fe^{III}(t^iPrp)(thf)_2]^+$, $[Fe^{III}(omtpp)(4\text{-}CNpy)_2]^+$, and $[Fe^{III}(oetpp)(4\text{-}CNpy)_2]^+$, the $Fe-N_p$ bond lengths range from 1.950(5) to 1.978(7) Å.[85,104,118] The axial bond lengths are quite long, ranging from 2.173(5) to 2.272(4) Å in the chiroporphyrin complexes.[104]

The Fe−Cl bond distances in the five-coordinate chloroiron(III) complexes, Fe^{III}(omtpp)Cl, Fe^{III}(oetpp)Cl, Fe^{III}(netpp)Cl (*n* = 2, 4, 6), and Fe^{III}(dpp)Cl, in which the mid-spin contributions to the $S = {}^3/_2,{}^5/_2$ spin-admixed ground states are most probably small, are not significantly different from those of the tetraphenyl-, octaethyl-, and chiroporphyrin derivatives, Fe^{III}(tpp)Cl, Fe^{III}(oep)Cl, and Fe^{III}(tmcp)Cl. These Fe−Cl bond distances range from 2.031(5) to 2.056(4) Å in the β-pyrrole-substituted tetraphenylporphyrin complexes and from 2.192 to 2.243 Å in the complexes without β-pyrrole substituents.[105,108−110,113] However, in the mid-spin ($S = {}^3/_2$), six-coordinate bis(ethanol) and mixed ethanol−water chiroporphyrin complexes, $[Fe^{III}(tmcp)(EtOH)_2]ClO_4$ and $[Fe^{III}(tmcp)(EtOH)(H_2O)]ClO_4$, the axial Fe−O bond distances are quite long, ranging from 2.173(5) to 2.272(4) Å.[104] It has been shown that the $Fe-N_{ax}$ axial bond distances in the six-coordinate iron(III) porphyrin derivatives $[Fe^{III}(p)(L)_2]^+$ (p = omtpp, oetpp, and tc_6tpp), bonded axially to various pyridines and imidazoles,[123,124] increase as the spin state of the iron center changes from the low-spin state, $S = {}^1/_2$ (Fe−

$N_{ax} \sim 2.00$ Å), to the mid-spin state, $S = {}^3/_2$ (Fe−$N_{ax} \sim 2.2$ Å).[85]

Overall, the work on model porphyrin complexes indicates that both the saddle and ruffle distortions destabilize the iron $d(x^2-y^2)$ orbital and therefore stabilize the mid-spin state. However, as shown by the studies of five-coordinate iron(III) porphyrin complexes with moderately strong axial ligands, the nonplanar distortions do not destabilize the iron $d(x^2-y^2)$ orbital to the degree of causing significant $S = {}^3/_2,{}^5/_2$ spin admixture. In contrast, significant $S = {}^3/_2,{}^5/_2$ spin admixtures have been obtained by a combination of nonplanar distortions with weak axial ligands. Thus, the net effects of the saddle and ruffle distortions of the heme in the cytochromes c' cannot easily be predicted, since, according to the model mono(imidazole) complexes of Nakamura et al.,[61,62] the axial imidazole-His ligand probably has moderately weak donor properties.

2.1.4. X-ray Absorption Spectroscopy

X-ray absorption spectroscopy (XAS) at the iron K-edge has been extensively applied to investigate the environment of iron in model and biological complexes of porphyrins.[125−127] Bond lengths and coordination numbers for a large number of complexes have been determined from the EXAFS portion of the XAS spectrum. There have been no systematic investigations published on $S = {}^3/_2,{}^5/_2$ spin-admixed systems. Pre-K-edge absorption features in the near-edge (XANES) region of the spectrum, representing excitation of 1s electrons to low-lying unoccupied orbitals with iron character, have received only limited attention by investigators. However, these transitions are highly sensitive indicators of iron site symmetry, valence, and spin state. The pre-K-edge features of iron porphyrins represent low-intensity 1s → 3d excitations arising through quadrupolar mechanisms.[127−129] Dipolar mechanisms can significantly enhance transition intensities through 3d−4p orbital mixing resulting from distortions that cause loss of inversion symmetry and additionally from ligand-induced 3d orbital destabilization, which results in closer energy matching between 3d and 4p orbitals. Recent investigation of a series of iron(III) porphyrin complexes[130] indicates that the energies and integrated intensities of the pre-edge transitions correlate with spin state. The pre-edge features of the bis(methanol) complexes of iron(III) tetramesityl chlorin,[131] porpholactone,[132] and porphyrin triflates can be resolved into two low-intensity features. Normalized to the edge jump, the total integrated intensities range between 7.4 and 9.5, only slightly exceeding the intensities expected for purely quadrupolar mechanisms. The absence of dipolar enhancement is consistent with the location of the iron in or near the porphyrin mean plane, conferring inversion symmetry. It is interesting to note that hyperfine structure observed at the pre-edge represents splitting of the 3d manifold. Based on the calculated energies of the allowed transitions, the lower energy peak is assigned to the mean of the 1s → $3d(z^2)$, $3d(\pi)$, and $3d(xy)$ transitions, and the higher energy peak to the 1s → $3d(x^2-y^2)$ transition. Weak coordination of the methanol ligands stabilizes the $d(z^2)$ orbital and also strongly enhances in-plane bonding, which, in turn, destabilizes the $d(x^2-y^2)$ atomic orbital. The net effect of these changes allows resolution of the 1s → $3d(x^2-y^2)$ transition and induces partial depopulation of $3d(x^2-y^2)$ to give the $S = {}^3/_2,{}^5/_3$ spin-state admixture, confirmed by solution EPR transitions at $g_\perp \cong 5.6-5.7$ (estimated from the zero crossing of the low-field line). In the absence of coordinating solvent, the triflate complexes are five-coordinate. Single pre-edge peaks for the triflate complexes of ferric tetramesitylporphyrin and the tetramesitylporpholactone have normalized, integrated intensities of 16.6 and 19.3, respectively, indicating some enhancement through 3d−4p mixing. Such mixing is in accord with loss of inversion symmetry through triflate coordination. Enhanced axial coordination by triflate predicts a decreased $S = {}^3/_2$ contribution to spin admixture, supported by values of $g_\perp \geq 5.8$ found in the EPR spectra. The predominance of a single pre-edge peak is in accord with the reported z-axis selective d−p mixing predicted for square pyramidal complexes and the narrow energy range expected for 1s → 3d transitions of complexes in predominantly high-spin states. The pre-edge spectra of hydroxoiron(III) tetramesitylporphyrin and chloroiron(III) tetraphenylporphyrin complexes, assigned pure $S = {}^5/_2$ spin states based on $g_\perp$ values of 5.9, are qualitatively similar to those of the five-coordinate triflates. However, integrated intensities of 30.7 and 32.7, respectively, show substantial 3d−4p mixing, in line with expected strong axial coordination and large displacement of iron from the porphyrin mean plane. An integrated intensity of 19.8 was observed for the single pre-edge feature of chloroiron(III) tetramesitylporphyrin. This value lies between those obtained for the strongly spin-admixed bis(methanol) complexes of the iron(III) triflates and those for the high-spin complexes and suggests a small $S = {}^3/_2$ admixture, although $g_\perp = 5.9$ (estimated from the zero crossing) is close to that of a pure high-spin state. As the pre-edge peak is highly sensitive to ligand field strength, this result suggests that the field strength ordering Cl ∼ OH proposed in the magnetochemical series[60] might be refined to Cl < OH.

2.1.5. Electronic Spectra, Resonance Raman Spectroscopy, Magnetic Circular Dichroism, and Mössbauer Spectroscopy of Model Compounds

The UV−visible absorption spectra of the five-coordinate spin-admixed iron(III) porphyrin complexes with one weakly basic axial ligand have been recorded and found to show strong similarities to those of known high-spin iron(III) porphyrin complexes. In acetone, the absorption spectrum of $Fe^{III}(oep)ClO_4$ shows bands at 392 (Soret), 497, and 628 nm. In contrast, in dichloromethane the bands appear at 380 (Soret), 500, and 633 nm, with the Soret band being broadened and slightly split.[86,87,119] In dichloromethane at 25 °C, the optical spectra of $[Fe^{III}(tmp)L]ClO_4$ (L = ImH, 2-RImH; R = Me, Et, ^{i}Pr, 1-EtPr, ^{t}Bu) display four bands appearing around 413, 511, 570, and 691 nm.[62] The absorption spectra of $Fe^{III}(tpp)ClO_4$ and $Fe^{III}(tpp)Cl$ have also been compared in toluene solution and found to be similar.[22]

Mixed-spin iron(III) complexes have been studied by resonance Raman spectroscopy.[133] Although the B_{1g} skeletal mode ν_{10} of the perchloratoiron(III) octaethylporphyrin complex $Fe^{III}(oep)ClO_4$ was observed at an anomalously high frequency of 1645 cm^{-1}, there did not appear to be a correlation between ν_{10} and magnetic moment, leading to the conclusion that this band was not an appropriate marker for spin state.[133]

Magnetic circular dichroism (MCD) spectra of five- and six-coordinate mixed-spin ferric octaethylporphyrin complexes, $Fe^{III}(oep)X$ (X = ClO_4^-, $SO_3CF_3^-$, SbF_6^-) and $[Fe^{III}(oep)(3,5\text{-}Cl_2\text{-}py)]ClO_4$, have been investigated in the Soret−visible (300−700 nm) and near-IR (700−2000 nm) regions.[67] MCD spectra of the iron(III) octaethylporphyrin

model complexes showed distinctive features in the NIR range and displayed characteristics similar to those of ferricytochromes *c′* from *Ach. xylosoxidans* NCIMB 11015. This result provides evidence for the utility of MCD spectroscopy, especially in the near-IR region, as a probe of spin state in ferric heme systems.[67]

A large number of $S = {}^3/_2,{}^5/_2$ spin-admixed iron(III) porphyrin model complexes have been studied by Mössbauer spectroscopy.[89,134] The spectra of such complexes are in general characterized by narrow-line symmetric doublets at all temperatures. In general, no gross line broadenings or resolution of separate quadrupole doublets is observed. These observations confirm the presence of only a single spin state in these compounds rather than a thermal equilibrium between unperturbed high-spin and low-spin states. Table 1 shows that the model complexes are characterized by large quadrupole splittings (ΔE_Q). Variation of ΔE_Q between compounds undoubtedly reflects varying quartet/sextet ($A_2{}^4$/$A_1{}^6$) ratios in the spin admixtures. The origin of the temperature dependence of ΔE_Q (Table 1) is not yet clear. Relaxation effects, thermal population of higher energy orbitals, and dynamic admixtures at different temperatures have been suggested as possible explanations.[14,134,135] Isomer shifts of spin-admixed complexes (Table 1) differ little from those of high-spin and low-spin ferric porphyrins. No relation is apparent between the Mössbauer parameters and the position of iron relative to the porphyrin core mean plane, with both five- and six-coordinate complexes having comparable δ and ΔE_Q values.[134]

2.2. Mono(imidazole) Iron(III) Porphyrin Complexes as Models for Cytochromes *c′*

Five-coordinate mono(imidazole) iron(III) porphyrin complexes have been of interest as models for the investigation of the properties of a variety of proteins containing 5-coordinate hemes with histidine axial ligands. Initial efforts to study (mono)imidazole complexes were frustrated by the tendency of imidazoles to form bis-adducts.[136] In the earliest report of 5-coordination of ferric porphyrins with imidazoles, these difficulties were overcome by titrating the ferric tpp complex of the weakly coordinating axial ligand, SbF_6^- in toluene with imidazole or 4-methylimidazole to give [Fe^{III}(tpp)(L)]SbF_6 (L = ImH, 4-MeImH).[137] Treatment of Fe^{III}(tpp)Cl or Fe^{III}(tpp)SbF_6 in toluene with the potassium imidazolate salts in a low ligand-to-porphyrin ratio (~2:1) yielded the corresponding mono(imidazolate) complexes. The 5-coordinated imidazole and imidazolate complexes were characterized as high-spin by comparison of their electronic spectra with those of a large number of ferric tetraphenylporphyrin complexes known to be high-spin. The imidazolate complexes were also determined to be high-spin by EPR spectroscopy.[137] However, assignments based on electronic spectra must be regarded with some caution. As described in detail in section 3.5 (Optical Spectroscopy), UV−vis spectra of iron(III) porphyrin complexes displaying a quantum mechanical spin admixture in the ground state are very similar to those in which the ground state is purely high-spin. In a study published contemporaneously with the work of Maltempo, the microcrystalline species obtained after treatment of a suspension of protohemin with imidazole in benzene was characterized as high-spin, based on a magnetic moment of 5.75 μ_B at 300 K and the Mössbauer parameters $\Delta E_Q = 0.783$ mm s^{-1} and $\delta = 0.52$ mm s^{-1} at 77 K.[138] Analytical data unequivocally establishing the compound as a monoimidazole complex were not provided. Subsequently, the oep complex, [Fe^{III}(oep)(2-MeImH)]ClO_4, has been crystallized from chloroform or dibromomethane by mixing equimolar quantities of 2-MeImH and Fe^{III}(oep)ClO_4. Structures of the chloroform and dibromomethane monosolvates have been determined by X-ray crystallography,[94,139] and in addition, the magnetic susceptibility and Mössbauer spectra of the chloroform solvate have been investigated in the solid state. As discussed in section 2.1.3, the displacement of iron from the porphyrin mean plane, Δ(core), and the Fe−N_p bond distances of [Fe^{III}(oep)(2-MeImH)]$^+$ lie between those of high-spin and $S = {}^3/_2,{}^5/_2$ spin-admixed ferric porphyrin model complexes. The magnetic moment μ_{eff} of [Fe(oep)(2-MeImH)]$^+$ and its temperature dependence are consistent with a high-spin state. However, a fit of the temperature-dependent susceptibility data required inclusion of weak antiferromagnetic interactions between face-to-face dimers in the solid state.[94] Mössbauer data were obtained in both the presence and absence of an applied magnetic field at 4.2 K. In zero field, a symmetric quadrupole doublet was observed with $\Delta E_Q = 1.39$ mm s^{-1} and an isomer shift δ of 0.40 mm s^{-1}. The value of the isomer shift was that expected for a high-spin ferric porphyrin complex. The quadrupole splitting was slightly larger than those observed for known high-spin, 5-coordinate ferric porphyrins with anionic ligands, but it was smaller than the quadrupole splittings generally observed for $S = {}^3/_2,{}^5/_2$ spin-admixed species with an appreciable $S = {}^3/_2$ contribution (Table 1). At neutral to acidic pH and low temperature, the quadrupole splitting (Table 11) of *Rs. rubrum* ferricytochrome *c′*, classified as predominantly high-spin, is somewhat larger than that of [Fe^{III}(oep)(2-MeImH)]$^+$. The weak antiferromagnetic interactions excepted, [Fe^{III}(oep)(2-MeImH)]ClO_4 appears, on the whole, to share the quadrupole splitting, temperature-dependence of magnetic behavior, and structural characteristics of the group of ferricytochromes *c′* that are considered to be predominantly high-spin.

In an investigation specifically directed towards modeling the spin states of the cytochromes *c′*, mono(imidazole) iron(III) porphyrin complexes were prepared in solution by addition of 2-alkyl- and 5-methyl-substituted imidazoles to iron(III) *meso*-tetramesitylporphyrin perchlorate, [Fe^{III}(tmp)]ClO_4, in methylene-d_2-chloride.[61] Effects of 2-alkyl substituents of increasing steric bulk, such as Me, Et, and ^{i}Pr, on spin state were determined. A spin-admixed ground state for the complexes was established by ^{1}H and ^{13}C NMR and EPR spectra. Consistent with the admixed spin state, a solution magnetic moment of 5.0 μ_B at 25 °C was reported for the 2-MeImH complex, [Fe^{III}(tmp)(2-MeImH)]ClO_4. Overall, the mid-spin contribution to the spin-state admixture was much smaller for the mono(imidazole) complexes than for Fe^{III}(tmp)ClO_4. However, the mid-spin contribution increased with the steric bulk of the 2-substituent of the axial imidazole ligand.[61] In a later publication, these authors extended the series of mono-imidazole complexes [Fe^{III}(tmp)L]ClO_4 to systematically investigate the factors affecting spin state. Complexes with L = HIm, 2-RImH (R = Me, Et, ^{i}Pr, 1-EtPr, ^{t}Bu), 1-Me-2-RIm (R = H, Me, Et, and ^{i}Pr), 4,5-Cl_2ImH, BzImH, 2-MeBzImH, 1,2-Me_2BzIm, and 5,6-Me_2BzImH were formed by treating Fe^{III}(tmp)ClO_4 with the appropriate base in methylene chloride.[62] The series of complexes were characterized in solution by UV−visible and ^{1}H and ^{13}C NMR spectroscopy and in frozen solution by EPR spectroscopy. While the ground states contained an $S = {}^3/_2,{}^5/_2$

quantum mechanical admixture, the magnitude of the $S = {}^3/_2$ component varied in a complex way with different axial ligands. Using ^{1}H NMR shifts of the pyrrole protons as a probe for the proportion of mid-spin state, the 2-alkyl imidazole complexes were ordered according to increasing $S = {}^3/_2$ contribution: 2-^{t}BuImH < 2-(1-EtPr)ImH < 2-MeImH < 2-EtImH < 5-MeImH = 2-^{i}PrImH. Although the 2-Me-, 2-Et-, and 2-^{i}Pr-substituted mono-alkyl(imidazole) complexes are ordered according to steric size, the two bulkiest substituents showed the least mid-spin contribution; in fact, the 2-^{t}BuImH complex was classified as high-spin using the criteria of pyrrole proton hyperfine shift and Curie law behavior. Unsubstituted imidazole, ImH, however, had a larger $S = {}^3/_2$ spin component in the ground-state admixture than any of the mono-alkyl(imidazole) complexes. The mid-spin contribution to the spin-state admixture of the dialkyl-substituted imidazoles, 1,2-diMeIm, 1-Me-2-EtIm, and 1-Me-2-^{i}PrIm, increases with the increasing steric bulk of the substituents at C-2, and all the complexes in this series contain a larger $S = {}^3/_2$ component than the mono-alkyl-substituted imidazoles. In order of increasing mid-spin contribution to the $S = {}^3/_2,{}^5/_2$ spin-admixed ground state, the mono(benzimidazole)complexes ranked as follows: 5,6-diMeBzIm < BzIm < 2-MeBzIm < 1,2-diMeBzIM. Overall, the $S = {}^3/_2$ spin contribution to the spin-state admixture in mono(benzimidazole) complexes is midway between those of the mono- and di-alkyl-substituted mono(imidazole) complexes. Coordination of the electron-deficient 4,5-dichloroimidazole, 4,5-Cl_2ImH, yielded a ground state with the largest $S = {}^3/_2$ contribution (68%) of all the mono(imidazole) complexes.[62] Using ^{13}C NMR shifts as a probe of spin-state admixture, the authors found that pyrrole α and β carbon shifts correlated closely with the pyrrole proton shifts (correlation coefficients 0.98 and 0.99, respectively), whereas correlation between the *meso* carbon and pyrrole proton shifts was poor.

The authors rationalize the global effect of bulky mono(imidazole) ligands as inducing an $S = {}^3/_2,{}^5/_2$ admixture in the five-coordinate $[Fe^{III}(tmp)L]^+$ complexes by weakening axial ligation through unfavorable ligand−porphyrin steric interactions. An increasing magnitude of $S = {}^3/_2$ contribution for the 2-alkyl substituents Me < Et < ^{i}Pr parallels an increase in steric bulk and was ascribed to an off-axis tilt resulting from increasingly unfavorable steric interactions between the alkyl groups and the mesityl *o*-methyls. As discussed above, in the absence of a crystal structure, the substantial *decrease* in $S = {}^3/_2$ contribution to the admixture in the case of the very bulky 2-^{t}Bu and 2-(1-EtPr) substituents was attributed to movement of iron out of the plane of the pyrrole nitrogens to avoid too pronounced a lengthening of the Fe−N_{ax} bond caused by severe steric interactions of these substituents with the porphyrin. However, the authors might also have considered a combination of saddling and ruffling of the porphyrin core with attendant rotating of the *meso* mesityl groups into the porphyrin plane in response to steric strain, allowing closer approach of the imidazole to iron. This possibility is suggested by the observation that the chemical shift of the mesityl *m*-H signal is significantly upfield from the position expected for a high-spin complex.

A reason for the large $S = {}^3/_2$ component in the unsubstituted parent (mono)imidazole complex $Fe^{III}(tmp)ImH^+$ is not evident from the hypothesis offered to explain the ordering of the mid-spin contributions in alkylated mono(imidazole) complexes, and this problem was not considered by the authors. The generally larger $S = {}^3/_2$ contribution to the spin admixture in mono(benzimidazole) complexes was not considered either but could be explained by a combination of increased steric hindrance and decreased ligand field strength resulting from fusion of the benzo ring. The authors reasonably attribute the large mid-spin component of the 4,5-Cl_2ImH complex to decreased ligand field strength resulting from the electron-withdrawing effect of the chloro substituents.

Effective magnetic moments were determined by the Evans method in CH_2Cl_2 solution at 25 °C. Because of difficulties with contamination by bis(imidazole) adducts and/or uncomplexed $[Fe^{III}(tmp)]ClO_4$, only three solution moments were reported: 5.9 μ_B for $[Fe^{III}(tmp)2$-^{t}BuImH$]ClO_4$, 5.2 μ_B for $[Fe^{III}(tmp)5,6$-Me_2BzImH$]ClO_4$, and 5.0 μ_B for $[Fe^{III}(tmp)(2$-MeImH$)]ClO_4$. The ordering of these moments parallels that based on ^{1}H and ^{13}C NMR shifts. The $S = {}^3/_2$ contributions (% $S = {}^3/_2$) to the $S = {}^3/_2,{}^5/_2$ admixture estimated by the $g^{eff}{}_\perp$ values {% $S = {}^3/_2 = 100(3 - g^{eff}{}_\perp/2)$} observed in the EPR spectra of frozen methylene chloride solutions at 4.2 K were significantly smaller than those determined by NMR spectrometry. An exception was the case of the 2-^{t}BuImH complex, which showed little or no admixture by either technique.

Unfortunately, the authors did not report an estimate for the 4,5-Cl_2ImH complex, which had the largest mid-spin component of all the mono(imidazole) complexes. All other admixtures contained between 5 and 15% $S = {}^3/_2$ by EPR. The authors ascribe the discrepancy between NMR and EPR estimates of mid-spin contribution to the effect of temperature. At low temperature, they suggest that the axial bond will contract, increasing ligand field strength and inducing a spin transition. They cite the contraction of the Fe^{III}−N(py) axial bond distance with decreasing temperature in the hexacoordinate complex $[Fe^{III}(oep)py_2]ClO_4$ to support this hypothesis. Nevertheless, in spin-admixed complexes with a quartet ground state, the opposing tendency to populate the ground state with decreasing temperature should also be considered, and thus the net effect of temperature may not be uniform between complexes.

Solvent polarity was reported to affect spin state. Addition of increasing amounts of the polar solvents methanol and acetonitrile to a methylene chloride solution of $[Fe^{III}(tmp)$-$(2$-MeImH$)]ClO_4$ increased the $S = {}^3/_2$ contribution, and addition of increasing amounts of the nonpolar solvent benzene decreased the $S = {}^3/_2$ contribution.[62] Methanol and acetonitrile compete with 2-MeImH for axial coordination sites. Although both are weaker field ligands than 2-MeImH, they occupy an increasing proportion of axial sites with increasing concentration, effectively lowering the ligand field strength experienced by iron and increasing the proportion of mid-spin state. Addition of benzene has the opposite effect because the positive charge on iron is destabilized as the polarity of the bulk solvent decreases, resulting in tighter coordination of 2-MeImH.

Reactions $[Fe^{III}(tpp)]ClO_4$ with various imidazoles have been examined by ^{1}H NMR in methylene-d_2-chloride solution.[140] Depending on the ligand and relative ligand/$[Fe^{III}$-$(tpp)]ClO_4$ ratio, variable proportions of μ-oxo dimer and mono- and bis(imidazole) complexes were detected. Formation of μ-oxo dimers was shown to occur when the imidazoles functioned as bases to abstract protons from coordinated water present in trace amounts in methylene-d_2-chloride. In the presence of sterically demanding 1,2-

Table 3. Crystal Structures of Cytochromes *c′*

bacterial source	PDB code	resolution (Å)	temp (K)
Rs. molischianum[a]	2CCY	1.67	ambient*[b]
Rp. palustris[c]	1A7V	2.3	ambient*[b]
Rs. rubrum[d]		2.8	283
Ch. vinosum[e]	1BBH	1.8	ambient*[b]
Ach. denitrificans NCTC 8582[f,g]	1CGN	2.15	ambient*[b]
Ach. xylosoxidans NCIMB 11015[f]	1CGO	1.8	ambient*[b]
Rb. capsulatus (strain M110, form B)[h]	1CPQ	1.72	ambient*[b]
R. gelatinosus[i]	1JAF	2.5	ambient
Ach. xylosoxidans NCIMB 11015[j]	1E83	2.05	100
Rb. sphaeroides[k]	1GQA	1.8	ambient

[a] Reference 153. [b] Ambient* indicates that, where crystallographic data collection temperatures were not specified, they are assumed to have been collected at or near ambient temperature. [c] Reference 25. [d] Reference 220. [e] Reference 28. [f] Reference 141. [g] Isostructural with *Ach. xylosoxidans* cytochrome *c′*. [h] Reference 148. [i] Reference 152. [j] Reference 143 and 144. [k] Reference 149.

dialkyl imidazoles and 2-alkyl and 2-aryl benzimidazoles, μ-oxo dimer was the only product observed. While mono(imidazole) complexes were detected with less sterically demanding ligands, this system was not examined as a model for spin states observed in the cytochromes *c′*.[140]

3. Cytochromes c′

3.1. Crystal Structures

Crystal structures of the five-coordinate ferricytochromes *c′* listed in Table 3 have been published. As indicated in this table, the structure of the cytochrome *c′* from *Ach. denitrificans* (NCTC 8582) is isomorphous and essentially identical to that of *Ach. xylosoxidans*.[141] Consequently, only the structure of the latter protein will be discussed here. In addition, as indicated in Table 3, where crystallographic data collection temperatures were not specified, they are assumed to have been collected at or near ambient temperature for the reports. Several structures of cytochromes *c′* bound to small molecule ligands have also been determined to study the energetics, mechanism, and structural rearrangements accompanying occupation of the sixth axial position. The ambient-temperature structure of the *n*-butylisocyanide adduct of ferrocytochrome *c′* from *Rb. capsulatus* (2.4 Å resolution, PDB accession code 1NBB) has been determined,[142] and the structures of the NO (1.35 Å resolution, PDB accession code 1E85) and CO (1.95 Å resolution, PDB accession code 1E86) adducts of the ferrocytochrome *c′* from *Ach. xylosoxidans* have been determined, at 100 K.[143,144]

An NMR-validated structural model of the oxidized state of a cytochrome *c′* homologue, cytochrome c_{556} from *Rp. palustris*, has been published recently.[145] In contrast to the ferricytochromes *c′*, which are five coordinate with a protoheme covalently bound to two cysteine residues and an adjacent histidine serving as the fifth ligand, the cytochromes c_{554} and c_{556} homologues are six-coordinate with a methionine residue as the sixth ligand.[146,147]

As described in section 1.1, these proteins, with the exception of cytochrome *c′* from *Rp. palustris*, are usually isolated as soluble homodimers, composed of two identical subunits of approximately 130 residues containing a *c*-type heme. However, the crystals of the cytochromes *c′* from *Rb. capsulatus* and *Ach. xylosoxidans* and the isostructural protein from *Ach. denitrificans* contain only one independent subunit (monomer) per asymmetric unit whereas those from *Ch. vinosum*, *Rb. sphaeroides*, *Rs. molischianum*, *Rs. rubrum*, and *R. gelatinosus* contain one independent dimer or two subunits.

The subunits or monomers show a similar folding pattern, constituted by a classic four-helix bundle, determined by the packing of hydrophobic side chains around the heme group. However, the modes of association in the crystals of these subunits have led to a classification of the resulting dimers as at least two types, types 1 and 2.[25,148,149] This aspect of the protein structure lies outside of the scope of this review; we shall not analyze the associations and types, but limit our description to the results related to the heme geometries and direct environment.

The crystal structural studies confirm the presence of the *c*-type heme protein binding sequence Cys−X−X−Cys−His and heme attachment near the C-terminal region of the protein. In all known cytochrome *c′* structures, the iron atoms are five-coordinate, bonded to the heme unit and axially to the imidazole ring of the His residue in the cytochrome *c* binding sequence. Fe−N_p bond distances range from 1.93 to 2.17 Å, with an overall average bond distance of 2.02 Å, which is only slightly smaller than the mean value of 2.04 Å corresponding to the Fe−N_p bond distance in the high-spin five-coordinate model complex, $[Fe^{III}(oep)(2\text{-MeImH})]^+$. The Fe−N(His) axial bond lengths vary between 1.93 and 2.18 Å, with an overall average distance of 1.98 Å that is clearly smaller than the Fe−N(2-MeImH) bond distance of 2.07 Å observed in the model complex, where there is an unfavorable steric interaction between the 2-methyl group and the porphyrin ring. As expected, the five-coordinate iron atoms of the cytochrome *c′* structures are displaced out of the four pyrrole nitrogen ($4N_p$) and porphyrin core (P(core)) mean planes toward the proximal His ligand. The $4N_p$ and P(core) mean planes are not generally superimposed; thus, most heme units are slightly domed.

In addition, the heme units show some saddle and ruffle distortions in almost all ferricytochrome *c′* structures. These saddle and ruffle distortions are indicated, respectively, by alternate displacement of the β-pyrrole (ΔC_β) and *meso* carbon (ΔC_m) atoms above and below the heme core mean plane. The mean values of the average displacements ΔC_β range from 0.06 to 0.14 Å. The ΔC_m values, which vary between 0.02 and 0.17 Å, indicate that ruffling of the heme units can become significant. Saddle and ruffle distortions of the prosthetic groups observed in the crystal structures of the ferricytochromes *c′* from *Ch. vinosum*, *Rb. sphaeroides*, *Ach. xylosoxidans* (NCIMB 11015), and *Rs. molischianum* have also been detected and characterized by the normal coordinate structural decomposition method (NSD) (see below).[150,151]

The axial histidine ligands are exposed to the solvent, and well ordered water molecules are often present in the proximal cavities of the proteins. Thus, the imidazole-His $N_\delta H$ (referred to as ND1H in the protein structures) is hydrogen bonded to a solvent molecule in the ferricytochromes from *Rp. palustris*, *Rb. capsulatus*, and *Ach. xylosoxidans* and in one subunit of the *Ch. vinosum* protein. In these proteins the $N_\delta H$- - -OH_2 distances range from 2.81 to 2.95 Å.[25,28,143,148] Ordered water molecules are also present in the structures of the ferricytochromes *c′* from *Rhodocyclus gelatinosus* (*R. gelatinosus*),[152] *Rs. molischianum*,[153] and *Rb. sphaeroides*.[149] However, the corresponding $N_\delta H$—OH_2 distances are larger than 3.25 Å, so that these bonds must

be very weak or absent. One subunit (chain A) of dimeric ferricytochrome c' from *Ch. vinosum* contains no ordered water molecule in the proximal cavity.[28]

Porphyrin model compound studies have shown that a hydrogen bond between ND1H (= $N_\delta H$) of an imidazole axial ligand and a basic residue or a water molecule increases the strength of the Fe−N(ImH) axial bond.[136,154] Similar observations have been made in heme proteins such as metMb, and a series of peroxidases.[155,156] *g* values and redox potentials were demonstrated to be a function of the field strength of the proximal histidine, which in turn was correlated with the $N_\delta H$ hydrogen bond strength measured by the $N_\delta H$ NMR hyperfine shift.[155]

It has been suggested that in heme proteins the ligand field strength of the axial histidine is largely determined by the strength of the hydrogen bond formed by the proximal histidine $N_\delta H$ and a neighboring protein group or water molecule.[155a] Thus, the hydrogen bonds of the $N_\delta H$- - -OH_2 type which are often present in the cytochromes c' could influence the axial field of the heme iron and therefore the quartet/sextet ($A_2{}^4/A_1{}^6$) ratio of this atom.[157] However, as observed above, in the known ferricytochromes c' X-ray structures, the corresponding $N_\delta H$- - -OH_2 distances range from 2.81 to 3.25 Å and no correlation could be established between these distances and the $A_2{}^4/A_1{}^6$ ratio determined by EPR spectroscopy.

The electrostatic environment of the axial ligand may also play a role in mediating the strength of the Fe−N(His) axial bond and has been cited as a factor in the activity of mutagenized peroxidases and globins as well as in the behavior of peroxidases and cytochromes P450.[156] Cation−π-electron interactions occur often within a protein between metal cations or protonated side chains of Arg or Lys residues and classical aromatic side chains of residues such as Phe, Tyr, and Trp.[158,159] The imidazole side chain of a His (ImH-His) residue can also participate in cation−π interactions, either as a π-system or, when protonated, as a cation.[159] Coordinated to a metal, the ImH-His remains a π-system and can, in principle, participate in cation−π interactions. It has also been suggested that the aromatic rings of Phe, Tyr, and Trp can act as hydrogen bond acceptors.[160−163] The π-system of the coordinated ImH-His should behave in a similar manner. As suggested by Dobbs *et al.*,[141] cation−π interactions and amino−aromatic hydrogen bonding of a positively charged group with the ImH-His axial ligand stabilize the negative charge on this ligand and, consequently, may reduce its ability to donate electrons to iron. Thus, guanidinium cation−π interactions or hydrogen bonding would reduce the field strength of the ImH-His axial ligand relative to an unperturbed ligand, a situation shown to lead to quantum mechanical $S = {}^3/_2,{}^5/_2$ spin-state admixtures.

The known amino acid sequences of cytochromes c'[164] indicate that a basic residue, either Arg or Lys, is present in the helix containing the cytochrome *c* binding sequence Cys−X−X−Cys−His, four residues toward the C-terminal from His. (With the availability of rapid DNA sequencing techniques, a number of bacterial genomes have been sequenced in which cytochrome c' proteins have been identified. Only protein sequences have been reported with no additional data. For this reason, these proteins are not addressed further in this review, other than to note that the motif Cys−X−X−Cys−His−X−X−X−(Arg/Lys) is scrupulously conserved. Accession numbers in the Swiss-Prot/TrEMBL database (accessible through www.expasy.org) are Q2CWD7, Q2W9CO, Q480K8, Q4FLB0, Q5LQ02, and Q8EBS9.) We classify cytochromes c' in which the basic group is Arg as group (i) proteins. These include proteins isolated from *Ch. vinosum*, *Rp. palustris*, *Rb. capsulatus*, *Ach. xylosoxidans* (NCIMB 11015), *Rb. sphaeroides*, *Rs. tenuis*, *Rs. photometricum*, *Rs. salexigens*, *Rhodopseudomonas* sp. strain TJ12, and *Paracoccus* sp. We classify the cytochromes c' in which the basic group is Lys as group (ii) proteins. These include proteins from *Rs. molischianum*, *Rs. rubrum*, *Rc. gelatinosus*, and *Rs. fulvum*. At weakly acidic to neutral pH, the guanidine-Arg and amino-Lys side chains are most probably protonated, and in the available crystal structures, the positively charged moieties are located in close proximity to the imidazole-His ring of the axial ligand. In the group (i) proteins from *Ch. vinosum* and *Rb. sphaeroides*, the guanidinium of the Arg side chain is stacked against the His-imidazole ring. In the two independent molecules present in the asymmetric unit of the crystals of these proteins, the interplanar angles α between the mean planes of the guanidinium-Arg and the imidazole-His moieties are 18.4°, 12.0° (*Ch. vinosum*) and 9.8°, 8.7° (*Rb. sphaeroides*).[28,149] The distances *D* between the guanidinium central carbon CZ and the centroid of the imidazole-His ring [D = CZ-(guanidinium-Arg)- - -centroid(ImH−His)] are 3.54, 3.64 Å (*Ch. vinosum*) and 3.51, 3.64 Å (*Rb. sphaeroides*).[28,149] These values of α and *D* indicate that the guanidinium-Arg cations are stacked in π fashion against the imidazole ring, making energetically favorable cation−π contacts.[163]

In contrast, in the ferricytochromes c' from *Rp. palustris*, *Ach. xylosoxidans*, and *Rb. capsulatus*, the values of the interplanar angle α are 34.7°, 45.2° (*Rp. palustris*), 53.6° (*Ach. xylosoxidans*), and 70.4° (*Rb. capsulatus*).[25,141,148] In these proteins, the values observed for α are larger than 30°, indicating no π-stacking between the guanidinium-Arg cation and the imidazole-His ring.[163] However, one of the guanidinium-Arg NH groups lies over the axial imidazole ring at distances of 3.56, 3.79 Å (*Rp. palustris*), 3.66 Å (*Ach. xylosoxidans*), and 3.79 Å (*Rb. capsulatus*) from the ImH-His centroid. These distances are compatible with weak amino−aromatic hydrogen bonds.[160,162]

A reorientation of the guanidinium-Arg mean plane takes place relative to the imidazole-His mean plane when the crystals are cooled from ambient temperature to 100 K. In the 100 K structure of the ferricytochrome c' of *Ach. xylosoxidans*, the interplanar angle α increases to 78.1° from 53.6° at ambient temperature.[143] Moreover, the distance between the guanidinium-Arg NH lying over the ImH-His ring and the ImH-His centroid increases significantly from 3.66 to 3.79 Å. Thus, cooling to 100 K appears to reduce the interaction between the guanidinium-Arg moiety and the imidazole-His axial ligand in this protein. The significance of the change as reflected in the electronic parameters of *Ach. xylosoxidans* has not been explored. *Ach. xylosoxidans* belongs to the group of cytochromes c' that is predominantly high-spin by all measurements, suggesting that the structural rearrangement does not have an important impact on the spin state of this protein. Nevertheless, the presence of effects of temperature on structure in the immediate environment of the heme suggests that the impact on spin state could be consequential for other cytochrome c' proteins and that subtle structural changes need to be considered in comparing spin-state assignments obtained by various techniques under different conditions.

At weakly acidic to neutral pH, the amino side chain of the Lys residue in the group (ii) proteins is also protonated and the corresponding ammonium cation is located near the imidazole-His ring of the axial ligand. In the ferricytochromes *c′* from *R. gelatinosus* and *Rs. molischianum*, the Lys ϵ-ammonium is bent away from the axial imidazole-His ring plane, and the distances between ϵ-nitrogen NZ and the centroid of imidazole-His in the two molecules of the asymmetric unit are 5.61, 5.60 Å and 5.63, 5.82 Å, respectively.[152,153] However, the C_ϵ (CE) carbon of cationic Lys bears a substantial positive charge, so that CE tends to be positioned closer to aromatic rings than NZ when cation$-\pi$ interactions with aromatic residues are present. [159] Consistent with this picture, the distances between CE and the centroid of the imidazole-His axial ligand are 4.41, 4.39 Å (*R. gelatinosus*) and 4.87, 5.23 Å (*Rs. molischianum*).[152,153]

Analysis of the crystallographic data shows that strong guanidinium-Arg- - -imidazole-His interactions are probably present in the ferricytochromes *c′* from *Ch. vinosum* and *Rb. sphaeroides*. Assuming that such interactions reduce the axial field of the ImH-His ligand,[141] these two proteins would be subject to the greatest effect. This seems to be borne out in an NMR study by La Mar *et al*.[16] of the *Ch. vinosum* ferricytochrome *c′* along with other reported spectroscopic data, which suggest that this protein does indeed contain an appreciable spin-state admixture at acidic to neutral pH and ambient temperature. The spin state of the protein from *Rb. sphaeroides* has recently been studied by ENDOR and EPR at 15 K.[165] This study has determined that *Rb. sphaeroides* contains a significant $S = {}^3/_2$ component, in accord with expectation based on the imidazole-His- - -guanidinium-Arg π-stacking. Unfortunately, there are no data available on *Rb. sphaeroides* that have a bearing on spin state in solution at physiological pH and ambient temperature. The NMR study of La Mar *et al*.[16] further indicates that the heme iron is in the high-spin state at ambient temperature in the group (i) ferricytochrome *c′* from *Rp. palustris* and the group (ii) proteins from *Rs. molischianum*, *R. gelatinosus*, and *Rs. rubrum*. Our structural analyses are compatible with these results, since they indicate that the interactions of the guanidinium-Arg and ammonium-Lys cations with the axial ImH-His ring are probably weaker in these proteins than in the proteins from *Ch. vinosum* and *Rb. sphaeroides*.

Cytochromes *c′* are able to bind small neutral ligands such as CO and NO and several larger alkylisocyanides,[34,36,37,39,41,142−144,166,167] as well as anionic ligands such as cyanide.[43,45,168] The low affinity of the ferrous and ferric proteins for CO, NO, and CN^- has been attributed to hindered access.[4,35,39] The sixth coordination position is blocked by hydrophobic side chains of aromatic or nonaromatic residues, which limits the entry of solvent molecules, although the higher affinity for the alkyl isocyanides is sufficient to overcome the steric effects. In *Ch. vinosum* ferricytochrome *c′*, the aromatic residue is Tyr, and in the cytochromes *c′* from *R. gelatinosus*, *Rb. capsulatus*, and *Rb. sphaeroides*, it is a Phe. The rings of the aromatic residues are nearly parallel to the heme mean plane at distances between 3.5 and 3.7 Å. The nonaromatic hydrophobic residues are Leu in the cytochromes *c′* from *Rp. palustris*, *Ach. xylosoxidans*, and *Rs. rubrum* and Met in the protein from *Rs. molischianum*. In the former cytochromes *c′*, one Leu methyl lies about 3.7 Å under the heme iron whereas, in the latter, the sulfur atom of the Met side chain lies in the distal cavity, about 3.7 Å from the heme iron.

The crystal structure of the *n*-butylisocyanide adduct of the ferrous cytochrome *c′* from *Rb. capsulatus* has been determined and refined to a resolution of 2.4 Å.[142] This study provided the first example of a ligand-bound structure of a cytochrome *c′*. Significant conformational changes of amino acid residues in the heme vicinity relative to the case of the native ferricytochrome *c′* were observed. The isocyanide adduct is coordinated in slightly bent form, with an Fe−C−N angle of 169° in subunit A and 160° in subunit B. The *n*-butyl group was sandwiched between the heme and the phenyl ring of Tyr 13 which is reoriented approximately perpendicular to its position in the native ferrocytochrome *c′*. Due to the binding of the sixth ligand, iron is displaced 0.3 Å toward the mean plane of the heme. This movement induces large conformational changes of side chains and displacements of several amino acid residues.[142] This work illustrates how the binding of a large sixth ligand can result in a series of concerted repositionings of side chains that connects internal alterations at the heme center to the molecular surface.[169]

The modes of association of the subunits, which have led to two groups of cytochrome *c′* crystal structures, have been proposed to account, in part, for the differences observed in carbon monoxide binding of the proteins.[142] The recent X-ray structure determinations at 100 K of the reduced cytochrome *c′* from *Ach. xylosoxidans* (1.90 Å resolution) also shed some light on the reasons for the low affinities for CO and NO.[143,144] The distal face of the heme is shielded from the solvent, and the size of the distal cavity is unusually small in both the reduced and oxidized states of this protein. One methyl group (CD2) of the Leu 16 residue lies directly under the heme iron, with the Fe—CH_3 separation being 3.66 Å.

Reduction of the heme iron from Fe^{3+} to Fe^{2+} leads to a major repositioning and rotation about the C_δ-N_ϵ (CD−NE) bond of the guanidinium-Arg cation. In the oxidized form at 100 K, as described above, the mean plane of the guanidinium-Arg is nearly perpendicular to the mean plane of the axial ImH-His ligand, with $\alpha = 78.1°$ and with the NH(guanidinium-Arg)- - -centroid(ImH-His) distance being 3.66 Å. In the ferrous form, the guanidinium-Arg mean plane rotates into a position nearly parallel to the mean plane of the ImH-His ligand, with an interplanar angle α of 8.5° and the NH(guanidinium-Arg)- - -centroid (ImH-His) distance 3.57 Å.[143,144] π-Stacking is now possible between the guanidinium-Arg and ImH-His, which might be expected to result in strong π-cation aromatic interactions.[163] This large variation of the orientation of the Arg residue by a simple reduction of Fe^{3+} to Fe^{2+} may also induce changes in other regions of this protein.

The crystal structures of the CO- (1.95 Å resolution) and NO- (1.35 Å resolution) bound forms of the reduced cytochrome *c′* from *Ach. xylosoxidans* at low temperature (100 K) have also been reported.[143,144] As in the case of *n*-butylisocyanide, CO binds to the distal side of the heme in a slightly bent form (Fe−C−O angle of 167°), yielding a six-coordinate heme. However, upon CO binding, the distal pocket undergoes a significant structural rearrangement. The Leu 16 residue located under the iron atom rotates around the $C_\alpha-C_\beta$ bond and induces flattening of the porphyrin ring. The oxygen atom of the carbonyl group comes into close contact with carbon C_β of Leu 16 and also with a carbon atom of Trp 56, with the corresponding distances being 3.23 and 3.66 Å.[143,144] The kinetic barrier associated with this

rearrangement has been assigned responsibility for the particularly low rates of CO and NO binding of the reduced form of this protein. The X-ray structure of the stable nitrosyl adduct (end product) reveals that NO disrupts the axial Fe−His bond and binds to the proximal face of the heme in two alternative bent conformations (Fe−N−O angles of 124 and 132°), each with half occupation.[143,144]

3.2. EXAFS Studies

An EXAFS study of the oxidized and reduced forms of the cytochromes *c*′ from *Rs. rubrum* and *Rs. molischianum* was performed at room temperature in pH 7 phosphate buffered solution.[13] The spectra indicated a coordination number of 5 in both oxidation states. By assuming Fe−N(His) axial bond distances of 2.07 and 2.10 Å from model mono(imidazole) ferric and ferrous heme structures, respectively, the EXAFS studies yielded an average $Fe-N_p$ bond distance of 2.01 ± 0.03 Å for the oxidized cytochromes *c*′ and 2.05 ± 0.03 Å for the reduced cytochromes *c*′. Using estimated out-of-mean-plane displacements Δ(core) = 0.27 and 0.3 Å for iron based on model ferric and ferrous porphyrin complexes, respectively, $Fe-C_t$ bond distances of 1.99 and 2.03 ± 0.03 Å have been calculated for the oxidized and reduced protein forms. The structural parameters of the ferric proteins are similar to those known for iron(III) porphyrin complexes with weakly basic axial ligands displaying quantum mechanical spin-admixed ground states. They are also consistent with results obtained by resonance Raman spectroscopy of the *Rp. palustris* ferricytochrome *c*′ in which the macrocycle was found to be more planar and closer in conformation to six-coordinate low-spin rather than five-coordinate high-spin ferric heme proteins.[12] Thus, the structural results obtained by EXAFS spectroscopy are compatible with the presence of an $S = {}^3/_2,{}^5/_2$ quantum mechanical spin-admixed ground state of the heme iron in the ferricytochromes *c*′ from *Rs. rubrum* and *Rs. molischianum*.[13] Unfortunately, these studies do not present any data on the edge or pre-edge portion of the XAS spectra.

3.3. Normal-Coordinate Structural Decomposition (NSD)

3.3.1. NSD of Heme Distortion in Model Compounds

Shelnutt and co-workers[170−172] have recently shown that the out-of plane distortions of a porphyrin or a heme prosthetic group correspond to displacements along the lowest frequency out-of-plane normal coordinates of a D_{4h}-symmetric macrocycle. Analysis by normal-coordinate structural decomposition (NSD) has been developed for classifying and quantifying distortions. The macrocyclic distortions can be described adequately by a linear combination of a set of orthonormal deformations including saddling (*sad*, B_{2u}), ruffling (*ruf*, B_{1u}), doming (*dom*, A_{2u}), waving (wav(*x*), wav(*y*), E_g), and propellering (*pro*, A_{1u}). NSD has been used to classify and quantify the distortions in structures determined by X-ray crystallography of a large number of synthetic and protein-bound porphyrin macrocycles.

3.3.2. NSD Applied to Cytochromes c′

The heme conformations in cytochromes *c*′ from the photosynthetic bacteria *Rs. molischianum* and *Ch. vinosum* and in the two polymorphs present in the denitrifying bacteria *Ach. xylosoxidans* NCIMB 11015 and *Ach. denitrificans* have been analyzed by NSD.[150,171] Unlike the mitochondrial ferricytochromes *c*, which are primarily ruffled, the ferricytochromes *c*′ show both saddling and ruffling. However, the saddling component of the deformations of all four cytochromes *c*′ is small and is dominant only for the protein from *Rs. molischianum*.

The absolute NSD displacements characterizing the saddle and ruffle deformations of the hemes in the cytochromes *c*′ from *Ch. vinosum* and *Rp. spaeroides*, the proteins in which strong cation−π interactions may be present, are 0.16−0.35 (*sad*) and ∼0.39 Å (*ruf*) (*Ch. vinosum*) and 0.14−0.21 (*sad*) and 0.19−0.27 Å (*ruf*) (*Rp. sphaeroides*). [151] The distortions are small, and saddling alone does not appear to be a critical determinant of spin-state admixture.[73,108−110] However, as indicated previously, the effects of a combination of small saddle and ruffle distortions of the hemes in the cytochromes *c*′ are not clear at present.

3.4. Magnetic Properties

3.4.1. EPR and Magnetic Susceptibility of Model Compounds

Iron(III) porphyrin complexes with weakly basic axial ligands displaying an $S = {}^3/_2,{}^5/_2$ quantum mechanical admixed spin state have been characterized. Excluding any possible solid-state effects, the magnetic moments lie between 3.9 and 5.9 μ_B at 300 K and the EPR spectra show effective $g_\perp$ values between 4 and 6, indicative of varying degrees of mid- and high-spin contributions to the ground states.[22,24] Mono(imidazole)iron(III) tetramesitylporphyrin perchlorate complexes ($[Fe^{III}(tmp)L]ClO_4$) have been prepared with bulky axial ligands and studied as models for the cytochromes *c*′. At 25 °C in CH_2Cl_2, complexes with L = 2-MeImH, 5,6-BzImH, or 2-^{t}BuImH had magnetic moments of 5.0, 5.2, or 5.9 μ_B, respectively. EPR studies yielded $g_\perp$ values from 5.7 to 6 for an extended series including complexes of dialkyl imidazoles, benzimidazoles, and 4,5-dichloroimidazole.[62]

3.4.1.1. Magnetic Studies Leading to Development of a Theoretical Basis for Quantum Mechanical Spin-State Admixture in Cytochromes *c*′. Prior to the synthesis and characterization of mixed-spin iron(III) porphyrin model complexes, unusual magnetic properties had been reported for several ferricytochromes *c*′. Bulk magnetic susceptibility measurements were reported on solution samples of several ferricytochromes *c*′ at room temperature,[5] or in the range 1.2−4.2 K,[6] in fields of 0.5 and 1 T and on solid samples obtained by precipitation with ammonium sulfate $[(NH_4)_2SO_4]$ at 4.2 and 150 K and different pH values.[173] The bulk magnetic susceptibility of the ferricytochrome *c*′ from *Rs. rubrum* at pH 6.5 and 10 in 50 mM NaCl was also determined by the NMR method.[174] The susceptibility data obtained by these measurements yielded the effective magnetic moments collected in Table 4, which shows that, at physiological pH, most μ_{eff} values are between those of high- and low-spin ferric heme proteins. The intermediate values were largely interpreted in terms of a low-spin/high-spin thermal equilibrium,[5,173] which appeared consistent with the observed changes in the electronic spectra of some of these proteins in variable-temperature studies.[5] However, Mössbauer and resonance Raman spectra of some proteins indicated that the electron distribution in the heme iron corresponds to a single d-electron configuration.[12,167]

Table 4. Effective Magnetic Moments μ_{eff} (μ_B) Observed for Several Ferricytochromes *c*′

bacterial source	pH	293 K	150 K	100 K	4.2 K	2.8 K
Rs. rubrum[a,c]	7.0	5.15				
Ch. vinosum[b,c]	7.0	5.03				
Ch. vinosum[b,c]	12.0	2.96				
Rp. palustris[b,c]	7.0	5.13				
Rs. rubrum[d,e]	6.0		5.2		3.82	
Rs. rubrum[d,e]	11		6.4		4.9	
Rs. rubrum[f]						3.8
Ch. vinosum[g,h]	7.0−10.8				3.4−4.7	3.4
Ch. vinosum[i,j]	7.2−10.5	6.0				
Rs. rubrum[k,l]	6.5−10.1	5.4−5.9				
Rb. capsulatus[m,n]				5.7−6.0		

[a] Also named *Rs. rubrum* heme protein (RHP). [b] By susceptibility measurements in solution at room temperature. [c] Reference 5. [d] By susceptibility measurements between 4.2 K and room temperature on samples precipitated from solution by adding ammonium sulfate. [e] Reference 173. [f] Reference 221. [g] By susceptibility measurements in solution between 1.2 and 4.2 K. [h] Reference 6. [i] By susceptibility measurements in solution at 20 and 30 °C using the NMR method. [j] Reference 17. [k] By susceptibility measurements at 26 °C in 50 mM NaCl solution using the NMR method. [l] Reference 177. [m] By susceptibility measurements in solution between 6 K and room temperature in two magnetic fields of 0.5 and 1 T using a SQUID. [n] Reference 20.

In EPR studies of the ferricytochrome *c*′ from the *Ch. vinosum*, Maltempo *et al.*[6] describe four magnetically distinguishable states labeled B_1, A (= A_1 + A_2), and B_2 between pH 1 and 11. At physiological pH the EPR trace is represented by A, which is a superposition of two spectral components A_1 and A_2 (Table 5) with a temperature-independent weight factor ratio of 40/1.[6] Maltempo *et al.* showed that reversible transitions between B_1, A, and B_2 are induced by changing the pH of the protein solution. At pH 1 (state B_1) or pH 11 (state B_2) the EPR spectra were similar to those of other high-spin heme proteins. However, at physiological pH (state A_1 + A_2) the EPR spectra were unusual. Simulations of the spectra using a Lorentzian line shape gave $g_\perp^{eff}$ ($g_\perp^{eff}$ = effective $g_\perp$), g_z, and line width Γ (10^{-3} T = mT) values of 4.75, 1.99, and 35.0 mT for A_1 and 5.27, 1.99, and 7.5 mT for A_2 (Table 5).

Magnetic moments of 3.4 and 5.07 μ_B were observed for *Ch. vinosum* at 2.8 and 293 K (Table 4). Maltempo *et al.*[6] explained the small magnetic moment of the *Ch. vinosum* protein by a quantum mechanical admixture of mid- and high-spin states, rather than a thermal mixture of the unperturbed low- and high-spin states. The Maltempo representation postulated that the quantum mechanical admixture represents a situation in which a pure spin state does not adequately account for electronic properties. In the case of models of cytochrome *c*′, a satisfactory wave function representing the heme iron(III) requires components of the $^6A_1$ and $^4A_2$ states. Ferric proteins or iron porphyrin model complexes displaying a spin-state admixture correspond to a single magnetic species with magnetic properties distinct from those of either pure species. In contrast, when a thermal mixture of spin states occurs, the protein molecules or the iron porphyrin model complexes can be monitored in two magnetically pure spin states.[7,22] Conditions under which quantum mechanical rather than thermal mixing of spin states occurs in ferric heme proteins were defined.[7] Spin−orbit interaction is the most likely mechanism for admixing. Even when allowed by the selection rules for the spin−orbit interaction between heme iron spin states, however, spin−orbit interaction between mid-spin and high-spin states will occur only if the energy separation is comparable to or less than the spin−orbit coupling constant, which was found to be close to 300 cm^{-1} for the ferric heme complexes.[175]

In most ferric heme proteins and iron porphyrin complexes, an energy separation (Δ) of several thousand inverse centimeters between the pure spin multiplets precludes any substantial mixing of spin states. The mid-spin state is the

Table 5. Experimental and Simulated EPR Parameters of Ferricytochromes *c*′ from Photosynthetic, Obligate Methylotroph *Methylococcus Capsulatus* Bath, Denitrifying, and Non-denitrifying Bacteria, at pH 7.2 unless Otherwise Indicated

bacterial source	exp/sim	*T* (K)	g_x	g_y	$g_\perp$[a]	g_z	Γ_x[b] (mT)	Γ_y (mT)	Γ_z (mT)	% ($S = 3/2$)
Ch. vinosum[c] (ATCC 17899)	exp	4.2	5.32	4.67	4.99	1.97				50.5
	sim		5.32	4.40	4.86	2.00	8.0	40.0	3.5	57
Ch. vinosum[d]	exp	7			4.77	1.99				61.5
	sim A_1				4.75	1.99		35.0		62.5
	sim A_2				5.27	1.99		7.5		36.5
Rb. capsulatus[c] (ATCC 11166)	exp	4.2	5.68	4.59	5.19	2.00				40.5
	sim		5.68	4.58	5.13	2.00	5.5	18.0	1.3	43.5
Rb. capsulatus[e] (37 b4) (pH 6.1)	exp	10	5.70	4.97	5.33	1.99				33.2
Rb. capsulatus[f] (MT 1141)	exp	4	5.73	4.62	5.17					41.5
Rp. palustris[c] (ATCC 17001)	exp	4.2	5.71	4.71	5.21	2.00				39.5
	sim		5.71	4.52	5.12	2.00	5.5	22.0	1.1	44
Rs molischianum[c] (ATCC 14031)	exp	4.2	5.96	5.51	5.74	2.00				13
	sim I		5.96	5.70	5.83	2.00	5.0	20.0	2.0	8.5
	sim II		5.65	5.45	5.55	2.00	5.0	20.0	2.0	22.5
Rs. rubrum[c] (ATCC 11170)	exp	4.2	6.00	5.48	5.74	1.99				13
	sim I		6.00	5.75	5.88	1.99	4.0	20.0	1.0	6
	sim II		5.70	5.45	5.58	1.99	4.0	20.0	1.0	21
M. capsulatus Bath[g] (pH 8.2) (major species)	exp	6	6.29	5.34	5.81	2				9.5
M. capsulatus Bath[g] (pH 4) (major species)	exp	6	6.06	5.34	5.70	2				15
Ach. xylosixidans[h] (NCIMB 11015)	exp	6	6.18	5.34	5.76	1.99				12
Ach. xylosixidans[h] (GIFU 543)	exp	6	6.23	5.36	5.80	1.99				10
Ach. xylosixidans[h] (GIFU 1048)	exp	6	6.19	5.35	5.77	1.98				11.5
	sim		6.19	5.35	5.77	1.95	5.0	7.0	2.5	11.5
Ach xylosixidans[h] (GIFU 1051)	exp	6	6.18	5.45	5.82	1.99				9
Ach xylosixidans[h] (GIFU 1764)	exp	6	6.17	5.47	5.82	1.99				9

[a] $g_\perp \cong [g_x + g_y]/2$. [b] Γ_x(mT), Γ_y(mT), and Γ_z(mT) = line widths in mT of the g_x, g_y, and g_z signals. [c] Reference 10. [d] Reference 6. [e] Reference 9. [f] Reference 20. [g] Reference 15. [h] Reference 11.

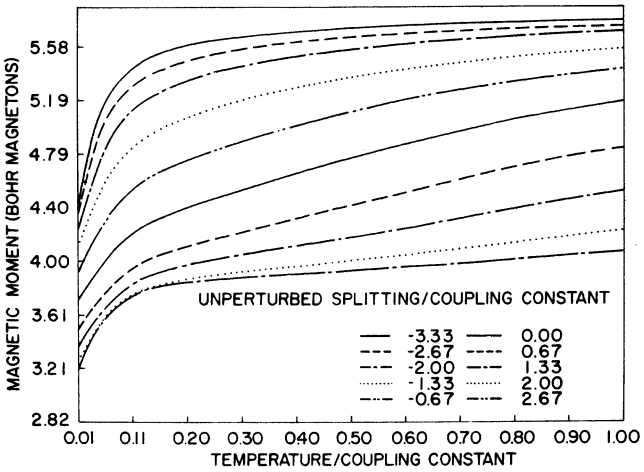

Figure 2. Effective magnetic moment μ_{eff} plotted as a function of T/λ, for different parametric values of Δ/λ. Reprinted with permission from ref 7. Copyright 1974 American Institute of Physics.

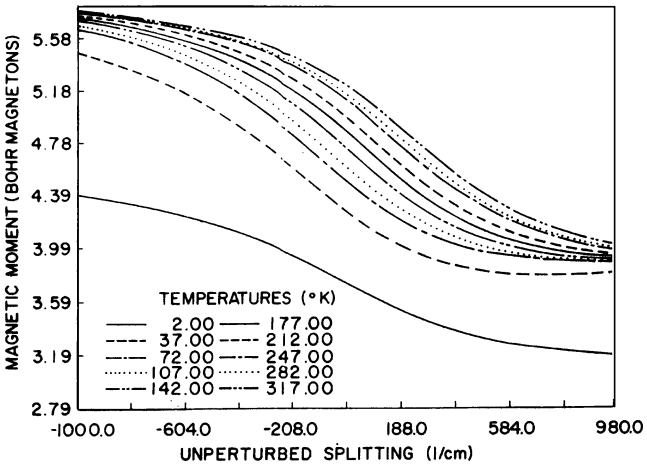

Figure 3. Effective magnetic moment μ_{eff} plotted as a function of Δ for different parametric values of T and the constant value of the free ion spin−orbit coupling constant $\lambda = 300$ cm^{-1}. Reprinted with permission from ref 7. Copyright 1974 American Institute of Physics.

lowest energy state when $\Delta > 0$, and the high-spin state is the lowest when $\Delta < 0$. The separation Δ is a function of both electrostatic and crystal field interactions. Since the magnitude of the electrostatic interaction is fixed for the $^4A_2$ and $^6A_1$ states, Δ is directly related to the crystal field strength.

Maltempo *et al*. also showed that the effective spin-only magnetic moment, μ_{eff}, of a paramagnetic species in a powder distribution can be obtained with the Van Vleck equation,[51] with the orientation average assuming fourfold symmetry. A double functional dependence has been found for the effective magnetic moment of a spin-admixed species, with μ_{eff} being a function of both T/λ and Δ/λ. In a moderate field, the spin-only magnetic moment, μ_S, should correspond closely to the total effective magnetic moment μ_{eff} of a spin-admixed species. The double functional dependence is depicted in Figure 2 by the family of curves for μ_{eff} plotted as a function of T/λ with different values of Δ/λ. This figure indicates that, in a quantum mechanically $S = {}^3/_2,{}^5/_2$ spin-admixed ferric heme protein or ferric porphyrin complex, the value of μ_{eff} can vary from a lower limit of 3.0 μ_B for $\Delta/\lambda \gg 1$ and $T/\lambda \ll \lambda/\Delta$ to an upper limit of 5.92 μ_B for $\Delta/\lambda \ll -1$ and $T/\lambda \approx 1$. Figure 3 shows the magnetic moment, μ_{eff}, plotted as a function of Δ for different parametric values of T and the constant value of the free ion spin−orbit coupling constant $\lambda = 300$ cm^{-1}.[7]

For the ferricytochrome c' from *Ch. vinosum*, $\Delta = 250$ cm^{-1} provides the best theoretical fit to the experimental values of $\mu_{eff} = 3.4$ μ_B at 2.8 K and $g_\perp = 4.75$ at pH 7.0 between 7 and 100 K and $\lambda = 300$ cm^{-1}. These calculations also indicate that the unperturbed state of lowest energy has a spin of $S = {}^3/_2$ ($\Delta > 0$). A value of Δ for the ferricytochrome c' from *Rs. rubrum* has been derived based on the experimental parameters $\mu_{eff} = 3.92$ and 5.05 μ_B at 2.8 and 150 K, respectively, with $\lambda = 300$ cm^{-1} (Table 4). The best computer fit was obtained for $\Delta = -170$ cm^{-1}, indicating a ground state of ≈62% high-spin and ≈38% mid-spin, with the high-spin state lower in energy than the mid-spin state.[7] Maltempo and Moss[8] also proposed that the degree of quantum mechanical $S = {}^3/_2,{}^5/_2$ spin admixture in a ferric heme may be deduced directly from the $g_\perp^{eff}$ in the frozen solution EPR spectrum. For axially symmetric ferric species, paramagnetic resonance within the $M_S = \pm{}^1/_2$ Kramers doublet is observed at $g_\parallel = 2$ and $g_\perp = 6$ for a pure $^6A_1$ state and at $g_\parallel = 2$ and $g_\perp = 4$ for a pure $^4A_2$ state. Consequently, for the ground Kramers doublet of a spin-admixed species of axial symmetry, $g_\parallel$ is close to 2 and $g_\perp$ varies from a minimum of 4 to a maximum of 6, with $g_\perp = 6(a_{5/2})^2 + 4(b_{3/2})^2$ (where $a_{5/2}$ and $b_{3/2}$ are the relative contributions of the unperturbed $S = {}^5/_2$ and ${}^3/_2$ spin states, respectively, to the admixed ground state). Since $(a_{5/2})^2 + (b_{3/2})^2 = 1$, $(a_{5/2})^2 = (g_\perp - 4)/2$ and the percentage of ${}^3/_2$ spin admixture was found to be $100(3 - {}^1/_2 g_\perp)$. An additional complication can be introduced by a small rhombic crystal field component splitting the $g_\perp$ signal into a more complex signal with g_x and g_y symmetrically spaced (to first order) about $g_\perp$ for a pure axial field. To the first order, in a rhombic field, the effective $g_\perp = {}^1/_2(g_x + g_y)$.

3.4.1.2. Magnetic Susceptibility and EPR Studies of Cytochromes c' Following the Maltempo Theory. Since the initial publication of studies on ferricytochromes c' from *Ch. vinosum* and *Rs. rubrum* by Maltempo *et al.*,[6,8,176] work on these two proteins has been repeated and the EPR properties of additional ferricytochromes c' from the photosynthetic bacteria *Rb. capsulatus*, *Rp. palustris*, and *Rs. molischianum* have been investigated.[9,10,14,20,177,178] Data from the studies cited above are summarized in Table 5. The EPR properties of the ferricytochromes c' recently isolated from the methanotroph *M. capsulatus* Bath[15] and from five strains of the chemoheterotrophic denitrifying bacteria, *Ach. xylosoxidans* NCIMB 11015,[179] *Ach. xylosoxidans* GIFU 543, GIFU 1048, GIFU 1051,[11,180] and the nondenitrifying strain GIFU 1764,[11,180] are also summarized in Table 5.

At pH ≈ 7, EPR studies of the ferricytochromes c' from the photosynthetic bacteria show that the electronic ground state of all these proteins is a quantum mechanical admixture of mid- and high-spin states, while, at pH ≈ 11, the electronic ground state of the heme iron is purely high-spin. In addition, at pH ≈ 7, the mid-spin state contribution to the admixed ground state varies with the bacterial source of the protein. EPR spectra indicate mid-spin contributions of about 50% for *Ch. vinosum*, 40% for *Rb. capsulatus* and *Rp. palustris*, and 10% for *Rs. molischianum* and *Rs. rubrum* (Table 5).[10,14] As indicated by Table 5, computer simulations of the EPR spectra are in accord with this diversity of admixtures. The basically high-spin electronic configuration determined in the later work on the *Rs. rubrum* protein is in contrast to the results of Maltempo.[7] The EPR study of the ferricytochrome

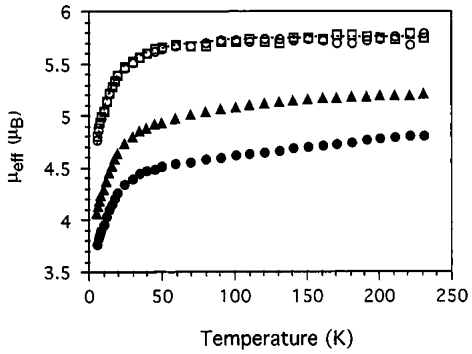

Figure 4. Temperature dependence of the molar effective magnetic moment of the *Rb. capsulatus* ferricytochrome *c*′ for two values of the magnetic field: open circles, 0.5 T; open squares, 1 T. The dashed line through the data is the magnetic moment curve calculated using the model of Maltempo ($\Delta = 726$ cm^{-1} and $\lambda = 228$ cm^{-1}) corresponding to a (90% $^5/_2$, 10% $^3/_2$) quantum-admixed spin state. The full circles and full triangles correspond to the molar effective magnetic moment of either a (40% $^5/_2$, 60% $^3/_2$) or a (60% $^5/_2$, 40% $^3/_2$) quantum-admixed spin state, respectively. Reprinted with permission from ref 20. Copyright 2001 American Chemical Society.

c′ from the methanotroph *M. capsulatus* Bath indicated that the ground states of the two slightly different forms present in the protein at pH 8 are predominantly high-spin, although, at pH 4, the $g_\perp$ values are in accord with an $S = {}^3/_2$ contribution to the admixture of ≈15% (Table 5).[15] Predominantly high-spin ground states with mid-spin contributions of only 9.5−12% have also been found for the five strains of the denitrifying and nondenitrifying bacteria *Ach. xylosoxidans* (Table 5).[11] In intact cells grown photoheterotrophically, the *Rb. capsulatus* protein is almost EPR silent. Appearance of EPR activity upon addition of the oxidizing agent $[Fe^{III}(CN)_6]^{3-}$ to the viable cells reveals that the in-situ cytochrome *c*′ from this bacteria probably exists largely in the ferrous state. The mid-spin contribution to the admixed ground state in a frozen, deuterated buffer mixture at pH 6.9 at 10 K was found by EPR spectroscopy to be close to 40% (Table 5).[9]

The magnetic susceptibility of ^2H_2O solutions of samples of ferricytochrome *c*′ from *Rb. capsulatus* has recently been investigated between 6 and 293 K, at magnetic fields of 0.5 and 1 T using a SQUID susceptometer.[20] While this study reports EPR spectral properties that are similar to those found by other investigators (Table 5), the temperature dependence of μ_{eff} reproduced in Figure 4 showed an effective magnetic moment between 5.7 and 6.0 μ_B above 100 K, with no indication of a spin transition at lower temperatures.

The value of μ_{eff}, which is very close to 5.92 μ_B and corresponds to a purely high-spin ferric heme protein, supports predominantly high-spin character for the iron center. The temperature dependence is very close to that previously observed in a six-coordinate iron(III) porphyrin model complex, $Fe^{III}(t_{piv}pp)(CF_3SO_3)(H_2O)$ ($t_{piv}pp$ = "picket-fence" porphyrin dianion), in which the mid-spin contribution to the admixed spin ground state was also found to be small.[68] The magnetic susceptibility data of the *Rb. capsulatus* protein was fitted assuming (i) a pure high-spin ground state or (ii) two neighboring $S = {}^3/_2$ and $^5/_2$ spin states, quantum mechanically spin admixed through spin−orbit interaction, as developed by Maltempo.[7] Both models provide good fits to the experimental data (Figure 4) with small residuals. Axial zero-field-splitting (ZFS) parameters, $D = 12.3$ and 14.3 cm^{-1}, were calculated from models (i) and (ii), respectively. A small rhombicity, $E = 1.3$ cm^{-1}, was determined with the pure high-spin model (i); rhombicity was not introduced into the Maltempo model (ii). The values of *D* derived from the magnetic moment models (i) and (ii) are consistent with the ZFS $D = 12$ cm^{-1} reported recently in an ^{1}H NMR study of the five-coordinate ferricytochrome *c*′ from *Rb. palustris*.[181] The parameters generating the fit for the Maltempo model (ii) were $^6A_1 - {}^4A_2$ = energy separation $\Delta = -726$ cm^{-1} and spin−orbit coupling constant $\lambda = 228$ cm^{-1}. These parameters correspond to a mid-spin contribution of 10% or less to the ground state. Using model (ii) with a 40% mid-spin/60% high-spin admixture based on the EPR data (Table 5) to fit the susceptibility curves gave a very poor fit, with an unreasonably low spin−orbit coupling constant of $\lambda = 62$ cm^{-1} and a very large residual. Figure 4 also shows the temperature dependence of the magnetic moment μ_{eff} calculated with model (ii) using a 60% mid-spin/40% high-spin admixture.[20] Both strong spin-state admixtures grossly underestimate the room-temperature effective magnetic moment μ_{eff}, giving values of 5.2 and 4.8 μ_B, respectively, at $T > 200$ K. The discrepancy in the magnitude of the $S = {}^3/_2$ spin-state contribution to the ground state determined from EPR and magnetic susceptibility data clearly shows that additional work is necessary to explain the electronic structure of a number of ferricytochromes *c*′.

The spin state of *Rb. sphaeroides* at the nominal pH 7 has recently been studied by ENDOR at 15 K.[165] Spin density was probed by measuring proton and nitrogen-14 splittings and comparison to splittings measured for high-spin hexacoordinate metmyoglobin and high-spin pentacoordinate Fe^{III}(oep)Cl. The results were rationalized by assignment of a significant $S = {}^3/_2, {}^5/_2$ spin-state admixture to the cytochrome *c*′. Splitting of the *meso* protons was ordered Fe^{III}(oep)Cl > *Rb. sphaeroides* > metmyoglobin, in accord with the theoretical considerations discussed above that spin density at the *meso* carbon decreases as iron approaches the porphyrin mean plane, with iron in the spin-admixed complex having an out-of-plane displacement intermediate between those of the 5- and 6-coordinate high-spin hemes and also in accord with crystal data. Larger splitting of the proximal imidazole $N_\delta H$ in *Rb. sphaeroides* than in metmyoglobin was interpreted as an indication, also consistent with crystal data, that spin transfer from the neutral His axial ligand of *Rb. sphaeroides* is more efficient because of the tighter N−H bond than in the case of metmyoglobin, where H-bonding with the Leu89 carbonyl imparts partial imidazolate character. This situation is in accord with the stabilization of the high-spin configuration in metmyoglobin relative to *Rb. sphaeroides*. Smaller nitrogen hyperfine coupling in *Rb. sphaeroides* than in metmyoglobin reflects the expected decrease in σ spin transfer to the heme from the $d(x^2-y^2)$ orbital in the spin-admixed cytochrome *c*′. Hyperfine coupling to the coordinated His ϵ2 nitrogen in *Rb. sphaeroides* is larger than that in metmyoglobin because coupling to the $d(z^2)$ component of a quartet state is $^5/_3$ larger than coupling to $d(z^2)$, which is a component of the sextet state. A fit to the EPR spectrum gave a value of $g_\perp = 5.15$. The authors concluded that ENDOR and EPR data support an admixed spin state, although the relative proportion of $S = {}^3/_2$ and $S = {}^5/_2$ components was not estimated. As discussed in section 3.2 on crystal structures, *Rb. sphaeroides*, in common with *Ch. vinosum*, has an Arg-guanidinium cation in close proximity and favorable orientation for π stacking against the proximal His. On this basis, *Rb. sphaeroides* might also

be expected to show significant spin-state admixture. However, ENDOR and EPR are low-temperature spectroscopies. A critical void is the absence of an ambient-temperature study by ^{1}H or ^{13}C NMR. As in the case of *Ch. vinosum*, a temperature-dependent magnetic susceptibility study would also be critical in arriving at a more conclusive characterization of spin state.

The complexity of the magnetic behavior of spin-admixed hemes is evident in the finding that, in contrast to the model studies described in section 2.2, estimates of mid-spin contribution to an $S = {}^3/_2,{}^5/_2$ admixture in the cytochromes c' by EPR are larger rather than smaller than estimates obtained by NMR. However, the variable-temperature magnetic susceptibility study on *Rb. capsulatus*[20] described above, which covers the range 6−293 K and represents the single published example of such a study on a cytochrome c' protein, yields results in direct opposition to estimates of a large mid-spin contribution by EPR. Thus, in the case of *Rb. capsulatus*, temperature effects appear to be ruled out as an explanation for the discrepancy between EPR and magnetic susceptibility results. In the study on *Rb. capsulatus*, subtle differences in the environment of the heme in samples used for EPR and magnetic susceptibility measurements are possible. Changes in heme environment might be explained by differences in protein concentration (the protein concentration of the magnetic susceptibility sample was higher by 6-fold than that of the EPR sample) and by the method of sample preparation. For susceptibility measurements, the protein was dialyzed against phosphate buffer at pH 6, and then lyophilized and dissolved in ^2H_2O. Thus, the amount of a mid-spin contribution to an admixture is probably a delicate balance of heme geometry and substituent pattern, ligand field strength, and external heme environment, which may have to be considered uniquely for each investigation.

3.4.2. NMR Spectroscopy

3.4.2.1. Model Complexes. NMR spectrometry serves as a sensitive probe of spin state for paramagnetic heme complexes. Pyrrole H signals of high-spin iron(III) *meso*-tetraarylporphyrin complexes typically appear downfield at ∼80 ppm. In $S = {}^3/_2,{}^5/_2$ spin-admixed iron(III) *meso*-tetraarylporphyrin model complexes, pyrrole protons show isotropic chemical shifts upfield relative to those of the corresponding high-spin complexes, with marked anti-Curie temperature dependence.[24,58,62,182] *meso*-H resonances of five-coordinate, high-spin iron(III) porphyrins bearing pyrrole β-substituents generally appear at high field in the −16 to −35 ppm range, while pyrrole β-methyl resonances are shifted downfield, in the 50−90 ppm range.[57] Fewer $S = {}^3/_2,{}^5/_2$ spin-admixed iron(III) pyrrole β-substituted complexes than *meso*-tetraarylporphyrins have been thoroughly characterized. The *meso* H resonances of the spin-admixed β-substituted models appear at lower fields than those of the corresponding high-spin complexes and are close to the diamagnetic envelope.[80−82,183] For both *meso*-tetraaryl and β-alkyl substitution patterns, the differences in isotropic shifts between high-spin and spin-admixed complexes can be ascribed to decreased σ-contact shift contribution accompanying partial depopulation of the $d(x^2-y^2)$ iron orbital. As in the case of the pyrrole protons of *meso*-tetraarylporphyrin complexes, the *meso* H resonances of pyrrole β-substituted complexes display anti-Curie temperature dependence,[80,82] which can be ascribed to an increase in the proportion of mid-spin state in the admixture with decreasing temperature.[58]

3.4.2.2. Proteins. ^{1}H NMR spectrometry is a frequently applied technique for solution studies of functionally relevant structural properties of the heme cavity in heme-containing proteins, particularly in the case of paramagnetic complexes.[184] Thus, a large number of results not directly related to the electronic structure of the heme iron in cytochromes c' have been reported by this technique. These studies and their results have been reviewed in detail in the *Porphyrin Handbook* (Vol. 5, Chapter 37)[184] and will not be discussed here.

Consistent with observations reported for the pyrrole β-substituted model compounds, *meso* proton resonances of the high-spin ferric hemes in proteins appear at high field. Based on the analysis of the ^{1}H NMR spectrum of the cytochrome c' protein of *Ch. vinosum*, for which there are strong indications of an $S = {}^3/_2,{}^5/_2$ spin-state admixture at ambient temperature, *meso* protons of the cytochrome c' hemes would be anticipated to shift downfield near the diamagnetic envelope on admixture of the mid-spin state, consistent with the models.[16] At pH above the ionization of the proximal His ligand, there is universal agreement that the proteins exist in the high-spin form, in accord with an increased ligand field strength of His on deprotonation. In addition to assignment of the proton signals, the NMR studies of the cytochromes c' have characterized the prosthetic hemes with regard to the pH profiles of peak width and hyperfine shifts in order to gain insights into electronic structure.

3.4.2.2.1. Ch. vinosum Cytochrome c′. In the 360 MHz ^{1}H NMR spectrum of *Ch. vinosum* ferricytochrome c' at 25 °C in D_2O at weakly acidic to neutral pH, the *meso* H resonances have been tentatively identified by La Mar *et al.*[16] between 0 and −5 ppm. At pH 10, these resonances are replaced by broad peaks upfield of the diamagnetic envelope between −15 and −30 ppm. These observations are consistent with conversion from an $S = {}^3/_2,{}^5/_2$ quantum mechanical, spin-admixed ground state at acidic pH to a high-spin state in alkaline solution. The appearance of the high-spin species is associated with a deprotonation having a pK_a of 9.13, attributed to ionization of the proximal histidine ligand. La Mar *et al.* have concluded that, in acidic to neutral solution at ambient temperature, a spin-admixed ground state is possible.[16]

In a contemporaneous ^{1}H NMR study of this *Ch. vinosum* ferricytochrome c' at 200 and 300 MHz over the pH range 4−11, Bertini *et al.* reported the ground state to be essentially high-spin over the entire pH range investigated.[17] This conclusion was based on the determination that the bulk magnetic susceptibility, measured by the Evans method, was identical at pH values of 7.2 and 10.5. The *meso* H resonances of the prosthetic heme were not identified in this work. The NMR trace at pH 4 is identical to that reported by La Mar for the acid form of the *Ch. vinosum* ferricytochrome c'; thus, the differing interpretation rests on the Evans measurement rather than the NMR spectrum. At pH 10.7, the methyl resonances show broadening and an upfield shift relative to the methyl signals in the spectrum recorded at pH 10 by La Mar *et al.* This difference would be expected for more complete conversion to a high-spin protein with increasing pH, in accord with the behavior of the model complex Fe^{III}(etio)ClO_4.[80] While the temperature dependence of the resonances identified by Bertini *et al.* was linear over the range investigated, the intercepts of several of the signals

fell considerably outside the diamagnetic limits. This behavior has been observed for other proteins in studies discussed below and has been interpreted as evidence of a thermally accessible excited-state Kramers doublet with appreciable $S = {}^3/_2$ character.[185] On the whole, the data derived from the NMR studies of the *Ch. vinosum* protein present a picture consistent with spin admixture at ambient temperature and acid-to-neutral pH, and this protein can tentatively be assigned an $S = {}^3/_2,{}^5/_2$ spin-state admixed state. However, the magnetic susceptibility measurements performed by the Evans method at pH 7.2 and 10.5 do not show any change in the bulk magnetic susceptibility of this protein at the temperatures of 20 and 30 °C, and a temperature-dependent magnetic susceptibility study performed with a SQUID susceptometer would be critical to a definitive conclusion.

3.4.2.2.2. Rb. capsulatus Cytochrome c′. In an early NMR and EPR investigation of the ferricytochrome *c′* from *Rb. capsulatus* in the pH range 7.5−10.5, Monkara *et al.* concluded that this protein exists in an $S = {}^3/_2,{}^5/_2$ admixed spin state at neutral pH and becomes predominantly high-spin at pH values above ~9, corresponding to the ionization of the proximal histidine ligand with a measured pK_a of 8.6.[9] NMR evidence for this conclusion was based on the observation of the increasing line width of the most downfield heme methyl signal with increasing pH as expected for a greater high-spin contribution to an $S = {}^3/_2,{}^5/_2$ admixture. The changes in methyl line width correlated with a change in $g^{\mathrm{eff}}{}_{\perp}$ from 5.34 at pH 6.1 to 5.95 at pH 9.8, supporting the investigators' conclusion. However, La Mar *et al.*[186] have reported that broadening of the methyl signals may result from both exchange and relaxation effects not directly correlated with spin state. Unfortunately, no features of the *Rb. capsulatus* protein NMR spectrum were described upfield of the diamagnetic envelope, where *meso* signals would be expected to appear, and thus, the *meso* proton shifts are not considered as probes of spin state for this study.

In a more recent and comprehensive study, Tsan *et al.*[20] determined the orientation and anisotropy of the magnetic susceptibility tensor of the ferric form of the *Rb. capsulatus* protein and, as well as the temperature dependence of the magnetic susceptibility, estimated the contact shifts of the heme protons and also the EPR spectrum in frozen solution. The NMR and EPR spectra were recorded at a nominal pH = 6.0. While not explicitly stated, the magnetic susceptibility curve was presumably also obtained at pH 6, so that the protein should have been in the acid/neutral form where spin-state admixture, if any, would be present. As discussed in section 3.4.1.2, the EPR and temperature dependence of the magnetic susceptibility reported in this study led to incongruent estimates of mid-spin contribution, with a mid-spin content of <10% estimated from the magnetic susceptibility experiments and an admixture with ~40% mid-spin content estimated from EPR. The larger $S = {}^3/_2,{}^5/_2$ admixture determined by EPR is in agreement with the Monkara study[9] cited above. The NMR data likewise led to divergent conclusions regarding a spin-state admixture. The susceptibility tensor was perpendicular to the porphyrin plane and axially symmetric, in agreement with results obtained from a determination based on $^1J_{\mathrm{HN}}$ dipolar coupling[187] and in accord with expectation for a predominantly high-spin ferric iron configuration. The pyrrole methyl signals showed strong downfield shifts. Downfield shifts of the α and β proton resonances of the thioether links showed increasing attenuation with distance from the porphyrin ring, consistent with σ-spin delocalization from a partially occupied d(x^2-y^2) iron orbital indicative of a high-spin configuration. However, a broad signal at −14 ppm was tentatively attributed to a *meso* proton. As the pH was raised, this signal disappeared and three broad signals appeared further upfield in the −20 to −35 ppm region. This pH dependence is qualitatively similar to that observed for the *Ch. vinosum* ferricytochrome *c′ meso* protons and, along with global broadening and upfield shifting of the methyl resonances with increasing pH through the His imidazole pK_a, suggests that the NMR data might be interpreted to support a spin-state admixture at acid pH. The authors considered this possibility, but despite a qualitative similarity in the pH dependence of the upfield signal to the *meso* signals of the *Ch. vinosum* protein, they concluded that they had not definitively assigned the upfield signals of *Rb. capsulatus* as *meso* proton resonances. On this basis, the authors speculate that the NMR spectrum might not be indicative of a spin-state admixture. The authors also cite as evidence against the spin-state admixture the observation that the line width of the methyl protons of the *Rb. capsulatus* protein, distinct from that observed in the NMR spectra of the *Ch. vinosum* protein, passes through a maximum at the pK_a. However, it might be noted that the origin of line broadening is not definitively established and at pH > 10 it is possible for equilibration with the low-spin form to result in narrowing of the signals. A linear dependence of chemical shifts with $1/T$ was observed for the *Rb. capsulatus* protein proton signals assigned to the macrocycle ring substituents, which suggests that, in the temperature range considered, no variation of spin-state population takes place. This result is consistent with the temperature-dependent magnetic susceptibility data, albeit over a small temperature range, and is cited by the authors as further support for a predominantly high-spin state. Nevertheless, a number of signals (not including those tentatively assigned to *meso* protons) have infinite-temperature intercepts considerably outside the diamagnetic envelope. At this juncture, NMR and EPR data do not rule out an $S = {}^3/_2,{}^5/_2$ spin-state admixture, but a serious argument against the admixture is the temperature-dependent magnetic susceptibility study, which shows, at most, a minor $S = {}^3/_2$ component. Until the magnetic susceptibility data can be explained, a conclusion regarding the presence of a spin-state admixture in the case of the ferricytochrome *c′* from *Rb. capsulatus* is precluded.

3.4.2.2.3. Rp. palustris, Rs. molischianum, Rs. rubrum, and R. gelatinosus cytochromes c′. Fewer data have been published for these proteins than for those from *Ch. vinosum* and *Rb. capsulatus*. NMR characterization of cytochromes *c′* from *Rp. palustris*, *Rs. molischianum*, and *Rs. rubrum* was included as part of the study on the *Ch. vinosum* protein by La Mar *et al.* cited above. The *meso* proton signals of these ferricytochromes *c′* were identified between −15 and −30 ppm at physiological pH. Based on the relative upfield shifts of the *meso* proton signals of these three proteins, La Mar *et al.* concluded that, in weakly acidic to neutral solution at 25 °C, the five-coordinate iron centers of these proteins must be primarily in a high-spin ($S = {}^5/_2$) state. However, at pH 10, the high-field *meso* proton signals seem to disappear. In contrast to the predictable behavior of the *meso* proton signals of the *Ch. vinosum* protein, this observation is rather puzzling, and there is currently no explanation for the reported behavior, unless the *meso* resonances become broadened beyond detection.

Table 6. Electronic Spectral Data at Several pH Values for the Ferricytochromes c' from *Rs. Rubrum*, *Ch. Vinosum*, and *M. Capsulatus* Bath

bacterial source	pH	λ_{max}/nm (E^a ($\times 10^{-6}$))	Soret	α/β	CT1
Rs. rubrum[b]	6−7		390 (159)	497 (21.5)	638 (5.86)
	8.0		396 (151)	500 (19.7)	638 (7.39)
	9.0		400 (153)	503 (18.9)	638 (8.26)
	10	368 (122)	402 (158)	505 (17.6)	638 (9.44)
	12	351 (53.5)	407 (225)	535 (18.1)	

bacterial source	pH	λ_{max}/nm	Soret	α	β	CT1
Rs. rubrum[c]	5.2		388	500		643
Rs. rubrum[d]	7.0		390			
	10.0	368	402			
	12.5	≈350	407			
Ch. vinosum[e]	1−10.5	≈375	396−408	500	535	635
Ch. vinosum[f] ($T = 77$, 293 K)	7.0		400	490		632
M. capsulatus Bath[g]	8	≈380 (sh)	401	502	≈535 (sh)	638

[a] E = molar extinction. [b] Reference 193. [c] Reference 40. [d] Reference 194. [e] Reference 6. [f] Reference 195. [g] Reference 15.

The pH dependences of the hyperfine shifts of the heme substituents of the *Rp. palustris* and *Rs. molischianum* cytochromes c' are similar and differ slightly from those of the *Rs. rubrum* and *Ch. vinosum* species, for which the lowest field methyl shows a distinct maximum between pH 7 and 8. The significance, if any, of this behavior has not been noted or explained. The pH profiles of methyl line widths are qualitatively similar for the ferricytochromes c' from *Rs. rubrum*[186] and *Rs. palustris*,[16,188] displaying a maximum in the vicinity of the ionization at high pH, in contrast to the case of *Ch. vinosum* ferricytochrome c', for which line broadening plateaus and remains constant.

The objectives of an NMR study of *R. gelatinosus* ferricytochrome c' by Bertini *et al.*[19] were to identify the ionizing groups and to make definitive assignments to paramagnetically shifted signals of the oxidized form. Spin state, per se, was not discussed. The pH dependence of the hyperfine shifts of the heme substituents is similar to those of the *Rp. palustris* and *Rs. molischianum* proteins.

Curie law studies have been reported for the proton signals of the ferricytochromes c' from *Rp. palustris*, *Rs. molischianum*, *Rs. rubrum*, and *R. gelatinosus*. Over the narrow temperature range accessible, shifts appear to vary linearly with $1/T$, as described above for the *Ch. vinosum* and *Rb. capsulatus* proteins. As in the case of these latter species, a number of the infinite-temperature intercepts fall outside the diamagnetic limits for all of the proteins.

3.4.2.3. Summary of NMR Results. ^{1}H NMR studies on the ferricytochromes c' have revealed a heme-linked ionization, with a pK_a between 8 and 9 at 25 °C,[9,16−18,177,188] which has been assigned to the deprotonation of the axial histidine ligand. For the ferricytochrome from *Ch. vinosum*, the behavior of the *meso* proton shifts associated with this ionization is consistent with a spin-state transition from a $S = {}^3/_2,{}^5/_2$ spin-admixed state to a pure high-spin state. The NMR studies on the *Ch. vinosum* cytochrome c' along with other reported spectroscopic data suggest that this protein does contain an appreciable spin-state admixture at acid to neutral pH and ambient temperature. However, to establish spin admixture definitively, the temperature dependence of the magnetic susceptibility would be important. The *meso* proton signals of the *Rb. capsulatus* protein show behavior similar to that of the *Ch. vinosum* cytochrome c', but other data, particularly the orientation of the magnetic susceptibility tensor and the temperature dependence of the magnetic susceptibility (both determined at nominal pH 6), support either a high-spin state or only a minimal contribution of mid-spin state to an $S = {}^3/_2,{}^5/_2$ admixture. At this juncture the apparent inconsistencies rule out assignment of spin-state admixture. There is insufficient data available on any of the remaining cytochromes c' to warrant speculation regarding the spin state of the proteins, at physiological pH and ambient temperature, although the proton shifts at acid pH suggest predominance of high-spin states for these proteins.

The active site structures of some ferrocytochromes c' have also been studied by NMR, and molecular structural studies have been reported for both oxidized and reduced states.[181,184,187,189−192]

3.5. Optical Spectroscopy

3.5.1. Model Complexes

As previously indicated, the absorption spectra of iron(III) porphyrin model compounds with well characterized spin-admixed ground states are similar in appearance to those of high-spin ferric porphyrin complexes. The absorption spectra of high-spin $S = {}^5/_2$ Fe^{III}(tpp)Cl and $S = {}^3/_2,{}^5/_2$ spin-admixed Fe^{III}(tpp)ClO_4 complexes have been compared in toluene and found to be similar.[22] In dichloromethane at 25 °C, the optical spectra of the $S = {}^3/_2,{}^5/_2$ spin-admixed (mono)imidazole complexes, [Fe^{III}(tmp)L]ClO_4 (L = ImH, 2-RImH; R = Me, Et, ^{i}Pr) are very similar to those of the 1-EtPr and ^{t}Bu derivatives, which are predominantly high-spin.[62] In addition, the absorption spectra of Fe^{III}(oep)ClO_4 in dichloromethane and in the solid state were found to be virtually identical to that of the ferricytochrome c' from *Rs. rubrum* observed at pH 5.2.[40,119]

3.5.2. Proteins

Tables 6−8 summarize the optical spectroscopic data available for various ferricytochromes c'. The first absorption spectrum reported for a ferricytochrome c' was that of the *Rs. rubrum* protein.[193] Table 6 gives the λ_{max} values of the optical spectra of this protein over the pH range from 5.2 to 12.5.[40,193,194] Imai *et al.* have shown that over the pH range 7.0−12.5 the Soret bands of this *Rs. rubrum* ferricytochrome c' appear as three distinct forms, designated type I (neutral, pH ≈ 7.0), type II (intermediate, pH ≈ 10.0), and type III (alkaline, pH ≈ 12.5). The type I Soret is a broad band peaking around 390 nm, the type II Soret band has a maximum at 402 nm with a shoulder around 368 nm, and

Table 7. Electronic Spectral Data for the Ferricytochrome *c′* from *Rb. Capsulatus*[a] (B100) at pH 7.2 and 11.0

pH	λ_{max} (ϵ in mM^{-1} cm^{-1})[b]					
7.2	375 sh (60)	400 (85.3)	465 sh (8.4)	500 (10.1)	535 sh (6.4)	635 (2.6)
11.0	370 sh (55)	405.5 (94.4)	455 sh (8.8)	500 (8.9)	535 sh (7.3)	637.5 (4.1)

[a] Reference 178. [b] Millimolar extinction coefficient expressed per heme.

Table 8. Electronic Spectral Data for the Ferricytochrome *c′* from *Ach. Xylosoxidans* (NCIMB 11015) at Various pH Values[a]

pH	λ_{max} (ϵ in mM^{-1} cm^{-1})[b]						
1.5			395.5 (128)		498 (7.1)	530 sh (5)	621 (2.9)
5.3			396 (76)	470 sh (9)	500 (10.6)	540 sh (7)	643 (2.9)
7.2		380 sh (70)	401.5 (80.0)	460 sh (8)	500 (10.0)	535 sh (8)	643 (3.8)
11.0		374 sh (60)	400 (82.9)	460 sh (9)	508 (9.1)	535 sh (8)	643 (4.9)
13.4[c]		374 sh	407	460 sh	508	535 sh	642
13.4[d]	355 (36)		410 (118)		540 (10.3)	570 sh (7)	635 sh (1)

[a] Reference 179. [b] Millimolar extinction coefficient expressed per heme. [c] Spectrum obtained immediately after sample preparation. [d] Spectrum obtained after keeping the sample one week in a frozen state.

Table 9. Porphyrin Skeletal Mode Frequencies (cm^{-1}) for Iron(III) Porphyrin Model Compounds in Different Coordination and Spin States (c = Coordination, HS = High Spin, LS = Low Spin, and QS = Spin-Admixed States)

compound	ν_4	ν_3	ν_{11}	ν_2	ν_{37}	ν_{10}
$[Fe^{III}(ppIX)(DMSO)_2]^+$[a] 6c, HS, $S = {}^5/_2$	1370	1480	1545	1560	1580	1610
$Fe^{III}(ppIX)Cl$[a] 5c, HS, $S = {}^5/_2$	1373	1491	1553	1570	1591	1626
$[Fe^{III}(ppIX)(ImH)_2]^+$[a] 6c, LS, $S = {}^1/_2$	1373	1502	1562	1579	1602	1640
$Fe^{III}(oep)SbF_6$[b] 5c, QS, $S = {}^3/_2, {}^5/_2$	1377	1513	1558	1581		1646
$Fe^{III}(oep)ClO_4$[c] (275 K) 5c, QS, $S = {}^3/_2, {}^5/_2$	1377					1629
$Fe^{III}(oep)ClO_4$[c] (77 K) 5c, QS, $S = {}^3/_2, {}^5/_2$	1378					1635

[a] Reference 222. [b] Reference 206. [c] Reference 133.

the type III Soret band is characterized by a further bathochromic shift to 407 nm with a shoulder close to 350 nm. Changes in the UV−visible spectra of the *Rs. rubrum* protein in the presence of sodium, potassium hydroxylamine, and hydrazine salts and molecules such as N_2O, NO, and CO have also been studied over the pH range from 5.2 to 12.0.[40] As previously indicated, only small mainly uncharged molecules were found to be able to penetrate the distal cavity. Temperature difference spectra between 283 and 310 K, recorded by Ehrenberg and Kamen,[5] for *Ch. vinosum*, *Rp. palustris*, and *Rs. rubrum* showed characteristic maxima and minima and were the basis for the initial proposal that the proteins were equilibrium mixtures of high-spin and low-spin forms.

The room-temperature optical absorption spectra of the *Ch. vinosum* ferricytochrome *c′* were obtained by Maltempo *et al.*[6] in the pH range 1−10.5. Over this pH range, the Soret band appears between 396 and 408 nm, with a shoulder at about 375 nm. Secondary maxima are present at 500 (β), 535 (α), and 635 nm. At pH 7.0, the spectra, which show bands at 400 (Soret), 500, and 632 nm, are very similar at 77 and 293 K (Table 6).[195] The λ_{max} values of the bands present in the spectrum of ferricytochrome *c′* from the obligate methylotroph *M. capsulatus* Bath at pH 8 are also given in Table 6. As indicated by these values, the optical spectra of this cytochrome *c′* and those of the other cytochromes *c′* (Tables 8 and 9) are very similar despite the differences in molecular mass, midpoint redox potentials, or structural changes resulting from reaction with carbon monoxide. [15]

Table 7 lists the $\lambda_{max}(\epsilon)$ values of the bands present in the optical spectra observed at pH 7.0 and 11.0, of the ferricytochrome *c′* from the photosynthetic bacterium *Rb. capsulatus* B100.[178] Spectra of the ferricytochrome *c′* from the chemoheterotrophic denitrifying bacterium *Ach. xylosoxidans* NCIMB 11015, in the pH range 1.5−13.4, have also been reported (Table 8).[179]

Taken together, the solution spectra of the ferricytochromes *c′* from different bacterial sources are, between pH 7 and 10, closely similar and, moreover, resemble those of high-spin heme proteins,[195,196] in accord with expectations based on iron(III) porphyrin model compounds.[22] However, with an increase of pH from 7 to ≥12, the bands originating from the porphyrin $\pi \rightarrow \pi^*$ transitions exhibit a bathochromatic shift and the charge-transfer, CT1, band also present in spin admixed species[196] disappears completely. The absorption spectra of the ferricytochromes *c′* are at pH ≥ 12 closely related to those of low-spin heme proteins, such as the cytochromes *c* of class I (Tables 5−7).

A study of the electronic absorption spectra of b-type heme proteins, such as the peroxidases, has shown that five- and six-coordinate, high-spin hemes can be distinguished by optical spectroscopy.[197] It was found that the extinction coefficients of the Soret bands of the six-coordinate, high-spin hemes are about 40% larger than those of the five-coordinate complexes and that the shoulder on the blue edge of the Soret band, which is prominent in five-coordinate heme, shows a concomitant decrease in intensity in the six-coordinate species.[198] Moreover, for proteins having a His residue as the fifth ligand, the wavelength of the charge-transfer CT1 band is sensitive to the coordination number of the heme iron. The wavelengths of the CT1 bands have been found to range from 600 to 637 nm in six-coordinate proteins and from 640 to 652 nm in five-coordinate proteins.[197,198]

As indicated previously, the optical spectra of the ferricytochromes *c′* often show markedly asymmetric Soret bands of lowered absorptivity at neutral pH.[29] Moreover, the wavelengths of the CT1 bands of these species (Tables 5−7), which are c-type heme proteins, range from 635 to 643 nm. The presence of asymmetric Soret bands of low absorptivities and red-shifted CT1 bands is consistent with the characterization of the ferricytochromes *c′* as five-coordinate in solution, as well as in the solid state.

Studies of the electronic absorption spectra of several plant peroxidases have shown that the wavelength of the CT1 band

Table 10. Comparison of High-Frequency Resonance Raman Modes (ν, cm^{-1}) in Weakly Acidic to Neutral Media for Various Ferricytochromes c' and High-Spin (HS) and Low-Spin (LS) Heme Proteins

	pH	λ_{exc}[a] (nm)	ν_4	ν_3	ν_{38}	ν_{11}	ν_{19}	ν_2	ν_{37}	ν_{10}
bacterial source										
R. palustris[d]	6.9	488	1372	1500		1559	1578	1581		1637
R. rubrum[e]	7.3	514	1373			1558	1577	1582		1637
C. vinosum[f]	7.0	407	1371	1502				1580		1637
R. molishianum[g]	6.8	407−413	1371	1494 + 1501	1553			1581	1605	1627 + 1635
R. sphaeroides[g]	7.2	407−413	1371	1490 + 1502	1551	1558		1582		1628 + 1635
HS and LS heme proteins										
metmyoglobin[h]			1373	1483		1544	1603	1563	1583	1614
cyt c[b,i]			1375	1504		1563				1637
cyt c[b,j]				1500	1547	1559		1582	1595	1633
cyt c[c,j]				1501	1539	1557		1583	1596	1634

[a] λ_{exc} = excitation wavelength. [b] Cytochrome c from horse heart. [c] Cytochrome c from yeast. [d] Reference 12. [e] Reference 202. [f] Reference 203. [g] Reference 204. [h] Reference 223. [i] Reference 224. [j] Reference 225.

is affected by the field strength of the sixth axial ligand through involvement in hydrogen bonding with water or an amino acid residue of the distal heme cavity. It has been observed that, when the axial ligand acts as a hydrogen bond acceptor, the CT1 band undergoes a red shift with increasing hydrogen bond strength and, when the axial ligand is a hydrogen bond donor, increasing hydrogen bond strength causes a blue shift.[197,199] The X-ray structures of several ferricytochromes c' (see section 3), have shown that no distal ligand is present but that the proximal axial histidine−imidazole ligand is often hydrogen bonded to a proximal water molecule. However, as yet, the effect of this proximal hydrogen bond on the wavelength of the CT1 band has not been studied.

3.6. Resonance Raman Spectroscopy

3.6.1. Model Complexes

The 1300−1700 cm^{-1} region in the resonance Raman (RR) spectra of hemes contains skeletal modes giving rise to bands assigned as core-size and spin-state markers. The core-size dependence of these marker bands reflects changes in the methine-bridge force constants as the porphyrin expands or contracts,[200] such that these core-size marker bands can be correlated with heme coordination and spin states. For six-coordinate, planar ferric heme units, a variation of the core size of 0.01 Å produces a change of about 5−6 cm^{-1} in the frequencies of the marker bands. In six-coordinate, high- or low-spin complexes, iron lies close to the heme mean plane, whereas, in five-coordinate complexes, iron is displaced out of the heme mean plane toward the fifth ligand. $Fe-N_p$ bond distances indicate a slight expansion of the porphyrin core in six-coordinate, high-spin iron(III) complexes relative to six-coordinate, low-spin complexes. Out-of-porphyrin-mean-plane displacement of iron toward the fifth ligand in five-coordinate high-spin ferric porphyrins results in core contraction relative to the case of six-coordinate, low-spin ferric complexes in which iron is situated in or close to the porphyrin mean plane. Table 9 shows that five-coordinate, high-spin and six-coordinate, high- and low-spin ferric porphyrin model compounds in well-defined coordination and spin states can be distinguished on the basis of skeletal mode frequencies. However, Table 9 also shows that the ν_{10} marker band of five-coordinate ferric porphyrin models in a quantum mechanically spin-admixed $S = {}^3/_2,{}^5/_2$ ground state does not fit into this scheme. RR spectra of the five-coordinate $S = {}^3/_2,{}^5/_2$ spin-admixed perchloratoiron(III) octaethylporphyrin model, $Fe^{III}(oep)ClO_4$, and the six-coordinate $S = {}^3/_2,{}^5/_2$ spin-admixed complexes $Fe^{III}(oep)(L)ClO_4$ (L = pyridine (py), 4-CHO-py, or 4-CNpy) have been recorded in the solid state and in various solvents at varying temperatures.[133] The frequency of the RR spin-state marker band ν_{10} varies with temperature and solvent (Table 9). In the solid state, the ν_{10} frequencies of the five- and six-coordinate perchlorato complexes, $Fe^{III}(oep)(L)ClO_4$ (L = none, pyridine (py), 4-CHO-py, or 4-CNpy), range from 1629 to 1630 cm^{-1} at 275 K and from 1634 to 1635 cm^{-1} at 77 K. No correlation was found between the frequencies of ν_{10} and the magnetic moments of these five- and six-coordinate perchloratoiron(III) porphyrin complexes (vide supra). However, the frequency of ν_{10} was empirically correlated with the coordination number and the nature of axial ligands. On this basis, the unusual RR spectra at neutral pH (type I) of the ferricytochromes c', showing high frequencies in the core-size marker band region (vide infra), were attributed to the coordination of carbonyl or carbonyl oxygen to the sixth position of the heme iron with a histidine imidazole as the fifth ligand.[133] In light of subsequent structural characterizations of a number of cytochromes c', this conclusion can be modified. As noted above, $Fe-N_p$ bond distances in spin-admixed ferric heme proteins or model compounds are shortened so that the porphyrin core is about the same size as that in low-spin ferric complexes. As a result, the resonance Raman frequencies of the core-size markers are comparable to those of the low-spin derivatives and, therefore, the spin-admixed ferric porphyrins and heme proteins cannot readily be distinguished from the low-spin species by RR spectroscopy alone.[200]

3.6.2. Proteins

Table 10 summarizes the RR spectroscopic data available for various cytochromes c', high-spin met-myoglobin, and low-spin ferricytochrome c. The earliest RR study of a ferricytochrome c' was done on the protein isolated from *Rp. palustris* at pH 6.9, 10.0, and 12.0 with laser excitation at both the Soret band and the $\alpha-\beta$ band frequencies.[12] The spectra were compared with those of other ferric heme proteins in well defined spin states. At pH 6.9, the ferric protein exhibited an anomalous RR spectrum, with core-size and spin-state marker band frequencies closer to values expected for low-spin rather than high-spin species, although magnetic moments, while intermediate, were closer to high-spin values. The presence of only a single set of marker bands ruled out a mixture of spin states to account for the apparent discrepancy, which was therefore attributed to a mid-spin state. As the pH was increased to 10.3, marker band

frequencies shifted toward high-spin values, indicative of a less planar structure. In strongly alkaline solution (pH > 11.5), the ferric form of *Rp. palustris* ferricytochrome *c′* showed resonance Raman spectra with band frequencies similar to those of low-spin heme proteins.

Three forms of the ferricytochrome *c′* from *Rs. rubrum*, correlated with the types I, II, and III defined by optical spectroscopy,[201] were observed in RR spectra with 514.5 nm excitation at pH 6.9, 10.3, and 12.0, respectively.[202] The type I spectrum (pH 6.9) showed unusual features, similar to those of the *Rp. palustris* protein, with the band corresponding to ν_{10} identified at 1637 cm^{-1}, a high value relative to those for high-spin proteins and model complexes. The investigators concluded that the anomalously high frequency of ν_{10} resulted from strain caused by the protein backbone rather than an intermediate or $^3/_2$,$^5/_2$ admixed spin state,[12] despite the low magnetic moment of 5.2 μ_B. This study also reported the conversion of type I directly to type III by addition of sodium dodecyl sulfate (SDS) or 2-propanol. However, the conversion accomplished by titration with NaOH occurred via the type II intermediate when the pH was increased from 6.9 to 12.0.[202]

Resonance Raman spectra of ferric *Ch. vinosum* ferricytochrome *c′* were also obtained at pH 7 (type I), pH 10 (type II), and pH 12 (type III) using Soret band excitation frequencies.[203] The core-size and spin-state marker bands were observed at 1371 (ν_4), 1502 (ν_3), 1580 (ν_2), and 1637 (ν_{10}) cm^{-1}. As in the case of the *Rp. palustris* and *Rs. rubrum* proteins, the ν_2, ν_3, and ν_{10} frequencies at pH 7 are close to those of heme proteins well characterized as low-spin. Following the pattern of the *Rp. palustris* and *Rs. rubrum* proteins, the spectrum of the type II form was consistent with a high-spin state and the spectrum of type III was consistent with a low-spin state.[203] Soret-excited resonance Raman spectra of solutions of the ferricytochromes *c′* from *Rs. molischianum* and *Rb. sphaeroides* were also obtained as a function of pH and compared with those from the proteins derived from *Rp. palustris*, *Rs. rubrum*, and *Ch. vinosum* (Table 10). In the spectra of the type I form of the proteins from *Rs. molischianum* and *Rb. sphaeroides*, two sets of bands were resolved in the ν_3 and ν_{10} regions (Table 10). One set was attributed to a normal high-spin form, and the second was attributed to an $S = {}^3/_2,{}^5/_2$ spin-admixed form, suggesting that, at physiological pH, these proteins exist as equilibrium mixtures of high-spin and spin-admixed states.[204]

In the RR spectra of the high-spin ferrous forms of the cytochromes *c′* from *Ch. vinosum*, *Rs. molishianum*, and *Rb. sphaeroides*, bands between 228 and 231 cm^{-1} were assigned to the Fe^{II}-His stretching vibration, $\nu(Fe^{II}\text{-His})$.[203,204] In the absence of H-bonding of $N_\delta H$ of the proximal histidine imidazole with a water molecule inferred from the crystal structure of the *Rs. molischianum* ferricytochrome *c′*,[153] the observed frequencies assigned to $\nu(Fe^{II}\text{-His})$ appeared to be outside the expected range (195−205 cm^{-1}). To account for the high frequency of $\nu(Fe^{II}\text{-His})$, several possibilities were considered:[204,205] (i) hydrogen bonding between the proximal histidine imidazole and a water molecule in solution (while the axial histidine imidazole is not hydrogen bonded in the crystal structure of the *Rs. molischianum* protein, a role for this interaction could not be ruled out in solution, since such hydrogen bonding to the axial ligand has been observed in crystal structures of other ferricytochromes *c′*); (ii) a hydrogen bonding interaction of the proximal histidine imidazole with a change in orientation of this imidazole ring relative to the orientation in the solid state; and (iii) a direct electrostatic interaction between the proximal histidine and a basic protein residue, stabilizing the axial His in the imidazolate form. This last suggestion was favored by the investigators. Such an electrostatic interaction has been suggested as playing a crucial role in the modulation of the magnetic properties of cytochromes *c′*.[204] The only crystal structure of a reduced cytochrome *c′* is that of the denitrifying bacterium *Ach. xylosoxidans* (1.90 Å resolution).[143] In both the oxidized and reduced states of this protein, the proximal His ligand is hydrogen bonded through $N_\delta H$ to an ordered water molecule that is accessible to bulk solvent. No basic protein residue is within Van der Waals distance of $N_\delta H$.[141,143]

More recently, Smulevich *et al.*[197] proposed that combined analysis of the electronic and vibrational spectra allows the distinction between low-spin and spin-admixed states to be made. Purified peroxidase preparations are frequently obtained as spin-state admixtures, as indicated by broadened or multiple resonance Raman peaks in the skeletal mode region from 1470 to 1640 cm^{-1}.[206] Resonance Raman spectroscopy shows different temperature-dependent coordination equilibria for native horseradish and cytochrome *c* peroxidase.[206] The Soret-enhanced A_{1g} mode, denoted as ν_3, proves useful for identifying individual components of spin-state mixtures. Though sometimes weak, ν_3 occurs in a region where there is no overlap with other fundamentals, in contrast to bands ν_2, ν_{10}, ν_{11}, and ν_{19}, which, though spin-state sensitive, occur in more congested spectral regions.[200] As a spin-state marker, ν_3 frequencies occur in heme proteins near 1480 cm^{-1} for 6-coordinate, high-spin; near 1490 cm^{-1} for 5-coordinate, high-spin; and in the range 1500−1510 cm^{-1} for 6-coordinate, low-spin species. [207] An abnormally high ν_3 frequency of 1499 cm^{-1} for HRP isozyme C, and similar high values near 1500 cm^{-1} (depending on pH) for ferricytochrome *c′* from *Rp. palustris* were originally considered to be "anomalous" since the ν_3 frequency (denoted as band E in early publications)[12,208,209] occurred closer to the low-spin than the high-spin range despite magnetic properties approaching high-spin character for both hemes. At the time, the anomalous nature of *Rp. palustris* ferricytochrome *c′* was concluded to be due to intermediate spin, while the heme structure of HRP-C was still felt to be "anomalous".[12,209] The ν_3 band region of the HRP A-1 and A-2 isozymes showed behavior comparable to the unusually high frequency (1499 cm^{-1}) observed for ν_3 of HRP-C. HRP A-1 exhibited an easily resolvable splitting of ν_3 into two components, at 1491 and 1505 cm^{-1}, which is reproducibly observed in purified preparations at neutral pH.[210] Virtually identical behavior is exhibited by HRP isozyme A-2.[211] Since the HRP-A isozymes are predominantly 5-coordinate, high spin, the 1491 cm^{-1} band was assigned as being characteristic of the 5-coordinate, high-spin heme, but the 1505 cm^{-1} component frequency was initially interpreted as being due either to the presence of a resonantly enhanced 6-coordinate, low spin component or to a Fermi resonance.[210] Subsequently, Smulevich *et al.* (1991) observed for HRP C at low temperature that the ν_3 band became resolved into two components at 180 K (three components with glycerol), which shifted to higher frequencies with further lowering of the temperature to 1503 cm^{-1}, indicative of a 6-coordinate, low-spin heme, and 1511 cm^{-1}, attributed to an intermediate spin state. Upon reinvestigating the 1491, 1505 cm^{-1} ν_3 doublet of HRP A-2 (now noted to have a third component at 1485 cm^{-1} characteristic of a 6-coordinate high-spin heme), Feis *et al.*[211]

noted that preparations containing a 6-coordinate, low-spin component would be expected to exhibit a Q_0 band at 570 nm as well as a red-shifted Soret band (402−414 nm) as observed for the 6-coordinate, low-spin complex of soybean seed coat peroxidase.[212] Maltempo *et al*.[213] had obtained EPR data for HRP A-2 and C-2, for which a $g_\perp = 5$ component was detected and assigned to a quantum mechanically admixed $S = {}^3/_2,{}^5/_2$ component. On this basis, Feis *et al*.[74,211] reassigned the 1505 cm^{-1} ν_3 band of HRP isozymes A-1 and A-2 to this quantum mechanical admixed spin component. It was noted that a quantum mechanically spin-admixed, 5-coordinate heme was a common feature of all class III secretory plant peroxidases.[73] A 6-coordinate, quantum mechanically spin-admixed component has recently been proposed for a peroxidase from artichoke flowers, *Cynara scolymus L*.,[214] as suggested by comparison with 6-coordinate benzohydroxamic-complexed peroxidases.[215]

As noted above, the optical spectra of ferricytochromes *c*′ are similar to those of high-spin heme proteins. In contrast, core-size and spin-state marker bands of most ferricytochromes *c*′ appear at frequencies higher than those of the pure high-spin species and comparable to those of low-spin ferric heme derivatives (Table 9). Taken together, a combined analysis of the electronic and vibrational spectra of various ferricytochromes *c*′ shows that these proteins are neither high- nor low-spin and thus are likely to be $S = {}^3/_2,{}^5/_2$ spin-admixed, as indicated by their EPR spectra.

3.7. Mössbauer Spectroscopy

3.7.1. Model Compounds

Mössbauer spectroscopy has shown that only a single spin state is present in the ferric quantum mechanically $S = {}^3/_2,{}^5/_2$ spin-admixed porphyrin model compounds (Table 1) rather than a thermal equilibrium between two species in unperturbed high-spin and low-spin states. The spin-admixed complexes are characterized by quadrupole splittings that are larger than those of pure high-spin complexes, increasing in magnitude with the relative size of the mid-spin contribution to the admixture. The magnitude of quadrupole splittings shows an inverse dependence on temperature. The origin of the observed temperature dependence of ΔE_Q is not clear; relaxation effects, thermal population of higher energy states, and dynamic admixtures at different temperatures have been invoked as explanations.

Mössbauer spectra of $Fe^{III}(oep)ClO_4 \cdot 2H_2O$, $Fe^{III}(oep)ClO_4$, and $Fe(tpp)ClO_4 \cdot 0.5$ *m*-xylene recorded at varying temperatures and external fields have been analyzed quantitatively.[87,135] The applicability of Maltempo's theory of quantum mechanical spin admixing[7] to $Fe^{III}(tpp)ClO_4$ has been studied. This model reproduces the sign, anisotropy, and temperature dependence of the internal field H^{int}. However, it does not satisfactorily reproduce the magnitude. To fit the data using Maltempo's model, the contact field, $B_0\kappa$, which is close to 21.6 T in high- and low-spin iron(III) porphyrins, has to be reduced to the unacceptably low value of ~10.8 T. The low value suggests that some modification of Maltempo's theory on quantum mechanical spin admixing is needed.[135] In contrast, a value of 24 T has been reported for the effective internal field at the ^{57}Fe nucleus of $Fe^{III}(oep)ClO_4$.[87] Currently, no theoretical interpretation of quantum mechanical $S = {}^3/_2,{}^5/_2$ spin admixture other than Maltempo's model has been proposed.

Table 11. Mössbauer Parameters Observed for the *Rs. rubrum* and *Ch. vinosum* Cytochromes *c*′

bacterial source	pH	*T* (K)	δ (mm s^{-1}) (/Fe:Cu)	ΔE_Q (mm s^{-1})
Rs. rubrum[a]		205	0.06 ± 0.02	1.56 ± 0.02
		77	0.08 ± 0.02	1.78 ± 0.02
		63	0.08 ± 0.02	1.94 ± 0.02
Ch. vinosum[a]		205	0.08 ± 0.02	1.97 ± 0.02
		77	0.11 ± 0.02	2.27 ± 0.02
		63	0.14 ± 0.02	2.53 ± 0.02
bacterial source	pH	*T* (K)	δ (mm s^{-1}) (/αFe)	ΔE_Q (mm s^{-1})
Rs. rubrum[b]	7.0	210	0.34 ± 0.04	1.5 ± 0.0 1
Ch. vinosum[c]	7.8	150	0.35 ± 0.01	2.31 ± 0.02
	7.8	4.2	0.29 ± 0.01	2.91 ± 0.01
	1.0	4.2	0.39 ± 0.01	0.82 ± 0.01
	10.5	4.2	0.39 ± 0.01	0.79 ± 0.01

[a] Reference 167. [b] Reference 14. [c] Reference 176.

3.7.2. Proteins

The ferric, ferrous, and ferrous carbonylated states of the cytochrome c_2 and cytochrome *c*′ (RHP, cc′) from the photosynthetic bacteria *Rs. rubrum*, as well as those of cytochrome c_{552} and cytochrome *c*′ from strain D of *Chromatium* (*Ch. vinosum*), have been studied by Mössbauer spectroscopy between 6 and 205 K.[166] The Mössbauer parameters observed over this temperature range for both ferricytochromes *c*′ are listed in Table 11.

Since the magnetic moments of the ferricytochrome *c*′ proteins determined by magnetic susceptibility measurements were found to be clearly smaller than the high-spin value of 5.9 μ_B,[5] a thermal equilibrium between high- and low-spin states was initially proposed for these proteins.[5,164] However, no such "thermally mixed" spin states could be resolved by the early Mössbauer studies of Moss *et al*.[167] Nevertheless, these authors indicated that spin states equilibrating rapidly on the time scale of the Mössbauer experiment could be masked by the apparent large temperature dependence of the quadrupole splitting of these proteins.[167]

The Mössbauer characteristics of the cytochromes *c*′ from the *Rs. rubrum* (ATCC 11170) and *Ch. vinosum* bacteria were later re-examined by Emptage *et al*.[14] and Maltempo *et al*.,[168] respectively. Spectra of the *Rs. rubrum* (ATCC 11170) ferricytochrome *c*′, buffered at pH 7, were obtained in a magnetic field of 0.6 T parallel to the direction of the incident γ-ray beam at 25 and 210 K and at 4.2 K in fields of 0.6 and 30 T parallel and of 0.6 T transverse to the incident beam.[14] The spectrum obtained at 210 K consists of a quadrupole doublet with $\delta/\alpha Fe = 0.34$ and $\Delta E_Q = 1.5$ mm s^{-1}. The quadrupole lines of the 25 K spectrum were broadened, and a reliable value for ΔE_Q could not be obtained. The investigators point out that when relaxation effects are taken into account, fits to the spectra at 4.2 and 210 K can be obtained with the same ΔE_Q values reported by Moss *et al*.[167] Thus, the apparent temperature dependence of ΔE_Q reported in these early studies can be explained by failure to consider relaxation effects. According to Emptage *et al*.,[14] reliable values of quadrupole splittings cannot be obtained in the temperature range 30−150 K, unless relaxation effects are properly taken into account. The external field spectra obtained at 4.2 K indicated the presence of two species, designated I and II, which could not be resolved at high temperature. The parameters for I (~60%) were estimated to be $D = 15(2)$ cm^{-1}, $\delta = 0.37$ mm s^{-1}, and $\Delta E_Q = 1.35$ (15) mm s^{-1}, and those for species II (~40%) were estimated to be $D > 20$ cm^{-1}, $\delta = 0.37$ mm s^{-1}, and

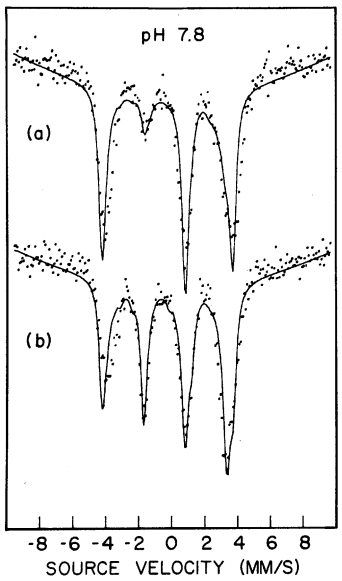

Figure 5. Mössbauer spectra of ferricytochrome *c′* from *Ch. vinosum* at pH 7.8 and 4.2 K in an applied field of ~0.2 T: (a) longitudinal field; (b) transverse field. Reprinted with permission from ref 176. Copyright 1980 American Institute of Physics.

$\Delta E_Q = 1.65(15)$ mm s^{-1}.[14] The parameters observed for the ferric cytochrome *c′* from *Rs. rubrum* most closely resemble those of ferric horseradish peroxidase (HRP). The wild-type HRP enzyme has subsequently been characterized as a mixture of several isozymes.[216] As noted above, the HRP isozymes, like the ferricytochromes *c′*, can exist in a quantum mechanical spin-admixed state.[213]

The oxidized form of cytochrome *c′* from *Ch. vinosum* was also studied by Mössbauer spectroscopy over the pH range 1.0−10.5 by Maltempo *et al.*[176] in the temperature range 4.2−150 K in the absence of an external field and at 4.2 K in magnetic fields of about 0.2 T applied longitudinally and transverse to the γ-ray beam. At 4.2 K and pH 1.0 and 10.5, the external magnetic field Mössbauer spectra consist, as expected, of a six-line hyperfine pattern typical of high-spin ferric heme proteins, while, at neutral pH, a four-line spectrum with a smaller overall width was observed (Figure 5). At 150 K and neutral pH in the absence of an external magnetic field, the protein showed a symmetric doublet with $\Delta E_Q = 2.31 \pm 0.02$ mm s^{-1} and an isomer shift (δ) relative to αFe of 0.35 mm s^{-1}.

At 150K, the spectra of samples at high and low pH were characterized by strongly asymmetric, diffuse doublets. Good fits have been obtained for the six-line spectra recorded at 4.2 K at high and low pH with a Hamiltonian having an effective spin of $S = {}^5/_2$. The four-line hyperfine spectrum recorded at 4.2 K could be fitted using the quantum mechanical $S = {}^3/_2,{}^5/_2$ spin-admixed model (Figure 5),[7] with the parameters $\Delta E_Q = 2.91$ mm s^{-1}, $\delta = 0.29$ mm s^{-1}, line width $\Gamma = 0.43$ mm s^{-1}, and a small value of the contact field $B_0\kappa$ of 12.4 T.[176] Again, as in the spin-admixed ferric porphyrin model complex Fe^{III}(tpp)ClO$_4$·0.5*m*-xylene, the value of 12.4 T found for the contact field is significantly smaller than 21.6 T, which is typical for high- and low-spin ferric porphyrin complexes. The investigators[176] recognized that their description of the internal field for the spin-admixed species may be incomplete and that the value of 12.4 T, required by their data, should be viewed as a parametrization accounting for mechanisms not included in their electronic model of $S = {}^3/_2,{}^5/_2$ spin admixing.[135]

The ΔE_Q values (Table 11) of the ferricytochromes from *Rs. rubrum* and *Ch. vinosum* follow the same trend of increasing magnitude when the temperature decreases, as observed in model iron(III) porphyrin complexes (Table 1). However, as in the case of the model complexes, spin relaxation effects have not been taken into consideration and such effects have been shown to be important in obtaining reliable values for the quadrupole splittings.[14] As in the model compounds, the ΔE_Q values also appear to increase as the $^4A_2/^6A_1$ ratio of the $S = {}^3/_2,{}^5/_2$ spin-admixed ground state increases. NMR and EPR studies have shown that, at neutral pH, the *Rs. rubrum* ferricytochrome *c′* belongs to the group of proteins that can be classified as predominantly high-spin.[10,16] Accordingly, between 63 and 205 K, this protein shows a smaller ΔE_Q than that of the ferricytochrome *c′* from *Ch. vinosum* (Table 11). In contrast, the *Ch. vinosum* ferricytochrome *c′*, which is believed to have a substantial mid-spin contribution to an $S = {}^3/_2,{}^5/_2$ spin-admixed ground state even at ambient temperature,[16,58] has a ΔE_Q ranging from 1.97 to 2.53 mm s^{-1} between 4.2 and 150 K, in line with the temperature dependence observed for the quadrupole splittings for model ferric porphyrin complexes known to be substantially $S = {}^3/_2,{}^5/_2$ spin admixed.[66,93]

3.8. CD and MCD Spectroscopy

3.8.1. Model Complexes

Kintner and Dawson[67] have investigated ferric octaethylporphyrin complexes by MCD spectroscopy as models for the various species of cytochromes *c′* observed at different pH values. The MCD spectra of the $S = {}^3/_2,{}^5/_2$ spin-admixed Fe^{III}(oep)X (X = Cl, ClO$_4^-$, SO$_3$CF$_3^-$, SbF$_6^-$) and [Fe^{III}(oep)(3,5-Cl$_2$pyridine)$_2$]ClO$_4$, the high-spin Fe^{III}(oep)-Cl, and the low-spin [Fe^{III}(oep)(L)$_2$]$^+$ (L = ImH, 1-MeIm) complexes were compared. Over the Soret−visible range (300−700 nm), the MCD spectra of the low-spin complexes were distinctive, but the MCD spectra of the high-spin and $S = {}^3/_2,{}^5/_2$ spin-admixed complexes were closely similar and not readily distinguished. By contrast, in the near-IR range (700−2000 nm), the MCD trace of each spin-state type was distinctive. High-spin Fe^{III}(oep)Cl gave a derivative-shaped feature with a crossover at ~1000 nm, in line with reports for high-spin, five-coordinate ferric protoporphyrin IX complexes. The near-IR MCD trace of low-spin [Fe^{III}(oep)-(1-MeIm)$_2$]$^+$ was positive, with a broad shoulder on the blue side of a maximum at 1557 nm. All of the spin-admixed complexes showed a broad, distinctive negative−positive−negative trace extending over nearly the entire near-IR range. Thus, the spectra of the spin-admixed species are easily distinguished from those of the high- and low-spin derivatives, and complexes reported to be in a high-spin/low-spin equilibrium appear as a composite of the high-spin and low-spin traces. This work strongly supports near-IR MCD spectroscopy as a sensitive probe of spin state.

3.8.2. Proteins

Unfortunately, the MCD studies of ferricytochromes *c′* preceded the studies on model complexes. Room-temperature near-IR MCD and CD spectra of the ferricytochromes *c′* from *Rs. rubrum*, *Ch. vinosum*, and *Rp. palustris* have been investigated.[217] Over the pD range of 1 to 13, four distinct species were identified and labeled A−D. The spectrum of B, the species present over the pD range 10−12, was assigned to be in a high-spin state by comparison with the

MCD spectra of known high-spin heme proteins. Similarly, species C and D at pH > 12 were unambiguously assigned to be in low-spin states. The spin-state assignments B−D are consistent with spectroscopic evidence from other techniques discussed in previous sections. In the absence at that time of any $S = {}^3/_2,{}^5/_2$ spin-admixed model for comparison, the MCD spectra of species A in the acidic to neutral pH range were judged to be consistent with a high-spin state for all three ferricytochromes c' examined. However, as pointed out by Kintner and Dawson,[67] the MCD traces A are virtually identical to those subsequently reported for the spin-admixed models. Thus, in light of the more recent work by Kintner and Dawson on model complexes, the MCD spectra of species A may be reinterpreted as supporting a spin-admixed ground state. The near-IR CD spectra were also recorded by Rawlings *et al*.[217] but were used to investigate ligation state, with no attempt to examine correlation with spin state. Nevertheless, the CD traces of species A, reproduced in the publication for the *Rs. rubrum*, *Ch. vinosum*, and *Rp. palustris* ferricytochromes c', are distinctly different from the CD spectra of B shown for the *Rs. rubrum* and *Rp. palustris* cytochromes c'. This result suggests that near-IR CD could also serve to probe the spin states of the ferricytochromes c'. A distinct disadvantage of CD as a spectroscopic probe is the need to identify models with asymmetric chromophores.

The remaining investigations of the ferricytochromes c' dichroism covered only the UV−visible range. Yoshimura *et al*.[179] recorded the CD and MCD spectra of the ferricytochrome from the denitrifying bacterium *Ach. xylosoxidans* NCIMB 11015 in the UV−visible region at pH 7.2. The CD spectrum (trace not reproduced in the citation) was described as similar to that of the *Rs. rubrum* protein reported earlier[218] and discussed below. The MCD trace was described as differing slightly from those of high-spin myoglobin and HRP and on this basis was considered to be inconclusive with respect to making an assignment of spin state. Comparison of the MCD spectrum of the ferricytochrome c' from *Ach. xylosoxidans*, published by Yoshimura *et al*.,[178] with those reported by Dawson *et al*.[67] for the high-spin and $S = {}^3/_2,{}^5/_2$ spin-admixed models in the UV−visible region favors the spin-admixed assignment. However, the observation that the MCD traces of high-spin and $S = {}^3/_2,{}^5/_2$ spin-admixed complexes vary only slightly in the UV−visible range demands caution in making such a spin-state assignment. Ferricytochromes c' isolated from the photosynthetic bacterium *Rb. capsulatus* B100 were reported to give UV−visible range MCD spectra similar to those of the *Ach. xylosoxidans* NCIMB 11015 protein.[178] No additional description of the MCD spectrum was provided by the authors, nor was the trace reproduced in the citation or used to support a spin-state assignment. In a study preceding both the Maltempo postulate of spin admixture[6] and the Kintner−Dawson study on model compounds, [67] CD spectra of the ferricytochromes c' from *Rs. rubrum* and *Rp. palustris* were examined over the range 205−500 nm at pH 7.0, 10.3, and 12.3.[218] The authors did not analyze the CD data with respect to information on spin state. Chromophores from the protein residues are probably major contributors to the CD spectra below 300 nm. Within the 300−500 nm range, traces recorded for the *Rs. rubrum* ferricytochrome c' at pH 7.0 and 10.3 corresponded closely to each other, and below 400 nm, they were distinctly different from the trace at pH 12.3. In the case of the *Rp. palustris* protein, CD spectra at pH 6.9, 10.4, and 12.3 were all close in appearance. In light of subsequent developments discussed in this and preceding sections, pure high- and low-spin forms with readily distinguishable CD traces could be anticipated at pH 10.3 and 12.3, respectively. At pH 7, the $S = {}^3/_2,{}^5/_2$ spin admixture would likely be difficult to demonstrate over the spectral range examined. The data reported for the *Rs. rubrum* ferricytochrome c′ are in accord with this expectation. In the absence of reference models, no significance can be assigned to results for the *Rp. palustris* protein. MCD and CD studies to date indicate that bands in the near-IR region of the electronic spectrum can provide information regarding spin state. MCD appears to offer an advantage over CD because an asymmetric chromophore is not prerequisite for spectroscopic activity, simplifying the use of model complexes.

4. Summary of Evidence on the Spin-State of Cytochromes c': Proposals for Additional Work

Interest in the spin state of the cytochromes c' spans nearly 40 years, since recognition of the unusual magnetic properties of the proteins. The earliest studies on the magnetic properties of these proteins were reported without the benefit of the Maltempo theory of quantum mechanical spin-state admixture or the extensive body of work on well characterized $S = {}^3/_2,{}^5/_2$ spin-admixed model complexes that was subsequently developed. However, despite progress in understanding the mechanisms of spin-state admixture, the picture presented by the totality of data accumulated on the cytochromes c' is not yet complete enough to support the definitive characterization of any of the proteins as an $S = {}^3/_2,{}^5/_2$ spin-state admixture. A major problem encountered in preparation of this review was that, despite application of a wide variety of physicochemical methods to studies of the cytochromes c', no single technique has been applied to all the proteins encompassed in this review. Thus, there are critical gaps in the characterization of the proteins. In addition, comparison of physicochemical properties under similar conditions across the entire family of cytochromes c' is difficult or impossible. Even for X-ray structures, temperatures at which data were collected were specified in only four of ten published studies, ruling out the assessment of temperature effects on structural features that might be related to spin state. In the single instance where structural data acquired at ambient and cryogenic temperatures is available, comparison of structures of *Ach. xylosoxidans* indicates that temperature has a significant effect on structure and, by implication, on spin state. However, as discussed above, *Ach. xylosoxidans* appears to be predominantly high-spin under all conditions, and lack of a companion temperature-dependent magnetic susceptibility study rules out the observation of even minor perturbations resulting from structural reorientation. In general, effects of temperature, crystal packing in the solid state, or protein and/or buffer concentration on physicochemical properties in solution are unknown.

Measurements directly yielding information on spin state include EPR, Mössbauer (through spectral simulation), magnetic susceptibility, and NMR spectroscopy. Studies of the ferricytochromes c' by EPR and Mössbauer spectroscopy support the presence of an $S = {}^3/_2,{}^5/_2$ quantum mechanical spin-admixed ground state in frozen solutions of most cytochromes c'. In particular, EPR spectroscopy of ferricytochromes c' at weakly acidic to neutral pH is consistent with mid-spin contributions to the ground-state ranging from

~10 to ~50%. Mössbauer studies of ferricytochromes *c*′ from *Ch. vinosum* and *Rs. rubrum* at varying temperatures yielded quadrupole splitting values ΔE_Q compatible with a spin-admixed ground state. Magnetic susceptibility measurements yield conflicting results. Effective magnetic moments reported at ambient temperature in solution at neutral pH and at low temperature on solids precipitated from slightly acidic solution gave magnetic moments for *Ch. vinosum*, *Rp. palustris*, and *Rs. rubrum* uniformly lower than those expected for purely high-spin proteins (Table 4). The single temperature-dependent magnetic susceptibility study on a cytochrome *c*′, recorded with a SQUID susceptometer on the ferricytochrome *c*′ from *Rb. capsulatus*, yielded a curve consistent with a spin state having 0−10% $S = {}^3/_2$ admixture and no evidence of a spin transition. The curve was qualitatively different from temperature-dependent curves over a similar range of temperatures reported for spin-admixed model complexes. In contrast, EPR spectroscopy in frozen solution determined by the same investigators led to an estimate of ~40% $S = {}^3/_2$ admixture. The inconsistency between the results of magnetic susceptibility curve and EPR measurements may ultimately be explained by medium effects attributable to sample preparation, but this inconsistency cannot be understood in terms of the current state of research. ^{1}H NMR spectroscopy of cytochromes *c*′ from *Rp. palustris*, *Rs. molischianum*, *Rs. rubrum*, and *Ch. vinosum* at room temperature and physiological pH indicates predominantly high-spin ground states with the possible exception of the cytochrome *c*′ from *Ch. vinosum*. The evidence for spin-state admixture at weakly acidic to neutral pH in the *Ch. vinosum* protein is based on the small upfield hyperfine shifts of the *meso* H signals, which appear in the 0 to −5 ppm region. Such small shifts are in accord with shifts observed in $S = {}^3/_2,{}^5/_2$ spin-admixed model complexes. The large upfield hyperfine shifts of the *meso* H signals of the other three ferricytochromes *c*′ are typical for high-spin heme proteins and model complexes.

Measurements indirectly related to spin state include resonance Raman, normal-coordinate structural decomposition, EXAFS and XAS, optical spectroscopy, MCD and CD, and X-ray crystallography. Structural metrics inferred from application of these techniques considered individually are intrinsically inconclusive regarding spin state but, when compared with data from model complexes and other proteins, may be useful in providing support for spin-state assignment. Evidence on spin state from resonance Raman spectroscopy is based on the observation that core-size and spin-state marker band frequencies of spin-admixed models appear in the range expected for low-spin complexes, whereas by other measurements, e.g., magnetic moments, the models are clearly not low-spin. On this basis, the resonance Raman spectra of proteins from *Ch. vinosum*, *Rs. rubrum*, *Rp. palustris*, *Rs. molischianum*, and *Rb. sphaeroides* in neutral to slightly acidic medium are compatible with the presence of spin-admixed forms. NSD analysis shows heme ruffling and saddling in the cytochromes *c*′, but the macrocycle distortions are within the ranges found for models and proteins in pure spin states and, in the absence of studies that correlate effects of combined macrocycle distortions and axial ligation on spin state, this analysis also is not diagnostic for spin-state admixture. Likewise, the structural metrics estimated from EXAFS studies on *Rs. rubrum* and *Rs. molischianum* encompass values of both high-spin and spin-admixed pentacoordinate hemes and are thus not informative with regard to spin admixture.

UV−visible spectra of spin-admixed and high-spin model complexes are closely similar, and in line with this observation, spectra of the cytochromes *c*′ recorded in weakly acidic to neutral solutions are also similar to those of high-spin model complexes and proteins. As a consequence, the electronic spectra alone do not provide support for spin-state assignment.

A comparison of the near-IR region (700−2000 nm) ambient-temperature MCD spectra of ferricytochromes *c*′ from *Rs. rubrum*, *Rp. palustris*, and *Ch. vinosum* with those of well characterized $S = {}^3/_2,{}^5/_2$ spin-admixed porphyrin model compounds supports an $S = {}^3/_2,{}^5/_2$ spin-admixed ground state for these proteins by virtue of a negative−positive−negative trace extending over the near-IR range. This feature was unique to the spin-admixed models on which the analysis was based; however, it must be recalled that the ambient-temperature ^{1}H NMR spectra of *Rs. rubrum* and *Rp. palustris* seem to favor the high-spin state for these proteins.

While the structural features of the porphyrins determined by X-ray crystallography are not definitive with regard to the presence of spin-state admixture, crystallographically determined relationships between the axial His ligand and the protein environment are potentially more informative. While several class III plant peroxidases are considered to be spin admixed, the cytochromes *c*′ are unique in the presence of ammonium-Lys or guanidinium-Arg cations within the distal pocket. In the structure of *Ch. vinosum*, which is most likely to be spin admixed by the measures applied to date, the mean plane of an guanidinium-Arg cation is within ~3.5 Å of the His-ImH and is optimally oriented for π-stacking against the axial His-ImH plane, which could weaken the ligand strength sufficiently to induce a spin-state admixture. This feature is shared with *Rb. sphaeroides*, which contains significant $S = {}^3/_2,{}^5/_2$ admixture by EPR and ENDOR analysis, and hence, it is tempting to suggest the importance of this interaction in spin-state admixture. Whether the π-stacking is indeed crucial is at the moment uncertain, because there are no measurements to support spin-state admixture in *Rb. sphaeroides* at ambient temperature.

In conclusion, the physicochemical characterization of the cytochromes *c*′ presents a mixed picture regarding the importance of an $S = {}^3/_2,{}^5/_2$ spin-state admixture in the ground state. Only in the case of the cytochrome *c*′ from *Ch. vinosum* do published studies, incomplete though they may be, consistently support the presence of an $S = {}^3/_2,{}^5/_2$ spin-state admixture.

To ascertain the presence of a quantum mechanical $S = {}^3/_2,{}^5/_2$ spin-admixed ground state in the cytochromes *c*′ and to clarify the significance and possible involvement of Arg/Lys-ImH interactions in these properties, additional studies are necessary. One might propose the following:

(i) Studies of the X-ray structures of several of Nakamura's model cytochrome *c*′ compounds and the synthesis, structure, and spectroscopic properties of other novel five-coordinate ferric complexes of β-pyrrole alkyl-substituted porphyrins and sterically hindered imidazoles to address ambiguities in Nakamura's models.

(ii) The role of the basic residue (Arg or Lys) in the ground-state spin states of the cytochromes *c*′ should be probed (a) by examination of novel site directed mutants of the proteins isolated from the *Ch. vinosum* and *Rb. sphaeroi-*

des bacteria, mutants in which residues Arg 129 (*Ch. vinosum*) and Arg 127 (*Rb. sphaeroides*) have been replaced by residues not able to undergo cation$-\pi$ interactions with the ImH-His axial ligand of iron present in both proteins; (b) by temperature-dependent magnetic susceptibility studies of both these proteins as well as an ambient-temperature ^{1}H NMR study of the *Rb. sphaeroides* cytochrome c' and ^{13}C NMR studies on both proteins; and (c) by high-resolution X-ray structures providing more accurate bond distances in the cytochromes c' from *Ch. vinosum* and in at least of one of the almost pure high-spin proteins, such the cytochromes c' from *Ach. xylosoxidans*, *Rb. capsulatus*, or *M. capsulatus* Bath.

5. Acknowledgment

The authors gratefully acknowledge the assistance of Jean Fischer and John Dawson in preparation of the manuscript and Robert Schoonhaven and Rebekkah Cote (supported in part by USPHS Grant P30ES10126) with the cover graphics and figures. R.W. gratefully acknowledges continuing support from Jean-Marie Lehn and the assistance of Véronique Bulach with the literature survey. This work was supported in part by USPHS Grant GM57042 (J.T.).

6. References

(1) Vernon, L. P.; Kamen, M. T. *J. Biol. Chem.* **1954**, *211*, 643.
(2) Bartsch, R. G.; Kamen, M. D. *J. Biol. Chem.* **1958**, *230*, 41.
(3) Morita, S. *Biochim. Biophys. Acta* **1968**, *153*, 241.
(4) Iwasaki, H.; Shidara, S. *Plant Cell Physiol.* **1969**, *10*, 291.
(5) Ehrenberg, A.; Kamen, M. D. *Biochim. Biophys. Acta* **1965**, *102*, 333.
(6) Maltempo, M. M.; Moss, T. H.; Cusanovich, M. A. *Biochim. Biophys. Acta* **1974**, *342*, 290.
(7) Maltempo, M. M. *J. Chem. Phys.* **1974**, *61*, 2540.
(8) Maltempo, M. M.; Moss, T. H. *Q. Rev. Biophys.* **1976**, *9*, 181.
(9) Monkara, F.; Bingham, S. J.; Kadir, F. H. A.; McEwan, A. G.; Thomson, A. J.; Thurgood, A. G. P.; Moore, G. R. *Biochim. Biophys. Acta* **1992**, *1100*, 184.
(10) Fujii, S.; Yoshimura, T.; Kamada, H.; Yamaguchi, K.; Suzuki, S.; Shidara, S.; Takakuva, S. *Biochim. Biophys. Acta* **1995**, *1251*, 161.
(11) Yoshimura, T.; Suzuki, S.; Kohzuma, T.; Iwasaki, H.; Shidara, S. *Biochem. Biophys. Res. Commun.* **1990**, *169*, 1235.
(12) Strekas, T. C.; Spiro, T. G. *Biochim. Biophys. Acta* **1974**, *351*, 237.
(13) Korszun, Z. R.; Bunker, G.; Khalid, S.; Scheidt, W. R.; Cusanovich, M. A.; Meyer, T. E. *Biochemistry* **1989**, *28*, 1513.
(14) Emptage, M. H.; Zimmermann, R. L.; Que, L. J.; Münck, E.; Hamilton, W. D.; Orme-Johnson, W. H. *Biochim. Biophys. Acta* **1977**, *495*, 12.
(15) Zahn, J. A.; Arciero, D. M.; Hooper, A. B.; DiSpirito, A. A. *Eur. J. Biochem.* **1996**, *1996*, 684.
(16) La Mar, G. N.; Jackson, J. T.; Dugad, L. B.; Cusanovich, M. A.; Bartsch, R. G. *J. Biol. Chem.* **1990**, *265*, 16173.
(17) Bertini, I.; Briganti, F.; Monnanni, R.; Scozzafava, A.; Carlozzi, P.; Materassi, R. *Arch. Biochem. Biophys.* **1990**, *282*, 84.
(18) Banci, L.; Bertini, I.; Turano, P.; Vicens Oliver, M. *Eur. J. Biochem.* **1992**, *204*, 107.
(19) Bertini, I.; Gori, G.; Luchinat, C.; Vila, A. J. *Biochemistry* **1993**, *32*, 776.
(20) Tsan, P.; Caffrey, M.; Daku, M. L.; Cusanovich, M.; Marion, D.; Gans, P. *J. Am. Chem. Soc.* **2001**, *123*, 2231.
(21) Palmer, G. In *The Porphyrins*; Dolphin, D., Ed.; Academic Press: New York, 1979; Vol. IV, p 313.
(22) Reed, C. A.; Mashiko, T.; Bentley, S. P.; Kastner, M. E.; Scheidt, W. R.; Spartalian, K.; Lang, G. *J. Am. Chem. Soc.* **1979**, *101*, 2948.
(23) Scheidt, W. R.; Reed, C. A. *Chem. Rev.* **1981**, *81*, 543.
(24) Reed, C. A.; Guiset, F. *J. Am. Chem. Soc.* **1996**, *118*, 3281.
(25) Shibata, N.; Iba, S.; Misaki, S.; Meyer, T. E.; Bartsch, R. G.; Cusanovich, M. A.; Morimoto, Y.; Higuchi, Y.; Yasuoka, N. *J. Mol. Biol.* **1998**, *284*, 751.
(26) Cusanovich, M. A. *Biochim. Biophys. Acta* **1971**, *236*, 238.
(27) Doyle, M. L.; Gill, S. J.; Cusanovich, M. A. *Biochemistry* **1986**, *25*, 2509.
(28) Ren, Z.; Meyer, T.; McRee, D. E. *J. Mol. Biol.* **1993**, *234*, 433.
(29) Meyer, T. E.; Kamen, M. D. *Adv. Protein Chem.* **1982**, *35*, 105.
(30) *Heme proteins*; Cusanovich, M. A., Meyer, T. E., Tollin, G., Eds.; Elesevier: Amsterdam, 1988; Vol. 7, p 37.
(31) Schmidt, T. M.; DiSpirito, A. A. *Arch. Microbiol.* **1990**, *154*, 453.
(32) Bergmann, D. J.; Zahn, J. A.; DiSpirito, A. A. *Arch. Microbiol.* **2000**, *173*, 29.
(33) Pettigrew, G. W.; Moore, J. R. *Cytochromes c*; *Biological Aspects*; Springer: Berlin, 1987.
(34) Gibson, Q. H.; Kamen, M. D. *J. Biol. Chem.* **1966**, *241*, 1969.
(35) Cusanovich, M. A.; Gibson, Q. H. *J. Biol. Chem.* **1973**, *248*, 822.
(36) Rubinov, S. C.; Kassner, R. J. *Biochemistry* **1984**, *23*, 2590.
(37) Doyle, M. L.; Weber, P. C.; Gill, S. J. *Biochemistry* **1985**, *24*, 1987.
(38) Yoshimura, T.; Suzuki, S.; Nakahara, A.; Iwasaki, H.; Masuko, M.; Matsubara, T. *Biochemistry* **1986**, *25*, 2436.
(39) Kassner, R. J. *Biochim. Biophys. Acta* **1991**, *1058*, 8.
(40) Taniguchi, S.; Kamen, M. D. *Biochim. Biophys. Acta* **1963**, *74*, 438.
(41) Moir, J. W. B. *Biochim. Biophys. Acta* **1999**, *1430*.
(42) Suzuki, S.; Nakahara, A.; Yoshimura, T.; Iwasaki, H.; Shidara, S.; Matsubara, T. *Inorg. Chim. Acta* **1988**, *153*, 227.
(43) Motie, M.; Kassner, R. J.; Meyer, T. E.; Cusanovich, M. A. *Biochemistry* **1990**, *29*, 1932.
(44) Yoshimura, T.; Shidara, S.; Ozaki, T.; Kamada, H. *Arch. Microbiol.* **1993**, *160*, 498.
(45) Yoshimura, T.; Iwasaki, H.; Shidara, S.; Suzuki, S.; Nakahara, A.; Matsubara, T. *J. Biochem.* **1988**, *103*, 1016.
(46) Mayburd, A. L.; Kassner, R. J. *Biochemistry* **2002**, *41*, 11582.
(47) Cross, R.; Aish, J.; Paston, S. J.; Poole, R. K.; Moir, J. W. B. *J. Bacteriol.* **2000**, *182*, 1442.
(48) Cross, R.; Lloyd, D.; Poole, R. K.; Moir, J. W. B. *J. Bacteriol.* **2001**, *183*, 3050.
(49) Dutton, P. L.; Leigh, J. S. *Biochim. Biophys. Acta* **1973**, *314*, 178.
(50) Prince, R. C.; Leigh, J. S.; Dutton, P. L. *Biochem. Soc. Trans.* **1974**, *314*, 178.
(51) Griffith, J. S. *The Theory of Transition Metal Ions*; Cambridge University Press: Cambridge, England, 1961.
(52) Harris, G. *Theor. Chim. Acta* **1968**, *10*, 119.
(53) Marathe, V. R.; Mitra, S. *Indian J. Pure Appl. Phys.* **1976**, *14*, 893.
(54) Loew, G. In *Iron Porphyrins*; Lever, A. B. P., Gray, H. B., Eds.; Addison-Wesley: London, 1983; Vol. 1, p 1.
(55) Bominaar, E. L.; Block, R. *J. Chem. Phys.* **1991**, *95*, 6712.
(56) Kahn, O. *Molecular Magnetism*; VCH: New York, 1993.
(57) La Mar, G. N.; Walker, F. A. In *The Porphyrins*; Dolphin, D., Ed.; Academic Press: New York, 1978; Vol. IV, p 61.
(58) Walker, F. A. In *The Porphyrin Handbook*; Kadish, K. M., Smith, K. M., Guilard, R., Eds.; Academic Press: San Diego, CA, 2000; Vol. 5, p 1.
(59) Gupta, G. P.; Lang, G.; Lee, Y. J.; Scheidt, W. R.; Shelly, K.; Reed, C. A. *Inorg. Chem.* **1987**, *26*, 3022.
(60) Evans, D. R.; Reed, C. A. *J. Am. Chem. Soc.* **2000**, *122*, 4660.
(61) Ikezaki, A.; Nakamura, M. *Chem. Lett.* **2000**, 994.
(62) Ikezaki, A.; Nakamura, M. *Inorg. Chem.* **2002**, *41*, 6225.
(63) Masuda, H.; Taga, T.; Osaki, K.; Sugimoto, H.; Yoshida, Z.; Ogoshi, H. *Bull. Chem. Soc. Jpn.* **1982**, *55*, 3891.
(64) Scheidt, W. R.; Geiger, D. K.; Haller, K. J. *J. Am. Chem. Soc.* **1982**, *104*, 495.
(65) Scheidt, W. R.; Geiger, D. K.; Hayes, R. G.; Lang, G. *J. Am. Chem. Soc.* **1983**, *105*, 2625.
(66) Scheidt, W. R.; Osvath, S. R.; Lee, Y. J.; Reed, C. A.; Shavez, B.; Gupta, G. B. *Inorg. Chem.* **1989**, *28*, 1591.
(67) Kintner, E. T.; Dawson, J. H. *Inorg. Chem.* **1991**, *30*, 4892.
(68) Gismelseed, A.; Bominaar, E. L.; Bill, E.; Trautwein, A. X.; Winkler, H.; Nasri, H.; Doppelt, P.; Mandon, D.; Fischer, J.; Weiss, R. *Inorg. Chem.* **1990**, *29*, 2741.
(69) Owens, J. W.; Robinson, J.; O'Connor, C. J. *Inorg. Chim. Acta* **1993**, *206*, 141.
(70) Sakai, T.; Ohgo, Y.; Ikeue, T.; Takahashi, M.; Takeda, M.; Nakamura, M. *J. Am. Chem. Soc.* **2003**, *125*, 13028.
(71) Cheng, R.-J.; Wang, Y.-K.; Chen, P.-Y.; Han, Y.-P.; Chang, C.-C. *Chem. Commun.* **2005**, 1312.
(72) Hoshino, A.; Ohgo, Y.; Nakamura, M. *Inorg. Chem.* **2005**, *44*, 7333.
(73) Howes, B. D.; Schiodt, B. B.; Welinder, K. G.; Marzocchi, M. P.; Ma, J.-G.; Zhang, J.; Shelnutt, J. A.; Smulevich, G. *Biophys. J.* **1999**, *77*, 478.
(74) Howes, B. D.; Veitch, N. G.; Smith, A. T.; White, C. G.; Smulevich, G. *Biochem. J.* **2001**, *353*, 181.
(75) Mitra, S.; Marathe, V. R.; Birdy, R. *Chem. Phys. Lett.* **1983**, *96*, 103.
(76) Nesset, M. J. M.; Cai, S.; Shokhireva, T. K.; Shokhirev, N. V.; Jacobson, S. E.; Jayaraj, K.; Gold, A.; Walker, F. A. *Inorg. Chem.* **2000**, *39*, 532.
(77) Weltner, W. *Magnetic Atoms and Molecules*; Van Nostrand Reinhold Co.: 1983; Chapter V.
(78) Nakamura, M.; Ikeue, T.; Ohgo, Y.; Takahashi, M.; Takeda, M. *Chem. Commun.* **2002**, 1198.

(79) Cheng, R.-J.; Chen, P.-Y.; Lovell, T.; Liu, T.; Noodleman, L.; Case, D. A. *J. Am. Chem. Soc.* **2003**, *125*, 6774.
(80) Goff, H.; Shimomura, E. *J. Am. Chem. Soc.* **1980**, *102*, 31.
(81) Boersma, A. D.; Goff, H. M. *Inorg. Chem.* **1982**, *21*, 581.
(82) Dugad, L. B.; Marathe, V. R.; Mitra, S. *Proc. Indian Acad. Sci.* **1985**, *95*, 189.
(83) Walker, A.; Simonis, U. In *Encyclopedia of Inorganic Chemistry*; King, R. B., Ed.; John Wiley & Sons: Chichester, 1994; Vol. 4, p 1814.
(84) Yatsunyk, L. A.; Sokhirev, N. A.; Walker, F. A. *Inorg. Chem.* **2005**, *44*, 2848.
(85) Yatsunyk, L. A.; Walker, F. A. *Inorg. Chem.* **2004**, *43*, 757.
(86) Ogoshi, H.; Watanabe, E.; Yoshida, Z. *Chem. Lett.* **1973**, 989.
(87) Dolphin, D. H.; Sams, J. R.; Tsin, T. B. *Inorg. Chem.* **1977**, *16*, 711.
(88) Summerville, D. A.; Cohen, I. A.; Hatano, K.; Scheidt, W. R. *Inorg. Chem.* **1978**, *17*, 2906.
(89) Gonzalez, J. A.; Wilson, L. J. *Inorg. Chem.* **1994**, *33*, 1543.
(90) Toney, G. E.; Gold, A.; Savrin, J. E.; terHaar, L. W.; Sangaiah, R.; Hatfield, W. E. *Inorg. Chem.* **1984**, *23*, 4350.
(91) Toney, G. E.; terHaar, L. W.; Savrin, J. E.; Gold, A.; Hatfield, W. E.; Sangaiah, R. *Inorg. Chem.* **1984**, *23*, 2563.
(92) Gupta, G. P.; Lang, G.; Scheidt, W. R.; Geiger, D. K.; Reed, C. A. *J. Chem. Phys.* **1986**, *85*, 5212.
(93) Gupta, G. P.; Lang, G.; Reed, C. A.; Shelly, K.; Scheidt, W. R. *J. Chem. Phys.* **1987**, *86*, 5288.
(94) Scheidt, W. R.; Geiger, D. K.; Lee, J. L.; Reed, C. A.; Lang, G. *J. Am. Chem. Soc.* **1985**, *107*, 5693.
(95) Ikeue, T.; Saitoh, T.; Yamaguchi, S.; Ohgo, Y.; Nakamura, M.; Takahashi, M.; Takeda, M. *Chem. Commun.* **2000**, 1989.
(96) Ikeue, T.; Ohgo, Y.; Yamaguchi, S.; Takahashi, M.; Takeda, M.; Nakamura, M. *Angew. Chem. Int. Ed.* **2001**, *40*, 2717.
(97) Ikeue, T.; Ohgo, Y.; Ongayi, O.; Vincente, M. G. H.; Nakamura, M. *Inorg. Chem.* **2003**, *42*, 5560.
(98) Sakai, T.; Ohgo, Y.; Hoshino, Y.; Ikeue, T.; Saitoh, T.; Takahashi, M.; Nakamura, M. *Inorg. Chem.* **2004**, *43*, 5034.
(99) Ohgo, Y.; Ikeue, T.; Takahashi, M.; Takeda, M.; Nakamura, M. *Eur. J. Inorg. Chem.* **2004**, 798.
(100) Kennedy, B. J.; Brain, G.; Murray, K. S. *Inorg. Chim. Acta* **1984**, *81*, L29−L31.
(101) Kennedy, B. J.; Murray, K. S.; Zwack, P. R.; Homborg, H.; Kalz, W. *Inorg. Chem.* **1986**, *25*, 2539−2545.
(102) Fitzgerald, J. P.; Haggerty, B. S.; Rheingold, A. L.; May, L. *Inorg. Chem.* **1992**, *31*, 2006.
(103) Fitzgerald, J. P.; Yap, G. P. A.; Rheingold, A. L.; Brewer, C. T.; May, L.; Brewer, G. A. *J. Chem. Soc., Dalton Trans.* **1996**, 1249.
(104) Simonato, J.-P.; Pécaut, J.; Le Pape, L.; Oddou, J.-L.; Jeandey, C.; Shang, M.; Scheidt, W. R.; Wojaczynski, J.; Wolowiec, S.; Latos-Grazynski, L.; Marchon, J.-C. *Inorg. Chem.* **2000**, *39*, 3978.
(105) Cheng, R.-J.; Chen, P.-Y.; Gau, P.-R.; Chen, C.-C.; Peng, S.-M. *J. Am. Chem. Soc.* **1997**, *119*, 2563.
(106) Cheng, R.-J.; Chen, P.-Y. *Chem.—Eur. J.* **1999**, *5*, 1708.
(107) Ohgo, Y.; Ikeue, T.; Nakamura, M. *Inorg. Chem.* **2002**, *41*, 1698.
(108) Schünemann, V.; Gerdan, M.; Trautwein, A. X.; Haoudi, N.; Mandon, D.; Fischer, J.; Weiss, R.; Tabard, T.; Guilard, R. *Angew. Chem., Int. Ed.* **1999**, *31*, 81.
(109) Weiss, R.; Fischer, J.; Bulach, V.; Shelnutt, J. *C. R. Chim.* **2002**, *5*, 405.
(110) Weiss, R.; Fischer, J.; Bulach, V.; Schünemann, V.; Gerdan, M.; Trautwein, A. X.; Shelnutt, J. A.; Gros, C. P.; Tabard, A.; Guilard, R. *Inorg. Chim. Acta* **2002**, *337*, 223.
(111) Barkigia, K. M.; Renner, M. W.; Fajer, J. *J. Porphyrins Phthalocyanines* **2001**, *5*, 415.
(112) Hoard, J. L. *Ann. N. Y. Acad. Sci.* **1973**, *206*, 18.
(113) Scheidt, W. R. In *The Porphyrin Handbook*; Kadish, K. M., Smith, K. M., Guilard, R., Eds.; Academic Press: San Diego, CA, 2000; Vol. 3, p 49.
(114) Pérollier, C.; Mazzanti, M.; Simonato, J.-P.; Launay, F.; Ramasseul, R.; Marchon, J.-C. *Eur. J. Org. Chem.* **2000**, 583.
(115) Manzzanti, M.; Marchon, J.-C.; Wojaczynski, J.; Woloviec, S.; Latos-Grazynski, L.; Shang, M.; Scheidt, W. R. *Inorg. Chem.* **1998**, *37*, 2476.
(116) Masuda, H.; Taga, T.; Osaki, K.; Sugimoto, H.; Yoshida, Z.-I.; Ogoshi, H. *Inorg. Chem.* **1980**, *19*, 950.
(117) Cheng, B.; Safo, M. K.; Orosz, R. D.; Reed, C. A.; Debrunner, P. G.; Scheidt, W. R. *Inorg. Chem.* **1994**, *33*, 1319.
(118) Ohgo, Y.; Saitoh, T.; Nakamura, M. *Acta Crystallogr.* **2001**, *C57*, 233.
(119) Ogoshi, H.; Sugimoto, H.; Watanabe, E.; Yoshida, Z.; Maeda, Y.; Sakai, H. *Bull. Chem. Soc. Jpn.* **1981**, *54*, 3414.
(120) Shelly, K.; Bartczak, T.; Scheidt, W. R.; Reed, C. A. *Inorg. Chem.* **1985**, *24*, 4325.
(121) Ohlhausen, L. N.; Cockrum, D.; Register, J.; Roberts, K.; Long, G. J.; Powell, G. L.; Hutchinson, B. B. *Inorg. Chem.* **1990**, *29*, 4886.
(122) Neal, T. J.; Cheng, B.; Ma, J.-G.; Shelnutt, J. A.; Schultz, C. E.; Scheidt, W. R. *Inorg. Chim. Acta* **1999**, *291*, 49.
(123) Ogura, H.; Yatsunyk, L.; Medforth, C. J.; Smith, K. M.; Barkigia, K. M.; Renner, M. W.; Melamed, D.; Walker, F. A. *J. Am. Chem. Soc.* **2001**, *123*, 6564.
(124) Yatsunyk, L. A.; Carducci, M. D.; Walker, F. A. *J. Am. Chem. Soc.* **2003**, *125*, 15986.
(125) Garner, C. D. In *Advances Inorganic Chemistry*; 1991; Vol. 36.
(126) Powers, L. *Biochim. Biophys. Acta* **1982**, *683*, 1.
(127) Lee, P. A.; Citrin, P. H.; Eisenberger, P.; Kincaid, B. M. *Rev. Mod. Phys.* **1981**, *53*, 769.
(128) Hahn, J. E.; Scott, R. A.; Hodgson, K. O.; Doniach, S.; Desjardins, S. R.; Solomon, E. I. *Chem. Phys. Lett.* **1982**, *88*, 595.
(129) Penner-Hahn, J. E.; Benfatto, M.; Hedman, B.; Takahashi, T.; Doniach, L.; Groves, J. T.; Hodgson, K. O. *Inorg. Chem.* **1986**, *25*, 2255.
(130) Kirk, M. L.; Gold, A. In preparation.
(131) Jayaraj, K.; Gold, A.; Austin, R. N.; Mandon, D.; Weiss, R.; Terner, J.; Bill, E.; Müther, M.; Trautwein, A. X. *J. Am. Chem. Soc.* **1995**, *117*, 9079.
(132) Jayaraj, K.; Gold, A.; Austin, R. N.; Ball, L. M.; Terner, J.; Mandon, D.; Weiss, R.; Fischer, J.; De Cian, A.; Bill, E.; Müther, M.; Schünemann, V.; Trautwein, A. X. *Inorg. Chem.* **1996**, *36*, 4555.
(133) Teraoka, J.; Kitagawa, T. *J. Chem. Phys.* **1980**, *84*, 1928.
(134) Debrunner, P. G., Lever, A. B. P., Gray, H. B., Eds.; VCH Publishers Inc.: New York, 1989; Vol. 3, pp 137.
(135) Spartalian, K.; Lang, G.; Reed, C. A. *J. Chem. Phys.* **1979**, *71*, 1832.
(136) Walker, F. A.; Lo, M.-W.; Ree, M. T. *J. Am. Chem. Soc.* **1976**, *98*, 5552.
(137) Quinn, R.; Nappa, M.; Valentine, J. S. *J. Am. Chem. Soc.* **1982**, *104*, 2588.
(138) Bullard, L.; Panayappan, R. M.; Thorpe, A. N.; Hambright, P. *Bioinorg. Chem.* **1974**, *3*, 161.
(139) Geiger, D. K.; Lee, Y. J.; Scheidt, W. R. *J. Am. Chem. Soc.* **1984**, *106*, 6339.
(140) Ikezaki, A.; Nakamura, M. *J. Inorg. Biochem.* **2001**, *84*, 137.
(141) Dobbs, A. J.; Anderson, B. F.; Faber, H. R.; Baker, E. N. *Acta Crystallogr.* **1996**, *D52*, 356.
(142) Tahirov, H. T.; Misaki, S.; Meyer, T. E.; Cusanovich, M. A.; Higuchi, Y.; Yasuoka, N. *Nat. Struct. Biol.* **1996**, *3*, 459.
(143) Lawson, D. M.; Stevenson, C. E. M.; Andrew, C. R.; Eady, R. R. *EMBO J.* **2000**, *19*, 5661.
(144) Lawson, D. M.; Stevenson, C. E. M.; Andrew, C. R.; George, S. J.; Eady, R. R. *Biochem. Soc. Trans.* **2003**, *31*, 553.
(145) Bertini, I.; Faraonee-Menella, J.; Gray, H. B.; Luchinat, C.; Parigi, J.; Winckler, J. R. **2004**, *9*, 224.
(146) Moore, G. R.; McClune, G. J.; Clayden, N. J.; Williams, R. J. P.; Alsaadi, B. M.; Angström, J.; Ambler, R. P.; Van Beeumen, J.; Tempst, P.; Bartsch, R. G.; Meyer, T. E.; Kamen, M. D. *Eur. J. Biochem.* **1982**, *123*, 73.
(147) Meyer, T. E.; Cheddar, G.; Bartsch, R. G.; Getzoff, E. D.; Cusanovich, M. A.; Tollin, G. *Biochemistry* **1986**, *25*, 1383.
(148) Tahirov, T. H.; Misaki, S.; Meyer, T. E.; Cusanovich, M. A.; Higuchi, Y.; Yasuoka, N. *J. Mol. Biol.* **1996**, *259*, 467.
(149) M.-Ramirez, L.; Axelrod, H. L.; Herron, S. R.; Rupp, B.; Allen, J. P.; Kantardjieff, K. A. *J. Chem. Cryst.* **2003**, *33*, 413.
(150) Jentzen, W.; Ma, J.-G.; Shelnutt, J. A. *Biophys. J.* **1998**, *74*, 753.
(151) Sun, L.; Shelnutt, J. A. Sandia National Laboratories, 2001−2005.
(152) Archer, M.; Banci, L.; Dikaya, E.; Romào, M. J. *J. Bioinorg. Chem.* **1997**, *2*, 611.
(153) Finzel, B. C.; Weber, P.; Hardman, K. D.; Salemme, F. R. *J. Mol. Biol.* **1985**, *186*, 627.
(154) Valentine, J. S.; Sheridan, R. P.; Allen, L. G.; Kahn, P. C. *Proc. Natl. Acad. Sci. U.S.A.* **1979**, *76*, 1009.
(155) Banci, L.; Rosato, A.; Turano, P. *J. Biol. Inorg. Chem.* **1996**, *1*, 364.
(156) (a) Poulos, T. L. *Adv. Inorg. Chem.* **1988**, *7*, 1. (b) Poulos, T. L. *J. Biol. Inorg. Chem.* **1996**, *1*, 356.
(157) Weber, P. *Biochemistry* **1982**, *21*, 5116.
(158) Dougherty, D. A. *Science* **1996**, *271*, 163.
(159) Gallivan, J. P.; Dougherty, D. A. *Proc. Natl. Acad. Sci. U.S.A.* **1999**, *96*, 9459.
(160) Burley, S. K.; Petsko, G. A. *FEBS Lett.* **1986**, *203*, 139.
(161) Perutz, M. F.; Fermi, G.; Abraham, D. J.; Poyard, C.; Bursaux, E. *J. Am. Chem. Soc.* **1986**, *108*, 1064.
(162) Lewitt, M.; Perutz, M. F. *J. Mol. Biol.* **1988**, *201*, 751.
(163) Mitchell, J. B. O.; Nandi, C. L.; McDonald, I. K.; Thornton, J. M.; Price, S. L. *J. Mol. Biol.* **1994**, *239*, 315.
(164) (a) Ambler, R. P.; Bartsch, R. G.; Daniel, M.; Kamen, M. D.; McLellan, L.; Meyer, T. E.; Van Beeumen, J. *Proc. Natl. Acad. Sci. U.S.A.* **1981**, *78*, 6854. (b) Ambler, R. P.; Daniel, M.; Meyer, T. E.;

Kamen, M. D. *Biochimie* **1994**, *76*, 583. (c) Bergmann, D. J.; Zahn, J. A.; Hooper, A. B.; DiSpirito, A. A. *J. Bacteriol*. **1998**, *180*, 6440.
(165) Usov, O. M.; Choi, P. S.-T.; Shapleigh, J. P.; Scholes, C. P. *J. Am. Chem. Soc*. **2005**, *127*, 9485.
(166) Doyle, M. L.; Gill, S. J.; Meyer, T. E.; Cusanovich, M. A. *Biochemistry* **1987**, *26*, 8055.
(167) Moss, T. H.; Bearden, A. J.; Bartsch, A. J.; Cusanovich, M. A. *Biochemistry* **1968**, *7*, 1583.
(168) Kassner, R. J.; Kykta, M. G.; Cusanovich, M. A. *Biochim. Biophys. Acta* **1985**, *831*, 155.
(169) Poulos, T. L. *Nat. Struct. Biol.* **1996**, *3*, 401.
(170) Jentzen, W.; Song, X.-Z.; Shelnutt, J. A. *J. Phys. Chem. B* **1997**, *101*, 1684.
(171) Shelnutt, J. A.; Song, X.-Z.; Ma, J.-G.; Jia, S.-L.; Jentzen, W.; Medforth, C. J. *Chem. Soc. Rev.* **1998**, *27*, 31.
(172) Shelnutt, J. A. In *The Porphyrin Handbook*; Kadish, K. M., Smith, K. M., Guilard, R., Eds.; Academic Press: San Diego, CA, 2000; Vol. 7, p 167.
(173) Tasaki, A.; Otsuka, J.; Kotani, M. *Biochim. Biophys. Acta* **1967**, *140*, 284.
(174) Phillips, W. D.; Poe, M. *Methods Enzymol*. **1972**, *24*, 304.
(175) Salmeen, L.; Palmer, G. *J. Chem. Phys*. **1968**, *48*, 2049.
(176) Maltempo, M. M.; Moss, T. H.; Spartalian, K. *J. Chem. Phys*. **1980**, *73*, 2100.
(177) Emptage, M. H.; Xavier, A. V.; Wood, J. M.; Alsaadi, B. M.; Moore, G. R.; Pitt, R. C.; Williams, R. J. P.; Ambler, R. P.; Bartsch, R. G. *Biochemistry* **1981**, *20*, 58.
(178) Yoshimura, T.; Suzuki, S.; Iwasaki, H.; Takakuwa, S. *Biochem. Biophys. Res. Commun*. **1987**, *144*, 224.
(179) Yoshimura, T.; Suzuki, S.; Nakahara, A.; Iwasaki, H.; Masuko, M.; Matsubara, T. *Biochim. Biophys. Acta* **1985**, *831*, 267.
(180) Iwasaki, H.; Yoshimura, T.; Suzuki, S.; Shidara, S. *Biochim. Biophys. Acta* **1991**, *1058*, 79.
(181) Clark, K.; Dugad, L. B.; Bartsch, R. G.; Cusanovich, M. A.; La Mar, G. N. *J. Am. Chem. Soc*. **1996**, *118*, 4654.
(182) Walker, F. A.; Simonis, U. In *Biological Resonance NMR*; Berliner, L. J., Reuben, J., Eds.; Plenum Press: New York, 1993; Vol. 12.
(183) Goff, H. M. In *Iron Porphyrins Part One*; Lever, A. B. P., Gray, H. B., Eds.; Addison-Wesley Publishing Company: London, 1983; Vol. 1, p 237.
(184) La Mar, G. N.; Satterlee, J. D.; De Ropp, J. S. In *The Porphyrin Handbook*; Kadish, K. M., Smith, K. M., Guilard, R., Eds.; Academic Press: San Diego, CA, 2000; Vol. 5, p 188.
(185) Pande, U.; La Mar, G. N.; Lecomte, J. T. J.; Ascoli, F.; Brunori, M.; Smith, K. M.; Pandey, R. K.; Parish, D. W.; Thanabal, V. *Biochemistry* **1986**, *25*, 5638.
(186) La Mar, G. N.; Jackson, J. T.; Bartsch, R. G. *J. Am. Chem. Soc*. **1981**, *103*, 4405.
(187) Déméné, H.; Tsan, P.; Gans, P.; Marion, D. *J. Phys. Chem*. **2000**, *104*, 2559.
(188) Jackson, J. T.; La Mar, G. N.; Bartsch, R. G. *J. Biol. Chem*. **1983**, *258*, 1799.
(189) Caffrey, M.; Simorre, M.; Brutscher, B.; Cusanovich, M.; Marion, D. *Biochemistry* **1995**, *34*, 5904.
(190) Caffrey, M.; Simorre, J. P.; Cusanovich, M.; Marion, D. *FEBS Lett*. **1995**, *368*, 519.
(191) Brutscher, B.; Cordier, F.; Simorre, J. P.; Caffrey, M.; Marion, D. *Biomol. NMR* **1995**, *5*, 202.
(192) Tsan, P.; Caffrey, M.; Daku, M. L.; Cusanovich, M.; Marion, D.; Gans, P. *J. Am. Chem. Soc*. **1999**, *121*, 1795.
(193) Horio, T.; Kamen, M. D. *Biochim. Biophys. Acta* **1961**, *48*, 266.
(194) Imai, Y.; Imai, K.; Sato, R.; Horio, T. *J. Biol. Chem*. **1969**, *65*, 266.
(195) Maltempo, M. M. *Biochim. Biophys. Acta* **1976**, *434*, 513.
(196) Adar, F. In *The Porphyrins*; Dolphin, D., Ed.; Academic Press: New York, 1978; Vol. III.
(197) Smulevich, G. *Biospectroscopy* **1998**, *4*, S3.
(198) Smulevich, G.; Neri, F.; Marzocchi, M. P.; Welinder, K. G. *Biochemistry* **1996**, *35*, 10576.
(199) Neri, F.; Kok, D.; Miller, M. A.; Smulevich, G. *Biochemistry* **1997**, *36*, 8947.
(200) Spiro, T. G.; Li, X.-Y. In *Biological Applications of Raman Spectroscopy*; Spiro, T. G., Ed.; Wiley: New York, 1988; Vol. III, p 1.
(201) Imai, Y.; Imai, K.; Sato, R.; Horio, T. *J. Biochem*. **1969**, *65*, 225.
(202) Kitagawa, T.; Ozaki, Y.; Kyogoku, Y.; Horio, T. *Biochim. Biophys. Acta* **1977**, *495*, 1−11.
(203) Hobbs, J. D.; Larsen, R. W.; Meyer, T. E.; Hazzard, J. H.; Cusanovich, M. A.; Ondrias, M. R. *Biochemistry* **1990**, *29*, 4166.
(204) Othman, S.; Richaud, P.; Verméglio, A.; Desbois, A. *Biochemistry* **1996**, *35*, 9224.
(205) Othman, S.; Le Lirzin, A.; Desbois, A. *Biochemistry* **1993**, *32*, 9781.
(206) Evangelista-Kirkup, R.; Crisanti, M.; Poulos, T. L.; Spiro, T. G. *FEBS Lett*. **1985**, *190*, 221.
(207) Reczek, C. M.; Sitter, A. J.; Terner, J. *J. Mol. Struct*. **1989**, *214*, 27.
(208) Spiro, T. G.; Strekas, T. C. *J. Am. Chem. Soc*. **1974**, *96*, 338.
(209) Rakshit, G.; Spiro, T. G. *Biochemistry* **1974**, *13*, 5317.
(210) Terner, J.; Reed, D. E. *Biochim. Biophys. Acta* **1984**, *789*, 80.
(211) Feis, A.; Howes, B. D.; Indiani, C.; Smulevich, G. *J. Raman Spectrosc*. **1998**, *29*, 933.
(212) Nissum, M.; Feis, A.; Smulevich, G. *Biospectroscopy* **1998**, *4*, 355.
(213) Maltempo, M. M.; Ohlson, P.-I.; Paul, K.-G.; Pertersson, P. L.; Ehrenberg, A. *Biochemistry* **1979**, *18*, 2935.
(214) Lopez-Minola, D.; Heering, H. A.; Smulevich, G.; Tudela, J.; Thorneley, R. N. F.; Garcià-Cànovas, F.; Rodrigues-Lopez, J. N. *J. Inorg. Biochem*. **2003**, *94*, 243.
(215) Indiani, C.; Feis, A.; Howes, B. D.; Marzocchi, M. P.; Smulevich, G. *J. Am. Chem. Soc*. **2000**, *122*, 7368.
(216) Dunford, H. B. *Adv. Inorg. Biochem*. **1982**, *4*, 41.
(217) Rawlings, J.; Stephen, P. J.; Nafie, L. A.; Kamen, M. D. *Biochemistry* **1977**, *16*, 1725.
(218) Imai, Y.; Imai, K.; Ikeda, K.; Hamaguchi, K.; Horio, T. *J. Biochem*. **1969**, *65*, 629.
(219) Scheidt, W. R.; Geiger, D. K.; Lee, Y. J.; Reed, C. A.; Lang, G. *Inorg. Chem*. **1987**, *26*, 1039.
(220) Yasui, M.; Harada, S.; Kai, Y.; Kasai, N.; Kusunoki, M.; Matsuura, Y. *J. Biochem*. **1992**, *111*, 317.
(221) Moss, T. H. Unpublished data.
(222) Choi, S.; Spiro, T. G.; Langry, K. C.; Smith, K. M.; Budd, L. D.; LaMar, G. N. *J. Am. Chem. Soc*. **1982**, *104*, 443.
(223) Hu, S.; Smith, K. M.; Spiro, T. G. *J. Am. Chem. Soc*. **1996**, *118*, 12638.
(224) Cartling, B. In *Biological Applications of Raman Spectroscopy*; Spiro, T. G., Ed.; John Wiley & Sons: New York, 1988; Vol. 3.
(225) Hildebrandt, P.; English, A. M.; Smulevich, G. *Biochemistry* **1992**, *31*, 2384.

CR040416L